NASA CR-165,919

NASA Contractor Report 165919

NASA-CR-165919
1982 0020390

Gust Response of Commercial Jet Aircraft Including Effects of Autopilot Operation

Joseph H. Goldberg
Villanova University
Villanova, PA 19085

Contract NAS1 - 16095
June 1982

LIBRARY COPY

JUL 28 1982

LANGLEY RESEARCH CENTER
LIBRARY, NASA
HAMPTON, VIRGINIA

NASA
National Aeronautics and
Space Administration

Langley Research Center
Hampton, Virginia 23665

GUST RESPONSE OF COMMERCIAL JET AIRCRAFT INCLUDING EFFECTS OF AUTOPILOT OPERATION

By Joseph H. Goldberg

Villanova University

SUMMARY

This paper presents a simplified theory of the vertical c.g. acceleration gust response of aircraft. The development is based on a three-degree of freedom model including pitch, vertical displacement, and longitudinal control deflection resulting from the autopilot pitch and vertical displacement feedbacks. Higher-order autopilot transfer functions are utilized to provide the necessary accuracy in the prediction of gust response characteristics such as the gust response parameters relating gust input to acceleration, the acceleration zero-level crossing number, and power spectral density properties. The method is applied to four representative commercial jet aircraft for a broad range of operating conditions and a comparison of all gust response characteristics is made. It is shown that autopilot operation relative to the controls - fixed case causes response attenuation of from 10 percent to approximately 25 percent depending on flight condition and increases in crossing number up to 30 percent, with variations between aircraft of from 5 percent to 10 percent, in general, which reflect the differences in autopilot design. A computer program description and listing of the calculation procedure suitable for the general application of the theory to any airplane - autopilot

N82-28266 #

combination is presented.

INTRODUCTION

Considerable effort, by industry and government agencies, has been devoted to the gust response problem beginning with the first NACA report. Currently the Safety and Operating Problems Branch at NASA Langley is engaged in an extensive study of digital flight recorder data from commercial jet operations. Central to this effort is the analysis of vertical c.g. acceleration records for the purpose of isolating the gust velocity input. A two-degree-of-freedom theory, unique in approach (ref. 1), was employed for the reduction and analysis of these data. (Additional important work is contained in references 2 through 9.) It was found (ref. 10) that a three-degree-of-freedom theory was required to account accurately for the influence of autopilot operation on the airplane gust response.

The study was undertaken for the purpose of extending the theory of reference 1 to include the longitudinal control autopilot; and to develop working methods for the prediction of gust response characteristics such as the gust response parameter A_σ, zero-crossing number N_0, and the power spectral density PSD, for various modes of autopilot operation. Four representative commercial jet designs were investigated over a wide range of flight conditions, loadings, and autopilot operating modes. The autopilots were modeled in a high-order linearized version to produce complex interactions with the airframe dynamics if present. The theoretical development included elastic airframe aerodynamics including compressibility effects over the

frequency range of interest. A computer program (appendix) was developed specifically for this purpose and structured for efficient calculation of the gust response parameters for each design, with varying aerodynamic and autopilot inputs corresponding to different combinations of gross weight, Mach number, altitude, and autopilot mode.

SYMBOLS

a wing lift-curve slope, rad^{-1}, based on wing area and wing local flow direction; real number coefficient in the airplane y transfer function

$\bar{a}$ imaginary number coefficient in the airplane y transfer function

a_0 complete airplane lift-curve slope, rad^{-1}, based on wing area and wing local flow direction

a_t horizontal tail lift-curve slope, rad^{-1}, based on horizontal tail area and tail local flow direction

A real number coefficient in the autopilot transfer function; subscripts indicate independent variable

A_σ ratio of normal acceleration increment to continuous gust velocity, g units/m/s (g units/fps)

A_w wing geometric aspect ratio

A_t tail geometric aspect ratio

A/P autopilot

APF autopilot factor, for A_σ or N_0

b real number coefficient in the airplane y transfer function

$\bar{b}$ imaginary number coefficient in the airplane y transfer function

B	imaginary number coefficient in the autopilot transfer function; subscripts indicate independent variable
c	real number coefficient in the airplane y transfer function
$\bar{c}$	imaginary number coefficient in the airplane y transfer function
c	wing mean geometric chord, m (ft)
c_t	horizontal tail mean geometric chord, m (ft)
e	effective wing moment arm, or distance from wing lift aerodynamic center to c.g. as required for S.M. simulation, positive forward of c.g., m (ft)
e_t	horizontal tail distance from tail aerodynamic center to c.g., positive aft of c.g., m (ft)
f	frequency, Hz
f_1	generalized airplane transfer function
f_c	upper integration limit, Hz
$F_\delta = \partial\alpha_t/\partial\delta$	
$F_{\dot{\delta}}$	tail $\partial\alpha_t/\partial\dot{\delta}$ factor
g	acceleration due to gravity, 9.81m/sec^2 (32.2 ft/sec^2)
hp	pressure altitude, m (ft)
i	imaginary number, $\sqrt{-1}$
k	nondimensional gust frequency, $\omega c/2V$
k_c	nondimensional upper integration limit, $\pi cf_c/V$
k_0	nondimensional acceleration zero-level crossing number, $\pi cN_0/V$
k	pitch radius of gyration, m (ft)
K	modified gust alleviation factor, based on σ_1 rather than σ_w

K'	K integral weighted by k^2, Kk_0
K_M	compressibility correction factors for $A\sigma$, single or double primed
L	Von Karman tubulence scale m (ft)
L_1	total wing lift, at c/4, N (lbf)
L_2	total horizontal tail lift, at $c_t/4$, N (lbf)
m	airplane total mass, kg (slugs)
M	Mach number
n	normal, i.e. vertical acceleration, g units
Δn	normal acceleration increment, n-1, g units
N_0	number of positive slope zero-level crossings of normal acceleration increment per second
PSD	power spectral density
r_0	wing lift slope ratio, a/a_0
r_1	weighted horizontal tail lift slope ratio, $S_t a_t/Sa_0$
r_2	horizontal tail nondimensional downwash point distance, $2e_t/c + c_t/c + \eta(2e/c-1)$
rms	root mean square
s	Laplace complex variable, $i\omega$
s_1	nondimensional w_1 distance from w_2, $2e/c-1 + 2e_t/c + c_t/c$
S	wing area, m^2 (ft^2)
S.M.	airplane controls - fixed static margin, fraction of c
S_t	horizontal tail area, m^2 (ft^2)
u	input gust velocity amplitude, positive up, m/s (ft/sec)
$U\sigma$	continuous gust velocity, m/s (ft/sec)
V	true airspeed, m/s (ft/sec)

w_1 wing downwash, at $3c/4$, positive up, m/s (ft/sec)

w_2 horizontal tail downwash, at $3c_t/4$, positive up, m/s (ft/sec)

y vertical displacement (inertial frame) of the c.g., m (ft)

y_1 vertical displacement of wing downwash point, m (ft)

y_2 vertical displacement of tail downwash point, m (ft)

α wing angle of attack, measured from local flow direction to zero lift line, rad

α_t tail angle of attack, measured from local flow direction to zero lift line, rad

β Glauret compressibility factor, $\sqrt{1-M^2}$

δ longitudinal control deflection, positive trailing edge down, rad

ε gust penetration time, sec

η tail downwash derivative, $\partial\varepsilon/\partial\alpha$, where ε is the downwash angle

μ mass ratio parameter, $2m/a_0\rho Sc$

ρ ambient air density, kg/m^3 (slugs/ft^3)

$\sigma_{\Delta n}$ rms acceleration, g units

σ_w rms gust velocity, m/s (ft/sec)

σ_1 rms modified gust velocity, $\sigma_w / \pi(2L/c)^2$, m/s (ft/sec)

ϕ airplane pitch angle, corresponds to wing angle of attack, rad

ϕ_w gust PSD, m^2/s^2/Hz (ft^2/sec^2/Hz)

$\phi_{\Delta n}$ acceleration PSD, (g units)^2/Hz

ω gust input frequency, rad/sec

EQUATIONS OF MOTION

The equations of motion are for a two-degree of freedom body with longitudinal control (elevator or full stabilizer motion as the primary control). A model based on two simplified lifting surfaces for the wing and horizontal tail is adopted. The analysis includes first order nonsteady lift effects, overall corrections for compressibility, first order corrections for gust penetration and gust lag effects on the tail relative to the wing. Since the primary frequency range of interest is low, downwash effects are included on the basis of a quasi-steady state condition. Static aeroelastic effects are considered by using aerodynamic characteristics at the equilibrium condition for the elastic airframe.

The equations of motion, provided by the author of reference 1, are extended herein to include an autopilot actuated control surface with autopilot modeling in a high-order version. The equation development follows that of reference 1 but is simplified by the use of a quasi-steady nonsteady lift assumption. Downwash expressions are given in terms of the three-degrees of freedom obtained when including control deflections. Solutions for vertical acceleration at the c.g. are developed in a closedform for the sinusoidal vertical gust input of unit magnitude. From these frequency response functions, spectral results are derived.

Referring to figure 1, the vertical displacements at wing and tail downwash control points are seen to be given by

$$y_1 = y + (e - \frac{c}{2})\phi$$

$$y_2 = y - (e_t + \frac{c_t}{2})\phi$$

The lift forces are

$$L_1 = \frac{a}{2} \rho S V w_1$$

$$L_2 = \frac{a_t}{2} \rho S_t V w_2$$

where the wing downwash is

$$w_1 = V\phi - \dot{y}_1 + u$$

and the tail downwash is

$$w_2 = V(\phi + F_\delta \delta) - \dot{y}_2 + F_\delta^{\cdot} \frac{c_t}{2} \dot{\delta} + (u)_{t-\varepsilon} - \eta w_1$$

In this last expression the factor F_δ is equivalent to the elevator or control lift effectiveness, i.e., $\partial \alpha_t / \partial \delta$ (unity for an all-moveable surface), and $F_\delta^{\cdot}$ is taken to be zero for elevator control and unity for an all-moveable primary control surface. Lift curve slopes for the wing and tail, a and a_t, are for the isolated components based on their individual areas and are the actual three-dimensional quantities at the equilibrium operating condition as required for this approach. The vertical gust input is u at the wing downwash point and is delayed by ε time when reaching the tail. A major effect, the steady state wing downwash velocity at the tail control point is given in terms of η denoting the familiar $\partial \varepsilon / \partial \alpha$ where ε is the downwash angle.

Taking the time derivatives of y_1 and y_2 and making substitutions leads to

$$w_1 = V\phi - \dot{y} - (e - \frac{c}{2}) \dot{\phi} + u$$

$$w_2 = V(\phi + F_\delta \delta) - \dot{y} + (e_t - \frac{c_t}{2}) \dot{\phi} + F_\delta^{\cdot} \frac{c_t}{2} \dot{\delta} + (u)_{t-\varepsilon}$$
$$-\eta \left[V\phi - \dot{y} - (e - \frac{c}{2}) \dot{\phi} + u \right]$$

Now the vertical force and pitching moment equations are developed. The vertical force is given by

$$m\ddot{y} = L_1 + L_2 = \frac{a}{2}\rho SVw_1 + \frac{a_t}{2}\rho S_t V w_2$$

The pitching moment equation for the complete configuration (including fuselage and mutual interference effects) can be expressed in terms of wing and tail by making the wing lift moment arm, e, that required to duplicate the moment characteristics of the overall configuration. The moment equation is then

$$mk^2\ddot{\phi} = eL_1 - e_tL_2$$

$$= e\frac{a}{2}\rho SVw_1 - e_t\frac{a_t}{2}\rho S_t V w_2$$

Nondimensionalizing the force and moment equation results in

$$\frac{2m}{a_0 \rho SV^2}\ddot{y} = \frac{a}{a_0}\frac{w_1}{V} + \frac{a_t}{a_0}\frac{S_t}{S}\frac{w_2}{V}$$

where a_0 is the complete airplane lift curve slope.

$$\frac{2mk^2}{a_0\rho SV^2 c}\ddot{\phi} = \frac{e}{c}\frac{a}{a_0}\frac{w_1}{V} - \frac{e_t}{c}\frac{a_t}{a_0}\frac{S_t}{S}\frac{w_2}{V}$$

Also, $\frac{2m}{a_0\rho SV^2} = \mu\left(\frac{c}{V^2}\right)$

where μ, the mass ratio parameter, is

$$\mu = \frac{2m}{a_0\rho Sc}$$

Thus,

$$\frac{2mk^2}{a_0\rho SV^2 c} = \mu\frac{k^2}{V^2}$$

The final simplified forms for the force, moment, wing downwash, and tail downwash in terms of the five variables considered at this stage are now derived. Here the equations are written in

the frequency rather than time domain. Thus the input variable u represents the amplitude of a sinusoidal vertical gust of frequency ω. Also to be noted is that the output or frequency response of interest is the vertical displacement y. (The lowest order in y in the preceeding is $\dot{y}$, and the magnitude of the vertical acceleration frequency response is $\omega|\dot{y}|$; but the control law for δ will be defined in terms of y and ϕ.) The four equations are

$$(\mu \frac{c}{V} \omega^2)\frac{y}{V} + (r_0)\frac{w_1}{V} + (r_1)\frac{w_2}{V} = 0 \qquad (1)$$

$$(\mu \frac{k^2}{V^2}\omega^2)\phi + (\frac{e}{c}r_0)\frac{w_1}{V} - (\frac{e_t}{c}r_1)\frac{w_2}{V} = 0 \qquad (2)$$

$$\frac{i\omega}{V}y + \left[(e-\frac{c}{2})\frac{i\omega}{V} - 1\right]\phi + \frac{w_1}{V} = \frac{u}{V} \qquad (3)$$

$$(1-\eta)\frac{i\omega}{V}y - \left\{(1-\eta) + \left[e_t + \frac{c_t}{2} + \eta(e-\frac{c}{2})\right]\frac{i\omega}{V}\right\}\phi$$

$$- (F_\delta + F_{\dot{\delta}}\frac{c_t}{2}\frac{i\omega}{V})\delta + \frac{w_2}{V} = (e^{-i\varepsilon\omega} - \eta)\frac{u}{V} \qquad (4)$$

where $r_0 = \frac{a}{a_0}$ and $r_1 = \frac{a_t}{a_0}\frac{S_t}{S}$

Now the forcing frequency is made dimensionless by normalizing on $2V/c$, thus the nondimensional input frequency is $k = \frac{\omega c}{2V}$.

Also the penetration time interval ε is given by

$$\varepsilon = \frac{1}{V}(e-\frac{c}{2}+e_t+\frac{c_t}{2})$$

Then $e^{-i\varepsilon\omega} = e^{-iks_1} = \cos ks_1 - i\sin ks_1$

where $s_1 = (\frac{2V}{c})\varepsilon = \frac{2e}{c} - 1 + \frac{2e_t}{c} + \frac{c_t}{c}$

The four equations now reduce to

$$\left[2\mu k^2(\frac{2V}{c})\right]y + r_0w_1 + r_1w_2 = 0 \qquad (1)$$

$$\left[4\mu\frac{k^2}{c^2}k^2\right]V\phi + \frac{e}{c}r_0w_1 - \frac{e_t}{c}r_1w_2 = 0 \qquad (2)$$

$$\left[k\left(\frac{2V}{c}\right)i\right] y + \left[\left(\frac{2e}{c}-1\right)ki-1\right] V\phi + w_1 = u \qquad (3)$$

$$\left[k(1-\eta)\left(\frac{2V}{c}\right)i\right] y - \left[(1-\eta)+r_2ki\right] V\phi - \left[F_\delta + F_\delta^{\cdot}\frac{c_t}{c}\, ki\right]V\delta$$

$$+ w_2 = \left[(\cos ks_1-\eta)-(\sin ks_1)i\right] u \qquad (4)$$

where $r_2 = \frac{2e_t}{c} + \frac{c_t}{c} + \eta\left(\frac{2e}{c}-1\right)$

The control law (the equation for $V\delta$ in terms of the transfer functions for $V\delta$ due to y and due to $V\phi$) is now developed for introduction into equation (4). It is initially given here in the Laplace variable s, later to be replaced by $i\omega$, or in nondimensional form as $\left(\frac{2V}{c}\right)ki$.

$$V\delta = \left(\frac{V\delta}{y}\right)y + \left(\frac{V\delta}{V\phi}\right)V\phi$$

where the bracketed terms are the two control transfer functions. As used in this study they are the linearized (limiter, dead-zone and hysteresis operations omitted) functions for the individual autopilot designs for each airplane. The general form found applicable to higher-order modeling for all autopilots, as given in terms of the computer program notation (see subroutine CALC in the appendix for the definitions), is

$$V\delta = \frac{DD}{DN}\left[\left(\frac{YN}{YD}\right)y + \left(\frac{PN}{PD}\right)V\phi\right]$$

Introducing the control effectiveness function, we now define the following

$$A_y + B_y i = -\left[F_\delta + \left(F_\delta^{\cdot}\frac{c_t}{c}\, k\right)i\right]\left(\frac{DD}{DN}\right)\left(\frac{YN}{YD}\right)$$

$$A_\phi + B_\phi i = -\left[F_\delta + \left(F_\delta^{\cdot}\frac{c_t}{c}\, k\right)i\right]\left(\frac{DD}{DN}\right)\left(\frac{PN}{PD}\right)$$

Equation (4), with $V\delta$ eliminated, then becomes

$$\left[k(1-\eta)\left(\frac{2V}{c}\right)i + (A_{\bar{y}}+B_y i)\right] y - \left[(1-\eta) + r_2 ki - (A_\phi+B_\phi i)\right] V_\phi + w_2 = \left[(\cos ks_1-\eta) - (\sin ks_1)i\right] u \qquad (4)$$

The preceding set of four equations is readily reduced to a 2x2 matrix by solving (3) for w_1 and (4) for w_2 and substituting in (1) and (2). With u set to unity for a unit gust input amplitude, the y solution is found to be

$$y = \frac{(c_1+\bar{c}_1)(b_2+\bar{b}_2) - (c_2+\bar{c}_2)(b_1+\bar{b}_1)}{(a_1+\bar{a}_1)(b_2+\bar{b}_2) - (a_2+\bar{a}_2)(b_1+\bar{b}_1)}$$

where

$$a_1 + \bar{a}_1 = \{r_1 A_y - 2\mu\left(\frac{2V}{c}\right)k^2\} + \{r_1 B_y + \left(\frac{2V}{c}\right)\left[r_0 + r_1(1-\eta)\right]k\}i$$

$$a_2 + \bar{a}_2 = \{-\frac{e_t}{c} r_1 A_y\} + \{-\frac{e_t}{c} r_1 B_y + \left(\frac{2V}{c}\right)\left[\frac{e}{c} r_0 - \frac{e_t}{c} r_1(1-\eta)\right]k\}i$$

$$b_1 + \bar{b}_1 = \{r_1 A_\phi - \left[r_0 + r_1(1-\eta)\right]\} + \{r_1 B_\phi + \left[r_0\left(\frac{2e}{c}-1\right) - r_1 r_2\right]k\}i$$

$$b_2 + \bar{b}_2 = \{-\frac{e_t}{c} r_1 A_\phi - \left[\frac{e}{c} r_0 - \frac{e_t}{c} r_1(1-\eta) + 4\mu\frac{k^2}{c^2} k^2\right]\} + \{-\frac{e_t}{c} r_1 B_\phi + \left[\frac{e}{c} r_0\left(\frac{2e}{c}-1\right) + \frac{e_t}{c} r_1 r_2\right]k\}i$$

$$c_1 + \bar{c}_1 = \left[r_0 + r_1(\cos ks_1-\eta)\right] - \left[r_1(\sin ks_1)\right] i$$

$$c_2 + \bar{c}_2 = \left[\frac{e}{c} r_0 - \frac{e_t}{c} r_1(\cos ks_1-\eta)\right] + \left[\frac{e_t}{c} r_1(\sin ks_1)\right] i$$

The y solution obtained here is the frequency response complex amplitude for a given input nondimensional k frequency. From this solution all of the gust response characteristics of interest in the study are obtained as described in the following section.

CALCULATION OF GUST RESPONSE CHARACTERISTICS

The vertical velocity frequency response is developed from the vertical displacement with

$$\dot{y} = i\,y = i\omega\left(\frac{2V}{c}\right)ky$$

Expressed in real and imaginary parts,

$$\dot{y} = \dot{y}_r + i\dot{y}_i$$

It should be noted that this quantity is nondimensional since $\dot{y}$ is per unit u, each in distance per time units. The absolute vertical velocity magnitude square (as required for the generalized transfer function below) is then

$$|\dot{y}|^2 = (\dot{y}_r + i\dot{y}_i)\ (\dot{y}_r - i\dot{y}_i)$$

An intermediate nondimensional response quantity termed the generalized airplane transfer function (developed in reference 1) and denoted as f_1, is first determined from

$$f_1 = \frac{4\mu^2 k^2\ |\dot{y}|^2}{\left(1 + \frac{1.5\pi}{\beta^2}\,k + \frac{\pi^2 M k^2}{\beta^2}\right)(1 + 0.55A_w k)}$$

where $\beta^2 = 1-M^2$ and A_w is the wing aspect ratio. In this equation the denominator factors provide the necessary corrections for gust penetration and spanwise gust distribution effects.

The generalized gust response PSD is obtained from the product of the airplane transfer function and the normalized gust input PSD. This gust input PSD is discussed in reference 1, and is given as

$$\frac{\phi_w}{\sigma_1^2} = \frac{\left(\frac{2L}{c}\right)^{5/3}\left[1 + \frac{8}{3}\left(1.339\,\frac{2L}{c}\,k\right)^2\right]}{\left[1 + \left(1.339\,\frac{2L}{c}\,k\right)^2\right]^{11/16}}$$

where the equivalent rms gust σ_1 is related to the actual rms σ_w by

$$\sigma_1^2 = \frac{\sigma_w^2}{\pi \left(\frac{2L}{c}\right)^{2/3}}$$

The turbulence scale L, a fundamental parameter but one having less influence at values of 2L/c in excess of about 100 (ref. 1), is taken as 305 m (1000 ft) throughout this study.

Response spectra are presented as the product of frequency and the PSD (affording an indication of the frequency intervals containing the greatest energy content). This generalized product of frequency and PSD for the acceleration response to gust is designated GFPSD and given as

$$\text{GFPSD} = k\left(f_1 \frac{\phi_w}{\sigma_1^2}\right)$$

Also, this quantity is identical to that contained in reference 1.

The equivalent gust alleviation factor is now found. It is so termed because it is based on σ_1 rather than σ_w. Designated by K it is calculated from the following integral.

$$K = \left[\int_0^{k_c} f_1 \left(\frac{\phi_w}{\sigma_1^2}\right) dk\right]^{\frac{1}{2}}$$

where k_c, the upper limit, is the nondimensional cut-off frequency given as

$$k_c = \frac{\pi f_c}{V/c}$$

Here f_c depends upon the specific airplane, and the value corresponds to that used in the reduction of flight response data in the Langley Digital VGH program. In general it is about five times the airplane's controls

- fixed short period natural frequency. This criterion permits inclusion of all spectral content contributing most significantly to the c.g. acceleration response. It should be noted that these alleviation factors are considerably greater than those based on the actual rms gust σ_w. The alleviation factor is increased by the term

$$\left[\pi \left(\frac{2L}{\bar{c}}\right)^{2/3}\right]^{1/2}$$

which is approximately 8 for the average configuration.

The gust response parameter A_σ relating the incremental load factor to the continuous gust velocity is defined as

$$A_\sigma = \frac{\Delta n}{U_\sigma}$$

and is determined from

$$A_\sigma = \left(\frac{V/c}{g\mu}\right) K$$

The two normalized frequency times PSD quantities of major interest are the frequency PSD products based on rms gust velocity and based on rms acceleration. The first is called the gust normalized frequency times PSD, or GNFPSD, and is obtained from

$$GNFPSD = \left(\frac{V/c}{g\mu}\right)^2 \frac{GFPSD}{\pi \left(\frac{2L}{c}\right)^{2/3}}$$

and can be denoted as

$$GNFPSD = \frac{f\phi\Delta n}{\sigma_w 2} \ , \ \left(\frac{g \text{ units}}{m/s}\right)^2 \left(\left(\frac{g \text{ units}}{ft/sec}\right)^2\right)$$

The second is called the acceleration normalized frequency times PSD, or ANFPSD, and is obtained from

$$ANFPSD = \frac{GFPSD}{K^2}$$

and can be denoted as

$$\text{ANFPSD} = \frac{f\phi_{\Delta n}}{\sigma_{\Delta n}^2} \text{ , nondimensional}$$

The zero level crossing number N_0 is the number of positive slope crossings per second of the zero-acceleration increment time history. It is found from

$$N_0 = \frac{V/c}{\pi} k_0$$

where

$$k_0 = \frac{K'}{K}$$

and

$$K' = \left[\int_0^{k_c} k^2 f_1 \left(\frac{\phi_w}{\sigma_1^2} \right) dk \right]^{1/2}$$

In summary, the theoretical development undertaken so far has shown the dependence of the response quantities of importance, such as A_σ, N_0, GNFPSD and ANFPSD, on the fundamental equation set comprising wing downwash, tail downwash, total lift, and total pitching moment, in conjunction with the autopilot control law. Inputs for the specific configurations to be considered are expressed in generalized and nondimensional form. Autopilot inputs are defined by gains and time constants in linearized transfer functions. These are kept in a higher-order version for the modeling process to retain the effects of all possible airplane-autopilot interactions.

AIRPLANE CHARACTERISTICS

Airplane inputs can be classified in three distinct groups; those constant for all cases for a given design; those that apply to one design only but that vary with flight condition (altitude

and Mach number); and those that are a function of the nondimensional forcing frequency k as well as flight condition for a particular airplane. Common to all configurations and considered constant throughout is the c.g. location at 0.25c and the turbulence scale of 305 m (1000 ft). Also, a standard atmosphere has been assumed. The airplane cut-off frequency f_c varied from 0.75 Hz to 1.50 Hz depending upon the configuration.

The complete airplane lift curve slope a_0 is used in combination with the wing aspect ratio, tail area ratio, tail aspect ratio and downwash derivative to calculate the isolated component wing and tail lift curve slopes. The two equations so employed are

$$a_0 = a + a_t \frac{S_t}{S}(1-\eta)$$

$$a_t = \frac{a}{1 + \frac{a}{0.9\pi}\left(\frac{1}{A_t} - \frac{1}{A_w}\right)}$$

In this manner, consistency is maintained between all three slopes, which, of course, figure independently in the analysis. Also, the wing and tail contributions to the complete configuration static longitudinal stability is used to determine the effective wing lift arm e from the following equation

$$\frac{e}{c} = \frac{a_t}{a}\frac{S_t}{S}(1-\eta)\frac{e_t}{c} - \frac{a_0}{a}(S.M.)$$

where S.M. is the controls-fixed static margin, in fraction of chord, for the specific airplane and flight condition. The controls-fixed short period mode natural frequency is found, in nondimensional form, from

$$k_{SP} = \frac{\omega_{sp}}{(2V/c)} = \frac{1}{2\mu(k/c)} \left[1.2 \left(\frac{a_t}{a_0}\right) \left(\frac{S_t}{S}\right) \left(\frac{e_t}{c}\right)^2 + \mu (S.M.) \right]^{\frac{1}{2}}$$

In the preceding, a_0, η and S.M. are considered to vary with flight condition and are taken at the corresponding altitude and Mach number for the elastic airframe.

Flight conditions for a given airplane are defined by pressure altitude, Mach number and gross weight. For each design a number of altitude and M combinations (varying from 7 to 14 depending on the individual case) were selected based on complete (take-off to maximum cruise to landing) flight profiles for each. Additionally, 3 gross weights were chosen for each condition as that corresponding to minimum, average, and maximum operational values. This approach lead to an excessively broad range of μ values for the analysis when considering the more restrictive conditions for autopilot operation but it was thought to be advantageous for correlation purposes.

A range of altitudes and Mach numbers was specified in order to identify three distinct operating conditions which would be applicable to all four airplanes. These are termed and defined as: Climb/Descent, M from 0.50 to 0.58, altitude from 3,050 m (10,000 ft) to 6,100 m (20,000 ft); Low Cruise, M from 0.80 to 0.81, altitude from 8,530 m (28,000 ft) to 9,140 m (30,000 ft); High Cruise, M from 0.84 to 0.89, altitude from 9,750 m (32,000 ft) to 12,220 m (40,000 ft). Table 1 presents the nondimensional geometric and aerodynamic parameters required for each airplane in the study. Noted are the nonvarying quantities S_t/S, c_t/c, e_t/c and k/c. At each general condition, the nondimensional wing and

tail slopes, a/a_0 and a_t/a_0, are given as well as the tail lift effectiveness r_1. Also included is the nondimensional effective wing moment arm e/c as required to simulate the overall static stability. Lastly, the nondimensional cut-off frequency kc, as defined in the integral limits, is given.

The autopilot modes of operation considered for the study are those which are appropriate to each design for climb, cruise, turbulent setting in cruise, and descent. It was found that all of these incorporated pitch-hold (with altitude-hold in cruise) with gains and signal shaping or filtering as required. Climb and descent involved altitude-rate as well in some cases, and two had provision for reduced gains in the turbulent setting. Three standard autopilot modes are then adopted and designated as: a combined climb and descent condition (Climb/Descent); basic cruise with pitch and altitude-hold (Cruise); and cruise with reduced gains excluding altitude hold (Turbulent). The autopilot-alone characteristics for each of the airplanes is illustrated in frequency plots for each autopilot. These have been evaluated as the log magnitude of the effective change in tail angle of attack (due to control deflection) with pitch angle and with vertical displacement, and are given by

$$\left|\frac{\alpha_t(k)}{\phi(k)}\right| = 20 \log_{10} |A_\phi + B_\phi i|$$

and

$$\left|\frac{\alpha_t(k)}{y(k)}\right| = 20 \log_{10} |A_y + B_y i|$$

where the A and B coefficients are as previously defined. It

should be noted that these quantities are not referenced to zero-frequency levels, hence they are not amplitude ratios in the usual sense. To permit a more general comparison of the individual autopilots, including the importance of static loop gains, they are so defined, as well as by including the aerodynamic control effectiveness. The frequency response results are presented in figure 2 as a function of nondimensional frequency (ratio of forcing frequency to the short period frequency) for the Low Cruise flight condition in the Cruise autopilot mode.

The frequency responses shown for each autopilot transfer function (pitch feedback and altitude feedback) provide a means of evaluating basic autopilot differences. Immediately evident is the fairly close correspondence between all pitch channels in the frequency band spanning the short period natural frequency. Larger differences are noted between the altitude channel frequency responses, but in general these are only secondary to the pitch frequency responses. It should be appreciated that only the combination of airframe and autopilot can determine the particular airplane gust characterization.

GUST RESPONSE PARAMETER A_σ

Initial studies were made of the A_σ parameter as a function of the principal operational variables. It was determined that regression functions were obtainable with about 1 percent average error when the independent variables were V/c, M and μ. Data correlations for each airplane were performed using equations of the form

$$\frac{gA_\sigma}{K_M(V/c)} = \frac{C_1}{\mu^n}$$

where the compressibility correction K_M is closely fitted with

$$K_M = \frac{C_2}{1 + \frac{C_3}{\beta^2}}$$

and C_1, C_2, and C_3 and n are constant for a particular design and autopilot mode combination. Significant here is the fact that these apply over the broad spectrum of flight encompassing take-off, climb, cruise, descent and landing at all gross weights; and also that the method is applicable to each of four autopilot modes. The procedure used was to generate first these regression functions for each autopilot mode and then derive an average compressibility correction factor for all airplanes at a given mode. The results so determined are presented as a function of μ in figures 3 through 6, in which the average compressibility correction is denoted as K_M'. Examination of the results here exhibit a close correspondence of the A_σ parameter for the different designs, with the exception of the low μ region in the Cruise mode. Since this is the one autopilot mode whose design would likely be optomized for cruise altitudes of 7,620 m (25,000 ft) or higher, autopilot effects at μ near landing may differ significantly.

Figure 3 for the fixed-control case can't be compared directly to the data in figures 4 through 6 for a direct indication of A_σ attenuation by the autopilots since each has a different K_M' function. However, the attenuation effects are quantitatively perceived when an autopilot factor APF is defined, as the ratio of

A_σ with A/P on to that with A/P off. The APF, denoted A_σ APF, is determined by the ratio of the ordinate value in either figure 4, 5 or 6 to the ordinate in figure 3 at the same μ. This approach results in the determination of the parameter

$$\frac{A_\sigma \text{ APF}}{K_M''} = f(\mu)$$

and the ratio of compressibility factors, denoted K_M'', is in general of the form

$$K_M'' = \frac{C_4 - C_5 M^2}{C_6 - M^2}$$

where C_4, C_5 and C_6 are additional constants for a given autopilot mode. The APF normalized now by the K_M'' compressibility factors are presented in figures 7, 8 and 9. Here the APF is shown in two different representations - the APF for any M and the APF for the specific M appropriate to that autopilot mode. The curves indicate that attenuation of gust response, increasing with μ, is achieved throughout except for one airplane at the extreme low end of the μ range in the A/P Cruise mode. Additionally, it is evident that a general consistency of trends exists for the APF parameter of the different designs considering the distinctive nature of the autopilot frequency responses as previously shown.

In summary, over the operative μ range for each aircraft, A_σ reductions due to autopilot and as a function of μ are: between 4 percent and 30 percent in the Climb/Descent mode; between -13 percent and 36 percent in the Cruise mode; and between 9 percent and 31 percent in the Turbulent mode (based on two of the four

aircraft).

ZERO-LEVEL CROSSING NUMBER N_0

An initial investigation of all N_0 results was conducted in order to establish the basic dependencies of N_0 on the operational variables, as was done for $A\sigma$. It was found from regression analysis that V/c and μ (M omitted) were the governing quantities but in a more complex manner than for the $A\sigma$ parameter. These fitting functions, semi-logarithmic in V/c and μ, were employed to generate curves of N_0 versus μ at selected V/c values for each of the A/P modes. N_0 results at V/c of 20 sec^{-1}, 30 sec^{-1}, and 40 sec^{-1} are presented in figures 10, 11 and 12 with the A/P off. These V/c magnitudes span the operating range from climb to high Mach number cruise conditions. It is seen that N_0 increases with V/c and decreases with μ, with an overall N_0 variation of from 0.2 to 0.6 crossings per sec. The variation of the N_0 level among airplane designs for a given condition is greater than it was in the case of $A\sigma$, as might be expected on the basis of the two-parameter (V/c and μ) versus three-parameter (V/c, M and μ) correlation.

With regard to the autopilot effect on N_0, again an APF is employed representing the ratio of N_0 with A/P on to that for A/P off (denoted N_0 APF) at the same conditions of V/c, μ and A/P mode. These factors however were not obtained from generalized N_0 values with A/P on (as with $A\sigma$) but rather were derived by a regression analysis of APF directly from the computer output. This procedure proved to be more convenient considering the added complexity of the N_0 fitting functions. Results so derived are

shown in figures 13 through 18. The Climb/Descent A/P mode factors are given in figures 13 and 14 for V/c of 20 sec^{-1} and 30 sec^{-1}, respectively. Except for one airplane in a limited low μ region, N_0 APF exceeds unity, as expected, with N_0 increases indicated of 10 percent to 32 percent depending on airplane configuration, μ, and V/c. An increase in APF with μ is evident, and the V/c effect is not well defined but is generally limited to only a few percent at a given μ. In the Cruise A/P mode results are presented for V/c levels of 30 sec^{-1} and 40 sec^{-1} in figures 15 and 16, respectively. In this autopilot mode wider variations in N_0 APF are shown with N_0 increases of from zero to 37 percent, again becoming greater with μ and, in general, with V/c. The Turbulent mode results are given in figures 17 and 18 at the same V/c values as for Cruise, for two of the aircraft. Again the same trends are illustrated with higher APF values compared to Cruise.

SPECTRAL RESPONSE RESULTS

Power spectral characteristics form the basis for the gust response parameters dealt with up to now, such as the A_σ and N_0 quantities. To gain better understanding of gust response these characteristics are now examined in some detail.

Power spectral density results are summarized in two generalized versions in figures 19 through 34 for the three representative flight conditions (Climb/Descent, Low Cruise, High Cruise) previously discussed. The basic spectral quantity studied is the product of frequency, in Hz, and the acceleration power spectral density, in g units squared/Herz. In figures 19 through 26, this

parameter is shown, in the first version, normalized by the square of rms gust velocity, in m^2/sec^2 (ft^2/sec^2). The abscissa scale in all of the figures is the nondimensional frequency k divided by k for the short period mode frequency as calculated using the previously given equation. Thus the scale is k/k_{SP}, or alternatively ω/ω_{SP}. This course of action was adopted because the peak response occurs at the short period natural frequency with A/P off, and thus provides a basic reference for comparison of the power spectral characteristics of the different airplanes.

It is seen in figures 19, 21, and 24 for the controls-fixed case that when based on the short period frequencies (which individually do vary, as noted on the figures, by as much as 87 percent) a very close correspondence among peak frequencies is achieved. Peak amplitudes differ considerably, and reflect the differences in airplane transfer function, f_1. Now focusing attention on the autopilot effect as seen in a comparison of figures 20, 22 and 25 with the preceding ones, what is evident is first, the marked gust alleviation achieved in all cases and second, the introduction of multiple response modes at frequencies both below and above the controls-fixed short period frequency. The lower coupled mode is fairly flat and wide in character; while the higher one (at the A/P on short period frequency of about 2.5 times the controls fixed frequency) is sharp and accentuated for two of the four airplanes. These high peaks in the spectra can indicate tendencies towards resonant-like responses if gust inputs at these frequencies are predominant. The major effect of the Turbulent mode (figures

23 and 26) - at least as seen for two of the four designs - is the reduction of sharp peaks when present for the standard A/P settings.

A similar set of spectral responses is given in figures 27 through 34 in which the ordinate scale is the acceleration-normalized frequency times PSD. This presentation is most convenient for use in correlation of flight recorder data since for each spectral record obtained a measure of $\sigma_{\Delta n}{}^2$ is also obtained. It should be noted that there is no difference in curve shape versus frequency for a given airplane in this set as compared to the former set. However, the magnitudes of the individual airplane distributions relative to each other are altered. Lastly, the results for the ANFPSD distributions have been correlated with those obtained from flight records for one of the designs. In all essential features the comparison proved to be satisfactory.

CONCLUDING REMARKS

A simplified approach to the study of aircraft gust response allows sufficient accuracy for the prediction of vertical c.g. acceleration for the frequency bands having the major energy content. In commercial jet operations, where autopilot operation is in common use, it is necessary to include the autopilot control degree of freedom for adequate precision of the gust response analysis.

Autopilot designs follow common trends but individual differences in automatic control performance, as seen in a frequency analysis, do produce significant differences in the gust response characteristics. As used in the four study cases, the pitch-hold

mode of the autopilot is of principal importance as compared to operation in the altitude-hold and turbulent modes.

Autopilot effects were such that the gust response parameter relating normal acceleration to gust velocity input was reduced from 10 to 25 percent depending on the aircraft operating condition. The number of zero-level acceleration crossings was increased up to 30 percent. Individual aircraft exhibited differences of from 5 percent to 10 percent, in general, for each of these response parameters at the same condition.

A computer program developed in the study is presented for the calculation of gust response characteristics of commercial jets with autopilots which are modeled in high order versions. Low order simplifications were found to result in significant error in the calculation of the response parameters.

APPENDIX

Computer Program

Donald E. Hawk, Jr
Villanova University

The appendix contains a complete presentation of the computer program used in the gust response study; the detail given here will facilitate reader usage. A particular effort in the development of the program was made to achieve minimum computation time for the complex operations involving high-order autopilot simulation, as well as to afford generality for application to a wide variety of autopilot designs.

The appendix is arranged in terms of the program major elements; each beginning with the definitions of all computer names, followed by a description of the program element, and ending with a flow chart for that portion of the program. The complete program is also given. Following is a flow diagram of the overall computer program.

Complete Program Flow Diagram

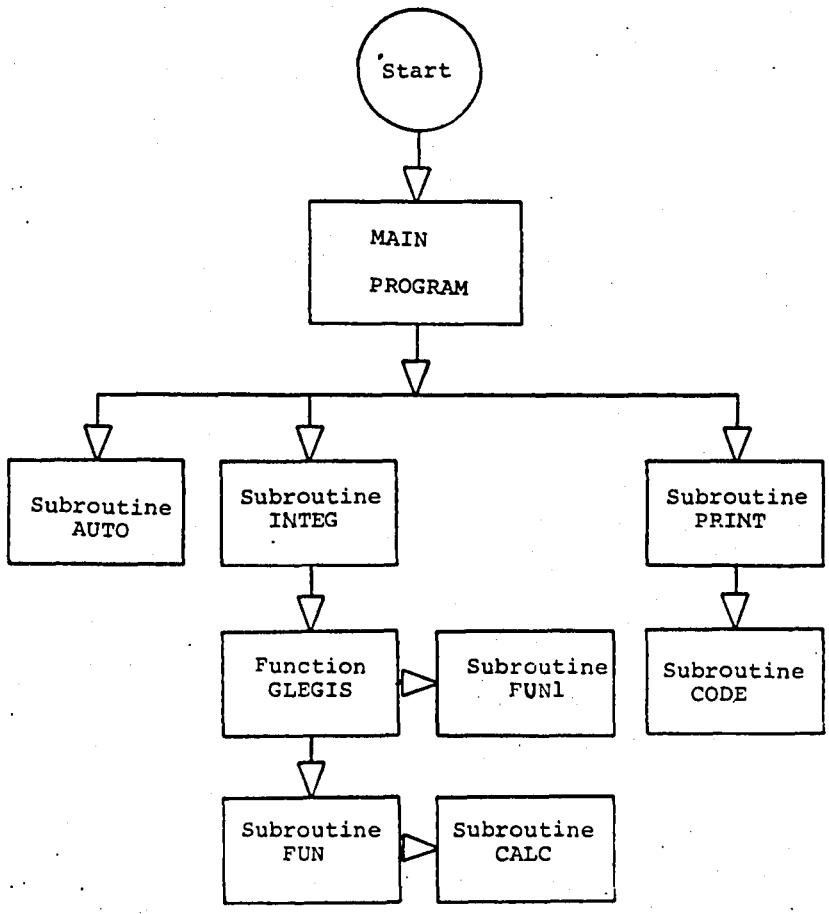

Main Program Definitions

NAPMAX	number of highest autopilot mode plus one
NOAPM	omitted autopilot mode
NFCMAX	number of flight conditions
LALT1 to 4	lowest flight condition number for a given autopilot mode
NALT1 to 4	highest flight condition number for a given autopilot mode
C	c, wing geometric chord, m (ft)
CT	c_t, geometric chord of horizontal tail, m (ft)
ET	e_t, tail moment arm, m (ft)
KAPPA	k, pitch radius of gyration, m (ft)
S	S, wing area, m^2 (ft^2)
ST	S_t, tail area, m^2 (ft^2)
AW	A_w, wing aspect ratio
AT	A_t, horizontal tail aspect ratio
L	L, turbulence scale, m (ft)
FC	f_c, cut-off frequency, Hz
FDLDT	$F_{\dot{\delta}}$, control rate effectiveness
PI	$\pi = 3.14159$
KAX(I)	k, reduced frequency (array)
HX(I)	H, altitude, 305m (1000 ft) (array)
XM(I)	M, Mach number (array)
RHOX(I)	ρ, air density, kg/m^3 ($slugs/ft^3$) (array)
AOX(I)	a_0, airplane lift curve slope, rad^{-1} (array)

VSX(I)	V_s, sonic speed, m/sec (ft/sec) (array)
ETAX(I)	$\eta = (\partial\varepsilon/\partial\alpha)$, tail downwash derivative (array)
FDELX(I)	$F_\delta = (\partial\alpha_t/\partial\delta)_t$, elevator effectiveness (array)
EX(I)	e, wing lift arm, m (ft) (array)
K1(I)	K1, A/P gain,function of flight condition (array)
K2(I)	K2, A/P gain,function of flight condition (array)
K4(I)	K4, A/P gain,function of flight condition (array)
KY(I)	K_y, A/P gain,function of flight condition (array)
AO	A_0, airplane lift curve slope, rad^{-1}
ETA	$\eta = (\partial\varepsilon/\partial\alpha)$, tail downwash derivative
PRI	prime, parameter of A' and B'
APRI	A', wing lift curve slope parameter
BPRI	B', wing lift curve slope parameter
SMLA	a, wing lift curve slope, rad^{-1}
SMLAT	a_t, horizontal tail lift curve slope, rad^{-1}
SM	S.M., static margin, percent mean geometric chord
MPA	A/P mode number plus one
APM	A/P mode
WX(1)	airplane weight A, 4448N (1000 lbf)
WX(2)	airplane weight B, 4448N (1000 lbf)
WX(3)	airplane weight C, 4448N (1000 lbf)
IP	print-out page number
JP	causes pages number to be printed
NFC	number of flight condition (used in do-loop)
M	M, Mach number of specific flight condition
H	H, altitude of specific flight condition 305m (1000 ft)

RHO	ρ, air density of specific flight condition, kg/m^3 (slugs/ft^3)
VS	V_S, sonic speed of specific flight condition, m/s (ft/s)
E	e, wing lift arm of specific flight condition, m (ft)
FDEL	F_δ, elevator effectiveness for given flight condition
V	V, true airspeed, m/s (ft/s)
VC	V/c, ratio of airspeed to wing chord, sec^{-1}
TVC	$2V/c$, sec^{-1}
RO	r_0, lift curve slope ratio
R1	r_1, weighted lift curve slope ratio
CO1	e_t/c, tail moment arm to wing chord ratio
CO2	c_t/c, tail chord to wing chord ratio
CO3	e/c, wing lift arm to wing chord ratio
GK1	A/P gain for given flight condition
GK2	A/P gain for given flight condition
GK4	A/P gain for given flight condition
GKY	A/P gain for given flight condition
R2	r_2, horizontal tail arm parameter
S1	s_1, horizontal tail distance parameter
NWT	number of the selected weight (used in do-loop)
W	W, weight of specific case, 4448N (1000lbf)
MU	μ, mass parameter
GK3	A/P gain for given autopilot mode
GKPHI	A/P gain for given autopilot mode

NDIV number of divisions to be integrated

Main Program Description

The main program performs two tasks - one, the reading of all geometric and flight condition dependent data; two, the calculation of variables which do not change with k, but do vary with flight condition, weight and autopilot mode.

The first read statement defines the autopilot modes to be used, the number of flight conditions, and the combination of the two for which a case should be run. The statement and an example of input are as follows:

```
READ(5,1)NAPMAX,NOAPM,NFCMAX,LALT1,NALT1,LALT2,NALT2, LALT3, NALT3,
LALT4,NALT4
1  FORMAT(11I3)
Col.- 3 6 9 12 15 18 21 24 27 30 33
      5 3 7  1  4  4  7  0  0  2  5
```

This would indicate that: there are 5 autopilot modes APM=0,1,2,3, 4 (col.3); that autopilot mode 3 is to be omitted (col.6); there are 7 flight conditions (col.9); that APM=1 is to be used for flight conditions 1 thru 4 (col.12,15), APM=2 for flight conditions 4 thru 7 (col.18,21), and APM=4 for flight conditions 2 thru 5 (col.30,33).

The next read statement inputs the geometric constants for the airplane. The statement and example of input are as follows:

```
READ(5,5)C,CT,ET,KAPPA,S,ST,AW,L,FC,FDLDT
5  FORMAT(11f6.0)
```

```
Col.- 1    6      12      18      24      30      36      42      48
      24.65 20.10  60.00  38.50  3648.  1338.  7.500  3.790  1000
      54     60        66
        1.200     0.000
```

These geometric quantities are then written out by the program in a series of write statements.

The program then calculates and stores the k's (KAX(I)) to be used in the detailed print-out. These can be altered by changing the do loops and the amount k is indexed.

The next read statement inputs the specific flight conditions parameters such as altitude, Mach number, airplane lift curve slope, etc. The following is an example of the statement and typical input.

```
READ(5,300)HX(I),XM(I),RHOX(I),AOX(I),VSX(I),ETAX(I),FDELX(I),EX(I)
300  FORMAT(8F8.0)
Col.- 1  8   16        24     32      40     48     56     64
      10. .43  .001755  4.96  1078.  .487  .580  4.17
```

Next, the gains K1, K2, K4, Ky which can vary with flight condition are read in. The statement and example of input follows;

```
READ(5,310)K1(I),K2(I),K4(I),KY(I)
310  FORMAT(4F10.0)
Col.- 1    10     20     30     40
      .379  1.00  1.00  .646
```

The quantities that vary with flight condition are then printed - that is, the previous two read statement quantities and the static margin.

The subroutine AUTO is then called-for each autopilot mode. Subroutine AUTO reads all the quantities that vary with autopilot mode and writes them out.

The next read statement is for inputing the weights, WX(1), WX(2),WX(3) in 4448N (1000 lbf) which corresponds to weights A, B, and C respectively. The statement and examples of input follows:

```
READ(5,420)WX(1),WX(2),WX(3)
420  FORMAT(3F5.0)
Col.- 1  5    10    15
       260 400.  555.
```

These weights are then printed out by a write statement

All required inputs have been read into the program at this point. Three nested do loops are then used to increment through the cases to be run. The outer do loop is for the indexing of flight conditions from 1 to NFCMAX. Between this do statement and the next are the quantities which vary by flight condition only. These quantities are either defined or calculated. The next do loop indexes the weight of the aircraft from 1 to 3, or A to C in other words. The quantity μ is calculated at this point. The inner-most do loop indexes the autopilot modes. Within this do loop the gains that vary with autopilot mode are defined. A series of if statements are then used to decide whether this case is to be run. This is accomplished by the use of the quantities LALT1 thru 4 and NALT1 thru 4 in the if statements. The subroutine INTEG is then called (if this case is to be run) and the required quantities calculated. These quantities are then written by the subroutine

PRINT. The program stops after all do loops have completed indexing the cases.

Main Program Flow Diagram

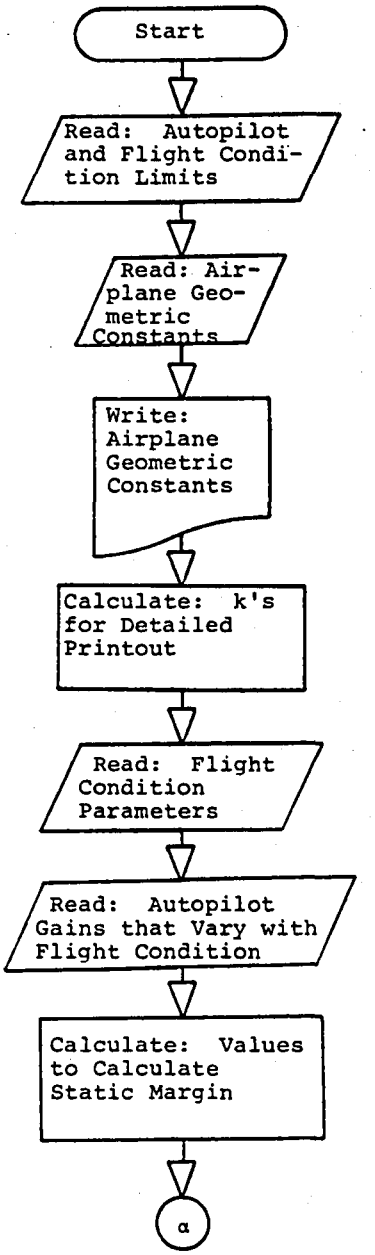

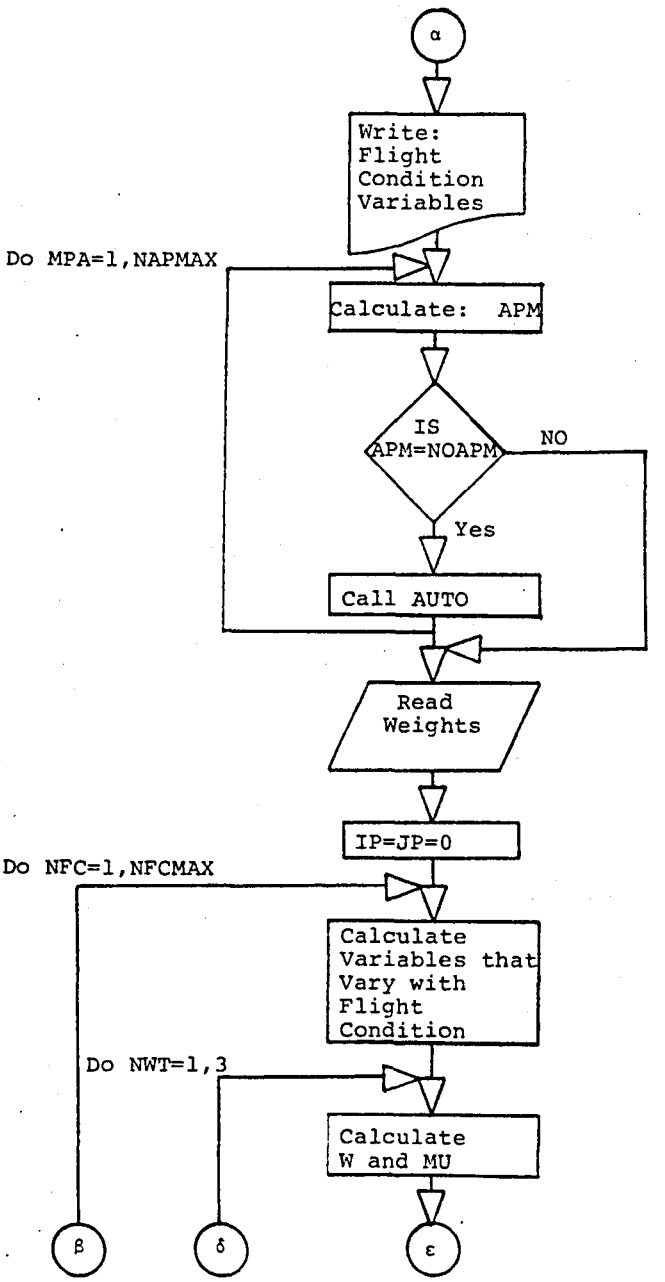
α
Write:
Flight
Condition
Variables
Do MPA=1,NAPMAX
Calculate: APM
IS
APM=NOAPM
NO
Yes
Call AUTO
Read
Weights
IP=JP=0
Do NFC=1,NFCMAX
Calculate
Variables that
Vary with
Flight
Condition
Do NWT=1,3
Calculate
W and MU
β
δ
ε

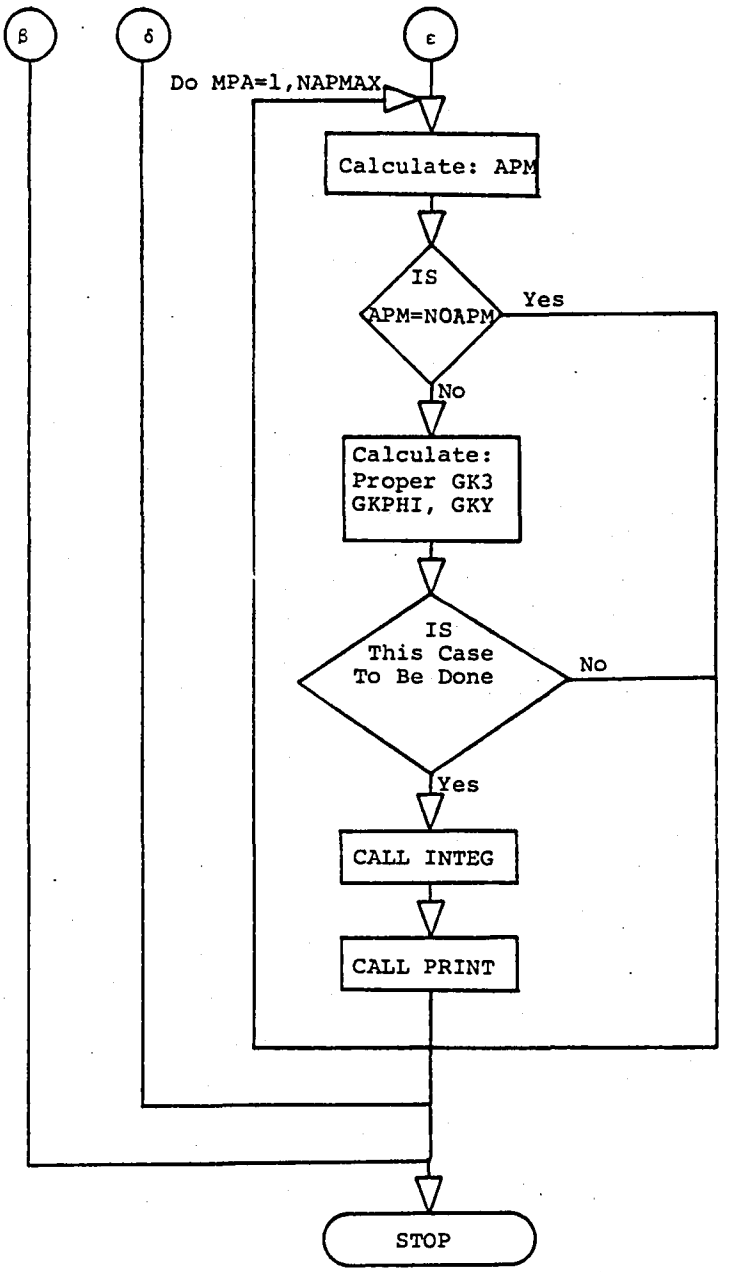
β
δ
ε
Do MPA=1,NAPMAX
Calculate: APM
IS
APM=NOAPM
Yes
No
Calculate:
Proper GK3
GKPHI, GKY
IS
This Case
To Be Done
No
Yes
CALL INTEG
CALL PRINT
STOP

Subroutine AUTO Definitions

I	autopilot mode
TPT(I,J)	τ_{ϕ_T}, tau's of phi term, numerator
TPB(I,J)	τ_{ϕ_B}, tau's of phi term, denominator
TYT(I,J)	τ_{Y_T}, tau's of y term, numerator
TYB(I,J)	τ_{Y_B}, tau's of y term, denominator
COND(I)	C_δ, constant of common term
CONP(I)	C_ϕ, constant of phi term
CONY(I)	Cy, constant of y term
QUADA(I)	A, coefficient of common term, numerator
QUADB(I)	B, coefficient of common term, numerator
TDB(I)	τ_{δ_B}, tau of delta term, denominator
QUAPTA(I)	A_{ϕ_T}, s^2 coefficient of phi term, numerator
QUAPTB(I)	B_{ϕ_T}, s coefficient of phi term, numerator
QUAYTA(I)	A_{Y_T}, s^2 coefficient of y term, numerator
QUAYTB(I)	B_{Y_T}, s coefficient of y term, numerator
QUAPA(I)	A_ϕ, s^2 coefficient of phi term, denominator
QUAPB(I)	B_ϕ, s coefficient of phi term, denominator
QUAYA(I)	Ay, s^2 coefficient of y term, denominator
QUAYB(I)	By, s coefficient of y term, denominator
K3(I)	A/P gain, function of autopilot mode
KPHI(I)	A/P gain, function of autopilot mode
NS	n, power of s in denominator of phi term
MS	m, power of s in denominator of y term
NPT	number of tau's in numerator of phi term
NPB	number of tau's in denominator of phi term

NYT number of tau's in numerator of y term

NYB number of tau's in denominator of y term

Subroutine AUTO Description

The purpose of this subroutine is to read in all quantities which are associated with the autopilot control law. All the quantities read in, except NPT,NPB,NYT and NYB, can vary with autopilot mode. The quanitites NPT,NPB,NYT,NYB are fixed at the maximum values required. If one autopilot mode has less than the maximum number of tau's, zero's are added as needed. The reader is referred to the definitions of variables used and the generalized control law for an understanding of the following read statements and examples of inputs.

```
READ(5,100)NPT,NPB,NYT,NYB
100  FORMAT(4I3)
Col.- 3 6 9 12
      3 3 5 3
READ(5,110)(TPT(I,J),J=1,NPT)
110  FORMAT(10F7.0)
Col.-     7     14    21    28    35    42    49    56    63    70
      .032 143.0  .957
TPB(I,J),TYT(I,J),andTYB(I,J) read in same manner.
READ(5,120)COND(I),CONP(I),CONY(I),QUADA(I),QUADB(I),TDB(I)
120  FORMAT(6F10.0)
Col.-     10    20    30    40    50    60
     0.638  1.00  2.0  3.0  4.0  .135
```

```
READ(5,123)QUAPTA(I),QUAPTB(I),QUAYTA(I),QUAYTB(I)
123  FORMAT(4F10.0)
Col.-       10        20    30    40
     .00117  0.5263  0.0  0.0
```

QUAPA(I),QUAPB(I),QUAYA(I),QUAYB(I) read in a similar manner.

```
READ(5,130)K3(I),KPHI(I)
130  FORMAT(2F10.0)
Col.-   10    20
      1.0  1.0
READ(5,135)NS(I),MS(I)
135  FORMAT(2I3)
Col.- 3 6
       1 0
```

The quantities read in are then written out with the proper descriptions.

Subroutine AUTO Flow Diagram

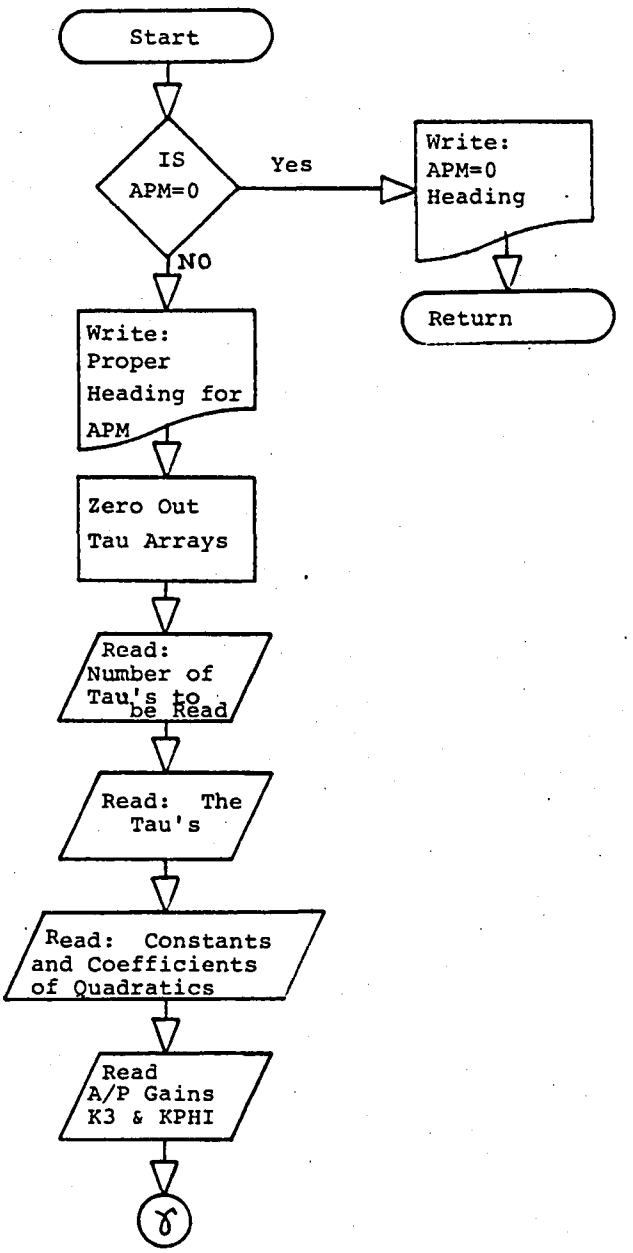

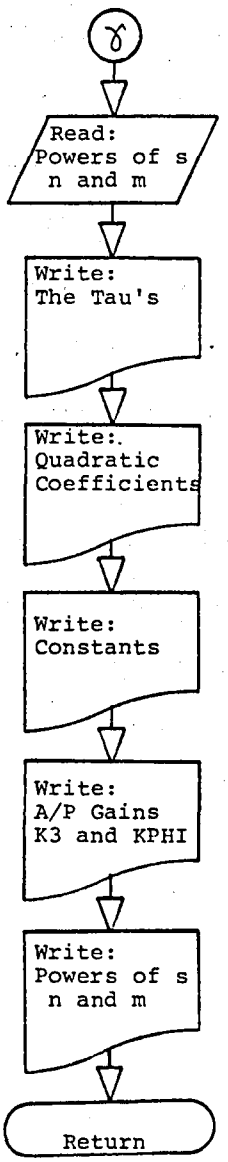
γ
Read:
Powers of s
n and m
Write:
The Tau's
Write:
Quadratic
Coefficients
Write:
Constants
Write:
A/P Gains
K3 and KPHI
Write:
Powers of s
n and m
Return

Subroutine INTEG Definitions

KC	kc, reduced cut-off frequency
DELTA	width of interval to be integrated
ANS	summation of values GLEG15
ANS1	summation of values GLEG15
BOT	lower limit of integration interval
TOP	upper limit of integration interval
BIGK	K, gust response parameter
KPRIME	K , gust response parameter
KO	k_0, ratio of gust response parameters
NO	N_0, number of positive-slope crossings per second of one-g load level due to gusts
GLEG15	function which equals value of integral
FUN, FUN1	names of subroutines which generate required values for integration

Subroutine INTEG Description

The purpose of this subroutine is to perform the integrations required for K and K′. The upper limit of the integral, k_c, is calculated and the interval from 0 to the upper limit, k_c, is divided into 10 equal divisions. Each division is then integrated twice, once for the K calculation and once for the K′ calculation. This integration is performed using a 15 point Gauss-Legendre Quadrature provided by the statement function GLEG15 and the integrals of the divisions are summed to provide the total integral from 0 to k_c. Then the quantities K, K′, k_0, and N_0 are calculated using

the previously found integrals.

Subroutine INTEG Flow Diagram

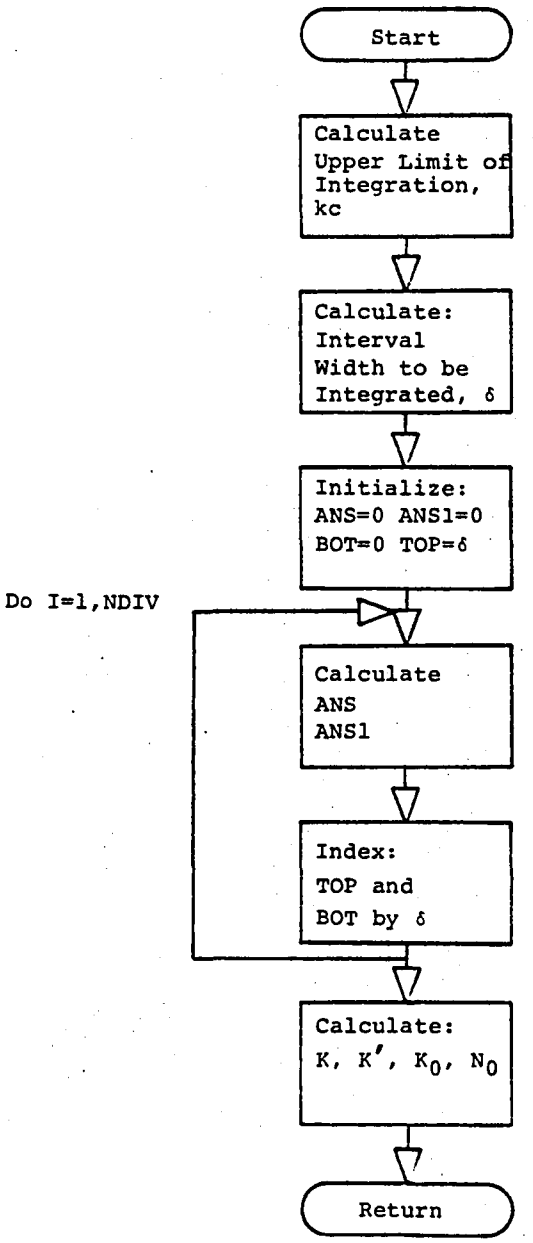

Function GLEG15 Definitions, evaluates integrals $\int_A^B G(x)dx$

W(1) to W(8)	W, weighting for results of function integrated, G(x)
R(1) to R(8)	R, weighting for location of point in interval
A	A, lower limit of integral
B	B, upper limit of integral
C	C, half the distance from A to B
D	D, average of A and B
KAG(I)	k, reduced frequency (array)
GLEG15	value of integral in interval A to B
FUNCT	external subroutine to calculate the value of G(x) at specified points. FUN, FUN1 are the external subroutines.

Function GLEG15 Description

The function GLEG15 evaluates the integral of a function from the lower limit, A, to the upper limit, B. The name of the function, and limits, A and B, appear in the function statement in subroutine INTEG. The two external subroutines which are used in conjunction with GLEG15 are FUN AND FUN1. Subroutine FUN calculates the function values for the integral used in the calculation of K. Subroutine FUN1 calculates the values for the integral used in the calculation of K'. After the integral is calculated over the interval using a 15 point Gauss-Legendre Quadrature the value is returned to subroutine INTEG.

Function GLEG15 Flow Diagram

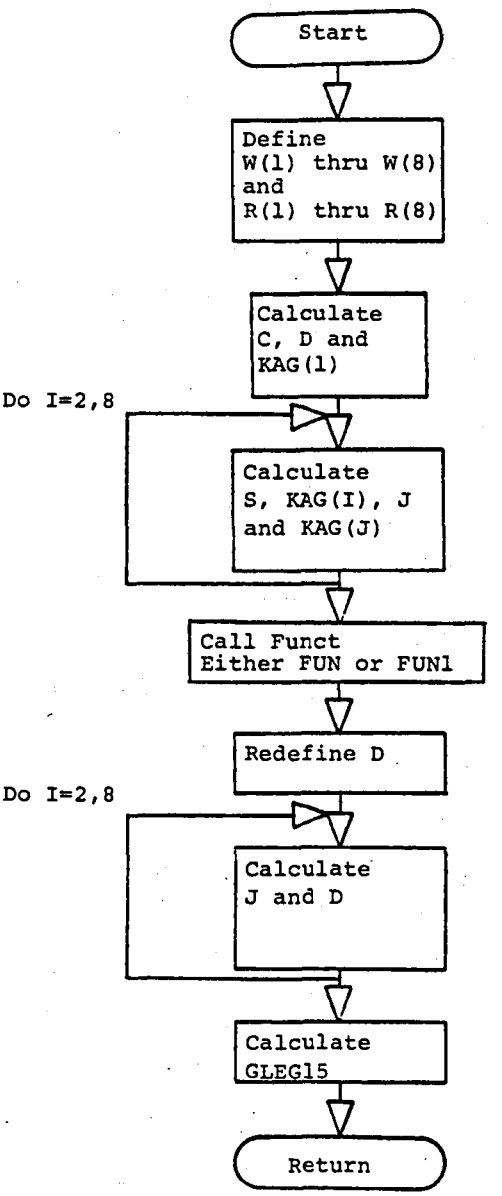

Subroutine FUN and FUN1 Definitions

KAG(J)	k, reduced frequency (array)
KAY	k, reduced frequency value
F1	f_1, airplane generalized transfer function
TLC	2L/c, twice the ratio of turbulence scale to wing chord
TLCK	parameter in ϕ_w/σ_1^2
PHISIG	ϕ_w/σ_1^2, ratio of vertical gust velocity PSD to rms vertical gust velocity square
F(J)	values of points to be used in Gauss Legendre Quandrature, GLEG15 (array)
CALF1(J)	f_1, stored value of f_1 calculated in subroutine FUN to be used again in subroutine FUN1 (array)

Subroutine FUN Description

This subroutine is used to obtain the function values necessary in the calculation of the integral for K. The calculations are performed at the 15 values of k specified by the Function GLEG15. Subroutine CALC is called upon to obtain the value of the airplane generalized transfer function f_1 at each specified k. These values are stored for use in subroutine FUN1. The function values to be used in the integration are calculated and returned to GLEG15 as the quantity F(15).

Subroutine FUN1 Description

This Subroutine is used to obtain the function values necessary in the calculation of the integral for K'. Calculations are performed at the 15 values of k specified by the function GLEG15. The basic quantity to be calculated is the airplane generalized transfer function f_1. Since FUN had already obtained these values at the same k's as FUN1 required them, the values of f_1 are stored in FUN and used again in FUN1. The function values to be used in the integration are calculated and returned to GLEG15 as the quantity F(15).

Subroutine FUN Flow Diagram

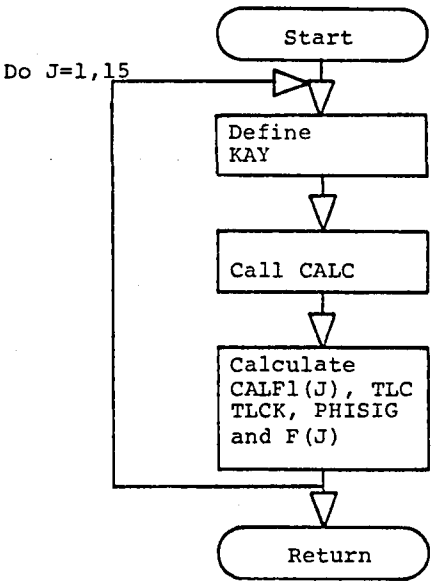

Subroutine FUN1

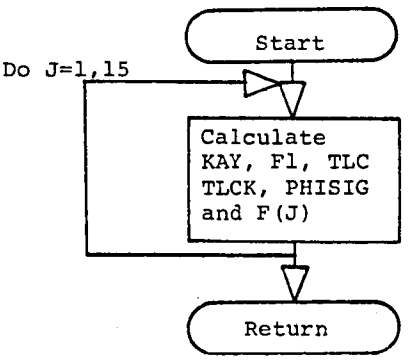

Subroutine CALC Definitions

KAY	k, reduced frequency specific value
OMEGA	ω, (2V/C)k, response frequency
SOP	s, Laplace operator
DN	denominator of common term of A/P equation
DD	numerator of common term of A/P equation
PN	numerator of phi term of A/P equation
PD	denominator of phi term of A/P equation
YN	numerator of y term of A/P equation
YD	denominator of y term of A/P equation
STAB	imaginary term of TAIL
TAIL	coefficient of ABPHI and ABY
ABPHI	airplane phi coefficient parameter
ABY	airplane y coefficient parameter
PAR1	component of a_1, real
PAI1	component of a_1, imaginary
PBR1	component of b_1, real
PBI1	component of b_1, imaginary
C1	c_1 airplane coefficient, real part
C1BAR	$\bar{c}_1$ airplane coefficient, imaginary part
PAR2	component of a_2, real
PAI2	component of a_2, imaginary
PBR2	component of b_2, real
PBI2	component of b_2, imaginary
C2	c_2 airplane coefficient, real part
C2BAR	$\bar{c}_2$ airplane coefficient, imaginary part

PA1	component of a_1, complex
PB1	component of b_1, complex
PA2	component of a_2, complex
PB2	component of b_2, complex
A1COM	$a_1 + \bar{a}_2$ airplane coefficient, complex
A2COM	$a_2 + \bar{a}_2$ airplane coefficient, complex
B1COM	$b_1 + \bar{b}_1$ airplane coefficient, complex
B2COM	$b_2 + \bar{b}_2$ airplane coefficient, complex
C1COM	$c_1 + \bar{c}_1$ airplane coefficient, complex
C2COM	$c_2 + \bar{c}_2$ airplane coefficient, complex
YTOP	numerator of vertical displacement equation
YBOT	denominator of vertical displacement equation
Y	y, vertical displacement, m (ft)
YDOT	$\dot{y}$, vertical velocity real component, m/s (ft/s)
YDTC	$\dot{y}_i$, vertical velocity imaginary component, m/s (ft/s)
YDOTSQ	$\lvert\dot{y}\rvert^2$, vertical velocity's magnitude squared, m^2/s^2 (ft^2/s^2)
BETASQ	β^2, Mach number correction, Glauret factor square
F2	f_2, airplane transfer function correction factor
F3	f_3, airplane transfer function correction factor
F1	f_1, airplane generalized transfer function

Subroutine CALC Description

The purpose of this subroutine is to obtain the value of the airplane generalized transfer function f_1, for a specified reduced frequency k. This required the calculation of the quantity $|\dot{y}|^2$, which is the absolute magnitude of the vertical velocity vector

square. This, in turn, would have necessitated determining the vertical displacement y from a 5x5 matrix. The matrix is composed of the two equations of motion, the two downwash equations, and the autopilot control law. The solution of this set of simultaneous equations for y was found in closed form to afford a threefold reduction in computer time. The solution was obtained by reducing the 5x5 matrix to a 2x2 matrix through successive substitutions and then applying Crammer's rule. The subroutine obtains the coefficients of the 2x2 matrix, which are termed a_1, b_1, c_1, a_2, b_2, and c_2. These coefficients are complex and the program recognizes them as such. The major part of the subroutine involves the calculation of components of these coefficients, both real and imaginary. Once y is obtained the calculation of $|\dot{y}|^2$ is performed. The airplane transfer function f_1 is then calculated and returned to the calling subroutine.

Subroutine CALC Flow Diagram

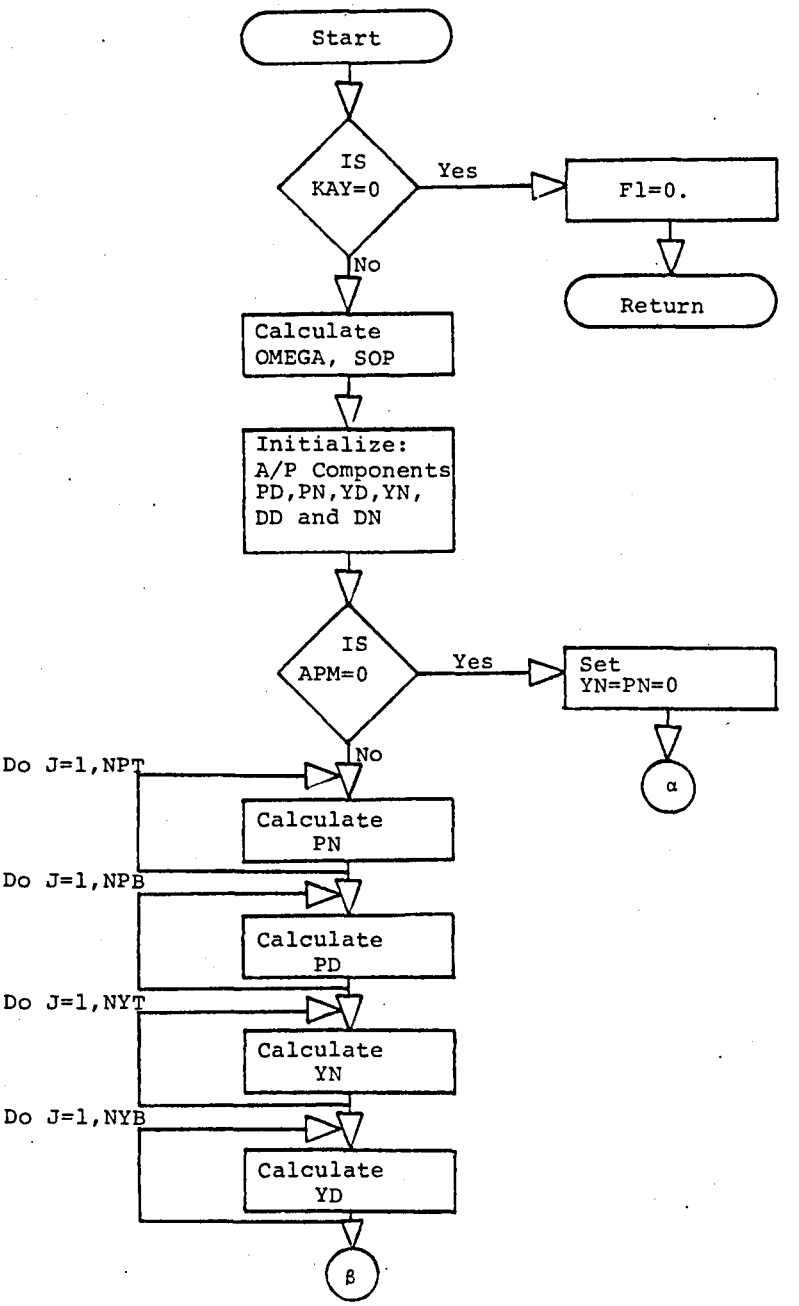

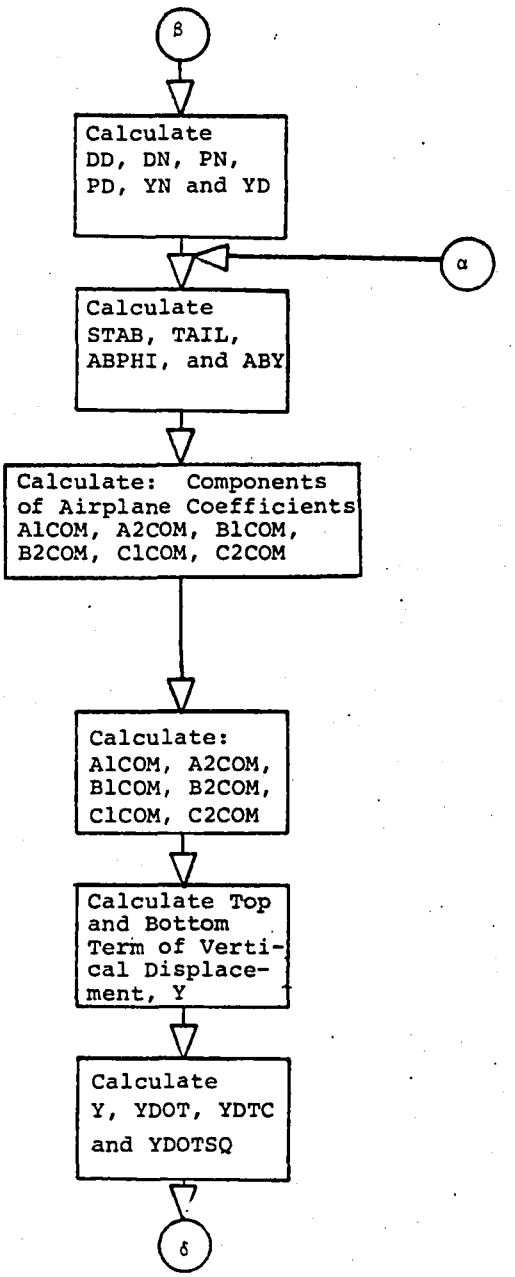
β
Calculate DD, DN, PN, PD, YN and YD
α
Calculate STAB, TAIL, ABPHI, and ABY
Calculate: Components of Airplane Coefficients A1COM, A2COM, B1COM, B2COM, C1COM, C2COM
Calculate: A1COM, A2COM, B1COM, B2COM, C1COM, C2COM
Calculate Top and Bottom Term of Vertical Displacement, Y
Calculate Y, YDOT, YDTC and YDOTSQ
δ

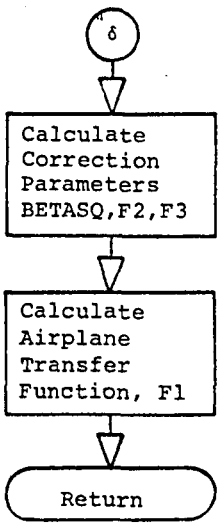
δ
Calculate Correction Parameters BETASQ,F2,F3
Calculate Airplane Transfer Function, F1
Return

Equations for Subroutine CALC

$$s = \frac{2V}{C}ki = i\omega$$

$$PN = C_\phi K_\phi (a_{\phi_T} s^2 + b_{\phi_T} s + 1)(\tau_{\phi_T} s + 1)_1 \ldots (\tau_{\phi_T} s + 1)_{NPT}$$

$$PD = s^n (a_{\phi_B} s^2 + b_{\phi_B} s + 1)(\tau_{\phi_B} s + 1)_1 \ldots (\tau_{\phi_B} s + 1)_{NPB}$$

$$YN = C_y K_y \frac{V}{57.3} (a_{y_T} s^2 + b_{y_T} s + 1)(\tau_{y_T} s + 1)_1 \ldots (\tau_{y_T} s + 1)_{NYT}$$

$$YD = s^m (a_{y_B} s^2 + b_{y_B} s + 1)(\tau_{y_B} s + 1)_1 \ldots (\tau_{y_B} s + 1)_{NYB}$$

$$DN = \frac{\tau_{\delta_B}}{K_4} s + 1$$

$$DD = C\, K_1 K_2 K_3\, (as^2 + bs + 1)$$

$$STAB = F_{\dot{\delta}} \frac{c_t}{c} k$$

$$TAIL = -F_\delta - (F_{\dot{\delta}} \frac{c_t}{c} k)i = -F_\delta - STABi$$

$$ABPHI = TAIL \left(\frac{DD}{DN}\right) \left(\frac{PN}{PD}\right)$$

$$ABY = TAIL \left(\frac{DD}{DN}\right) \left(\frac{YN}{YD}\right)$$

$$PAR1 = -2\mu\left(\frac{2V}{c}\right)k^2$$

$$PAI1 = \left(\frac{2V}{c}\right)\left[r_0 + r_1(1-\eta)\right]k$$

$$PBR1 = -\left[r_0 + r_1(1-\eta)\right]$$

$$PBI1 = \left[r_0\left(\frac{2e}{c} - 1\right) - r_1\, r_2\right]k$$

$$C1 = c_1 = r_0 + r_1\left[\cos kS_1 - \eta\right]$$

$$C1BAR = \bar{c}_1 = -r_1(\sin kS_1)i$$

$$PAR2 = 0$$

$$PAI2 = \left(\frac{2V}{c}\right)\left[\frac{e}{c} r_0 - \frac{e_t}{c} r_1 (1-\eta)\right] k$$

$$PBR2 = -\left[\frac{e}{c} r_0 - \frac{e_t}{c} r_1 (1-\eta) + \frac{4\mu k^2 k^2}{c^2}\right]$$

$$PBI2 = \left[\frac{e}{c} r_0 \left(2\frac{e}{c} - 1\right) + \frac{e_t}{c} r_1 r_2\right] k$$

$$C2 = c_2 = \frac{e}{c} r_0 - \frac{e_t}{c} r_1 (\cos kS_1 - \eta)$$

$$C2BAR = \bar{c}_2 = \frac{e_t}{c} r_1 (\sin kS_1)$$

$$PA1 = -2\mu\left(\frac{2V}{c}\right)k^2 + \left(\frac{2V}{c}\right)\left[r_0 + r_1 (1-\eta)\right] ki$$

$$= PAR1 + PAI1i$$

$$PB1 = -\left[r_0 + r_1 (1-\eta)\right] + \left[r_0\left(\frac{2e}{c} - 1\right) - r_1 r_2\right] ki$$

$$= PBR1 + PBI1i$$

$$PA2 = 0 + \left(\frac{2V}{c}\right)\left[\frac{e}{c} r_0 - \frac{e_t}{c} r_1 (1-\eta)\right] ki$$

$$= PAR2 + PAI2i$$

$$PB2 = -\left[\frac{e}{c} r_0 - \frac{e_t}{c} r_1 (1-\eta) + 4\mu \frac{k^2}{c^2} k^2\right] + \left[\frac{e}{c} r_0 \left(2\frac{e}{c} - 1\right) + \frac{e_t}{c} r_1 r_2\right] ki$$

$$= PBR2 + PBI2i$$

$$A1COM = a_1 + \bar{a}_1 = r_1 A_y - 2\mu\left(\frac{2V}{c}\right)k^2 + \left\{r_1 B_y + \left(\frac{2V}{c}\right)\left[r_0 + r_1 (1-\eta)\right] k\right\} i$$

$$= r_1 (A_y + B_y i) - 2\mu\left(\frac{2V}{c}\right)k^2 + \left(\frac{2V}{c}\right)\left[r_0 + r_1 (1-\eta)\right] ki$$

$$= R1 \quad ABY + PA1$$

$$A2COM = a_2 + \bar{a}_2 = -\frac{e_t}{c} r_1 A_y + \left\{-\frac{e_t}{c} r_1 B_y + \left(\frac{2V}{c}\right)\left[\frac{e}{c} r_0 - \frac{e_t}{c} r_1(1-\eta)\right] k\right\} i$$

$$= -\frac{e_t}{c} r_1 (A_y + B_y i) + \left(\frac{2V}{c}\right)\left[\frac{e}{c} r_0 - \frac{e_t}{c} r_1(1-\eta)\right] ki$$

$$= -CO1\ R1\ ABY + PA2, \quad (CO1 = e_t/c)$$

$$B1COM = b_1 + \bar{b}_1 = r_1 A_\phi - \left[r_0 + r_1(1-\eta)\right] + \left\{r_1 B_\phi + \left[r_0\left(\frac{2e}{c} - 1\right) - r_1 r_2\right] k\right\} i$$

$$= r_1 (A_\phi + B_\phi i) - \left[r_0 + r_1(1-\eta)\right] + \left[r_0\left(\frac{2e}{c} - 1\right) - r_1 r_2\right] ki$$

$$= R1\ ABPHI + PB1$$

$$B2COM = b_2 + \bar{b}_2 = -\frac{e_t}{c} r_1 A_\phi - \left[\frac{e}{c} r_0 - \frac{e_t}{c} r_1(1-\eta) + 4\mu \frac{k_2^2}{c^2} k^2\right]$$

$$+ \left\{-\frac{e_t}{c} r_1 B_\phi + \left[\frac{e}{c} r_0 \left(\frac{2e}{c} - 1\right) + \frac{e_t}{c} r_1 r_2\right] k\right\} i$$

$$= -\frac{e_t}{c} r_1 (A_\phi + B_\phi i) - \left[\frac{e}{c} r_0 - \frac{e_t}{c} r_1(1-\eta) + 4\mu \frac{k_2^2}{c^2} k^2\right]$$

$$+ \left[\frac{e}{c} r_0 \left(\frac{2e}{c} - 1\right) + \frac{e_t}{c} r_1 r_2\right] ki$$

$$= -CO1\ R1\ ABPHI + PB2$$

$$C1COM = c_1 + \bar{c}_1 = r_0 + r_1(\cos kS_1 - \eta) - r_1 (\sin kS_1) i$$

$$= C1 + C1BARi$$

$$C2COM = c_2 + \bar{c}_2 = \frac{e}{c} r_0 - \frac{e_t}{c} r_1(\cos kS_1 - \eta) + \frac{e_t}{c} r_1 (\sin kS_1) i$$

$$= C2 + C2BARi$$

$$YTOP = (c_1 + \bar{c}_1)(b_2 + \bar{b}_2) - (c_2 + \bar{c}_2)(b_1 + \bar{b}_1)$$

$$= C1COM\ \ B2COM - C2COM\ B1COM$$

$$YBOT = (a_1+\bar{a}_1)(b_2+\bar{b}_2) - (a_2+\bar{a}_2)(b_1+\bar{b}_1)$$

$$= A1COM\ B2COM - A2COM\ B1COM$$

$$Y = y\ \frac{(c_1+\bar{c}_1)(b_2+\bar{b}_2) - (c_2+\bar{c}_2)(b_1+\bar{b}_1)}{(a_1+\bar{a}_1)(b_2+\bar{b}_2) - (a_2+\bar{a}_2)(b_1+\bar{b}_1)}$$

$$= \frac{YTOP}{YBOT}$$

$$YDOT = \dot{y} = i\omega y = i\left(\frac{2V}{c}\,k\right)y = (\dot{y})r + (\dot{y})i$$

$$YDTC = \text{conjugate of } \dot{y} = (\dot{y})r - (\dot{y})i$$

$$|\dot{y}|^2 = (\dot{y})_r^2 - (\dot{y})_i^2$$

$$= \left[(\dot{y})_r + (\dot{y})_i\right]\left[(\dot{y})_r - (\dot{y})_i\right]$$

$$= (YDOT)(YDTC)$$

$$BETASQ = \beta^2 = 1-M^2$$

$$F2 = f_2 = \frac{1}{1 + \frac{1.5\,\pi k}{\beta^2} + \frac{\pi^2\,Mk^2}{\beta^2}}$$

$$F3 = f_3 = \frac{1}{1 + .55\,A_w k}$$

$$F1 = f_1 = 4\mu^2\,k^2\,|\dot{y}|^2\,f_2\,f_3$$

Subroutine PRINT Definitions

IPRT	controls whether detailed print-out is to be obtained for that case

The following arrays are found for detailed print-out at the selected reduced frequencies.

KAY	k, selected reduced frequency
KAX(J)	k, reduced frequency (array)
F1X(J)	f_1, airplane generalized transfer function (array)
TLC	2L/c, twice the ratio of turbulence scale to wing chord
TLCK	parameter in $\phi w/\sigma_1^2$
YDTSQ(J)	$\lvert\dot{y}\rvert^2$, absolute value of velocity square (array)
F2X(J)	f_2, airplane transfer function correction factor (array)
F3X(J)	f_3, airplane transfer function correction factor (array)
FISIG(J)	$\phi w/\sigma_1^2$, ratio of vertical gust velocity PSD to rms vertical gust velocity square (array)
JP	causes page number to be printed
KP	causes page number to be printed
IP	page number of print out
ASIG	$A\sigma$, gust response parameter
ASIGVC	$A\sigma/(V/c)$, generalized gust response parameter
F2F3	$f_2\ f_3$, airplane transfer function correction factor
FUNF1	values generated to find K
FUN1F1	values generated to find K′
GFPSD	GFPSD, generalized frequency times power spectral density

GNFPSD	GNFPSD, gust normalized frequency times power spectral density
ANFPSD	ANFPSD, acceleration normalized frequency times power spectral density

Subroutine PRINT Description

The purpose of this subroutine is to print out the results for the cases run. The standard printout is performed for all cases. The detailed printout is done only for the medium weight, B, cases. The standard printout is of the following quantities: case number, M, h, V, V/c, μ, kc, a_0, a, a_t, r_0, r_1, r_2, s_1, K, K', $A\sigma$, $A\sigma/(V/c)$, k_0, N_0. The detailed printout are the values of the quantities: $|\dot{y}|^2$, $f_2 x f_3$, f_1, $\phi w/\sigma_1^2$, $f_1(\phi w/\sigma_1^2)$, $k^2 f_1 \phi w/\sigma_1^2$, GFPSD, GNFPSD, ANFPSD calculated for specific values of k. The values of k are specified in the main program and run for three decades, 10^{-3} to 1. The purpose of the detailed printout is to generate the PSD graphs. Subroutine CODE, which is used in conjunction with subroutine PRINT, prints out the case number when called upon. Once the required printout for the case is performed the program returns to the Main Program.

Subroutine PRINT Flow Diagram

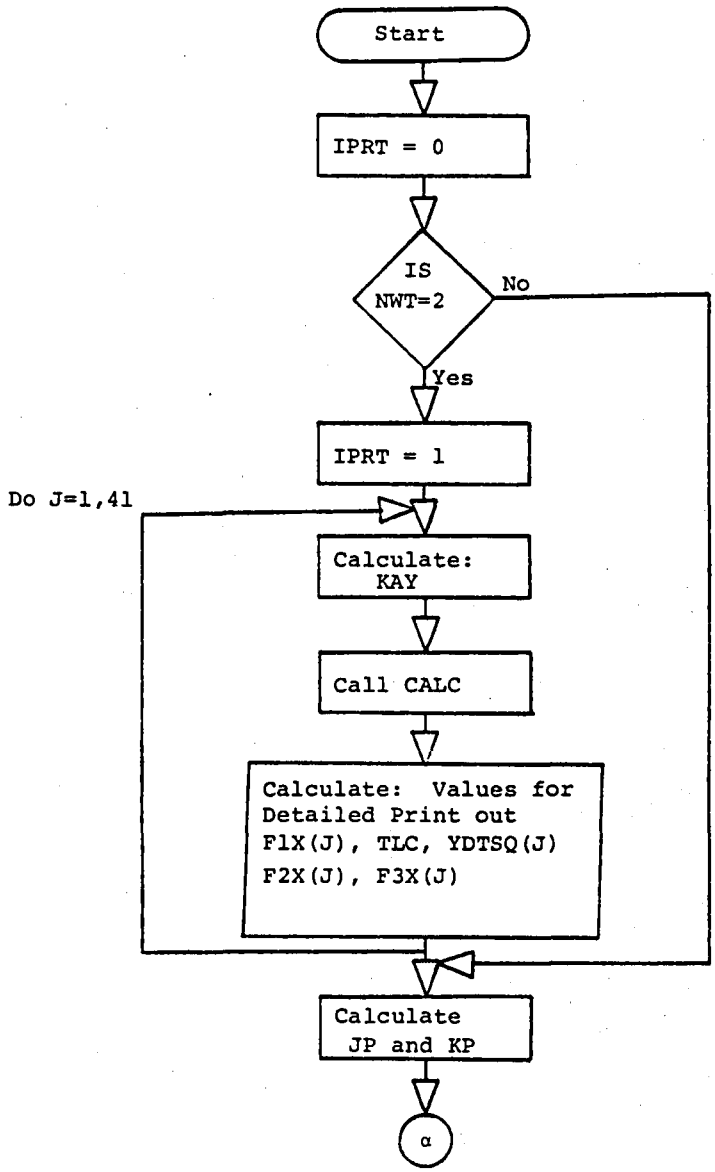

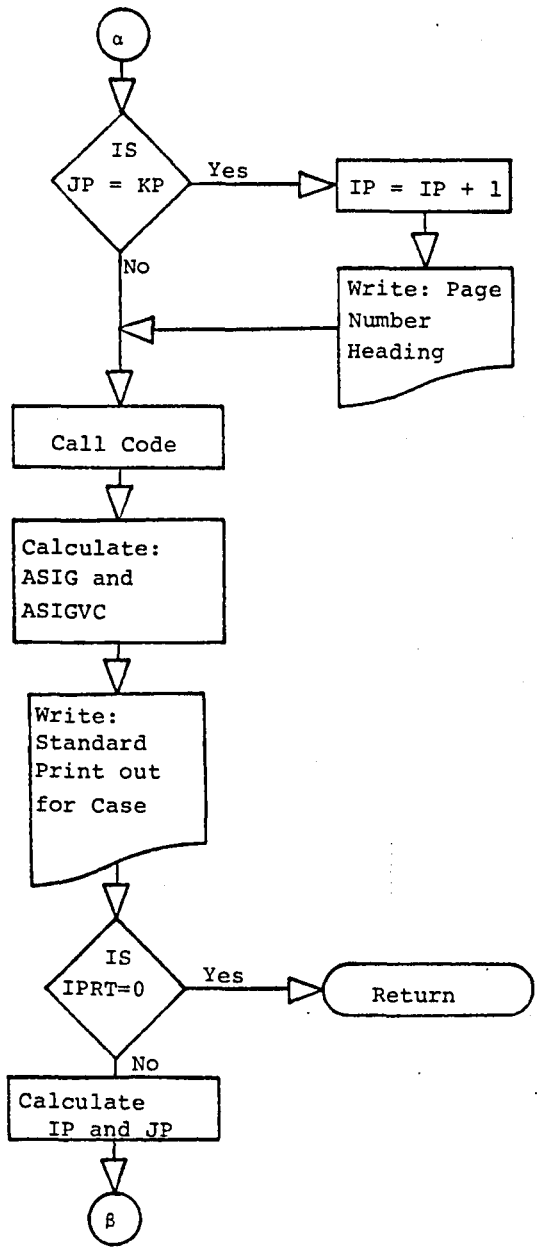
α
IS
JP = KP
Yes
IP = IP + 1
No
Write: Page
Number
Heading
Call Code
Calculate:
ASIG and
ASIGVC
Write:
Standard
Print out
for Case
IS
IPRT=0
Yes
Return
No
Calculate
IP and JP
β

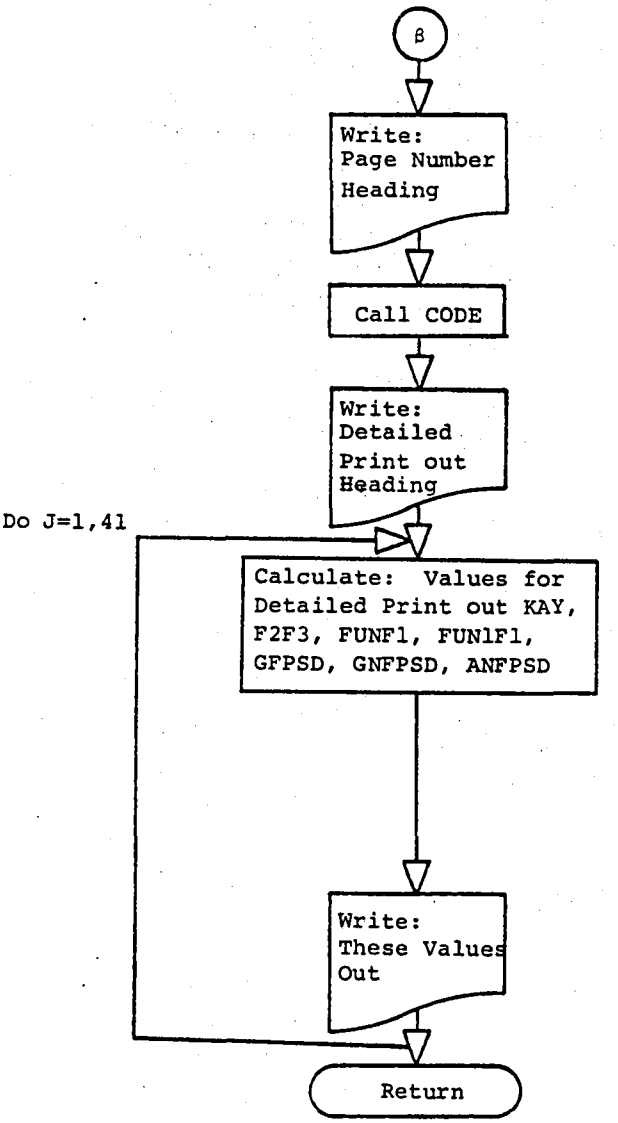
β
Write:
Page Number
Heading
Call CODE
Write:
Detailed
Print out
Heading
Do J=1,41
Calculate: Values for
Detailed Print out KAY,
F2F3, FUNF1, FUN1F1,
GFPSD, GNFPSD, ANFPSD
Write:
These Values
Out
Return

Subroutine CODE Flow Diagram

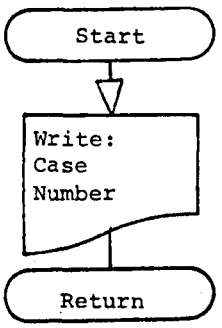

Program Listing

```
* $$ JOB JNM=HAWK,CLASS=A
* $$ PRT CLASS=M
// JOB HAWK,3610051010
// EXEC PROC=FRTCLG
      IMPLICIT REAL*8(A-H,K,O-Z)
      REAL*8 MU,M,NRSQ,NISQ,L
      INTEGER APM
      COMMON/INP/H,RHO,VS,AO,ETA,FDEL,FDLDT,W,C,CT,ET,S,ST,AW,AT,FC
     1,KAX(60),KAPPA,KAY,M,L
      COMMON/FLT/APM,NFC,NWT
      COMMON/CALCU/V,VC,PI,APRI,BPRI,SMLA,SMLAT,R0,R1,E,CO1,CO2,CO3,R2,S
     11,MU
      COMMON/INT/BIGK,ASIG,F1,KPRIME,KC,KO,NO
      COMMON/PRT/YDOTSQ,F2,F3,IP,JP
      COMMON/FAST/TVC,GK1,GK2,GK3,GK4,GKPHI,GKY
      COMMON/DIV/NDIV
      COMMON/GEN/TPT(4,10),TPB(4,10),TYT(4,10),TYB(4,10),COND(4),CONP(4)
     1,CONY(4),QUADA(4),QUADB(4),TDB(4),QUAPA(4),QUAPB(4),QUAYA(4),QUAYB
     2(4),QUAPTA(4),QUAPTB(4),QUAYTA(4),QUAYTB(4),NS(4),MS(4)
      COMMON/GEN2/K3(4),KPHI(4),NPT,NPB,NYT,NYB
      DIMENSION XM(20),HX(20),RHOX(20),VSX(20),AOX(20),ETAX(20),FDELX(20
     1),EX(20),K1(20),K2(20),K4(20),KY(20),WX(3)
      READ(5,1)NAPMAX,NOAPM,NFCMAX,LALT1,NALT1,LALT2,NALT2,LALT3,NALT3,L
     1ALT4,NALT4
      READ(5,5)C,CT,ET,KAPPA,S,ST,AW,AT,L,FC,FDLDT
      PI=3.14159
      WRITE(6,10)
      WRITE(6,15)C
      WRITE(6,20)CT
      WRITE(6,25)KAPPA
```

```
      WRITE(6,30)ET
      WRITE(6,35)S
      WRITE(6,40)ST
      WRITE(6,45)AW
      WRITE(6,50)AT
      WRITE(6,55)L
      WRITE(6,60)FC
      WRITE(6,65)FDLDT
      KAX(1)=0.001
      DO 100 I=2,10
      KAX(I)=KAX(I-1)+.001
  100 CONTINUE
      DO 120 I=11,28
      KAX(I)=KAX(I-1)+.005
  120 CONTINUE
      DO 140 I=29,33
      KAX(I)=KAX(I-1)+.02
  140 CONTINUE
      DO 160 I=34,41
      KAX(I)=KAX(I-1)+.1
  160 CONTINUE
      WRITE(6,250)
      DO 390 I=1,NFCMAX
      READ(5,300)HX(I),XM(I),RHOX(I),AOX(I),VSX(I),ETAX(I),FDELX(I),EX(I
     1)
  390 CONTINUE
      DO 400 I=1,NFCMAX
      READ(5,310)K1(I),K2(I),K4(I),KY(I)
      AO=AOX(I)
      ETA=ETAX(I)
      PRI=.9*PI/((1./AT)-(1./AW))
      APRI=AO-(1.+(ST/S)*(1.-ETA))*PRI
      BPRI=AO*PRI
```

```
      SMLA=(APRI/2.)+DSQRT((APRI/2.)**2+BPRI)
      SMLAT=SMLA/(1.+SMLA/PRI)
      SM=(SMLA/C/AO)*100.*(SMLAT*ST*(1.-ETA)*ET/SMLA/S-EX(I))
      WRITE(6,340)I,XM(I),HX(I),RHOX(I),VSX(I),AOX(I),ETAX(I),FDELX(I),E
     1X(I),SM,K1(I),K2(I),K4(I),KY(I)
  400 CONTINUE
      DO 410 MPA=1,NAPMAX
      APM=MPA-1
      IF(APM.EQ.NOAPM)GOTO410
      CALL AUTO
  410 CONTINUE
      READ(5,420)WX(1),WX(2),WX(3)
      WRITE(6,500)
      WRITE(6,550)WX(1),WX(2),WX(3)
      IP=0
      JP=0
      DO 600 NFC=1,NFCMAX
      M=XM(NFC)
      H=HX(NFC)
      RHO=RHOX(NFC)
      VS=VSX(NFC)
      AO=AOX(NFC)
      ETA=ETAX(NFC)
      E=EX(NFC)
      FDEL=FDELX(NFC)
      V=M*VS
      VC=V/C
      TVC=2.*VC
      PRI=.9*PI/((1./AT)-(1./AW))
      APRI=AO-(1.+(ST/S)*(1.-ETA))*PRI
      BPRI=AO*PRI
      SMLA=(APRI/2.)+DSQRT((APRI/2.)**2+BPRI)
      SMLAT=SMLA/(1.+SMLA/PRI)
```

```
      R0=SMLA/AO
      R1=(SMLAT/AO)*(ST/S)
      CO1=ET/C
      CO2=CT/C
      CO3=E/C
      GK1=K1(NFC)
      GK2=K2(NFC)
      GK4=K4(NFC)
      GKY=KY(NFC)
      R2=(2.*CO1)+CO2+(ETA*(2.*CO3-1.))
      S1=2.*CO3+2.*CO1-1.+CO2
      DO 650 NWT=1,3
      W=WX(NWT)
      MU=2.*W*1000./(32.2*AO*RHO*S*C)
      DO 700 MPA=1,NAPMAX
      APM=MPA-1
      IF(APM.EQ.NOAPM)GOTO 700
      GK3=0.0
      GKPHI=0.0
      IF(APM.NE.0)GK3=K3(APM)
      IF(APM.NE.0)GKPHI=KPHI(APM)
      GKY=0.
      IF(APM.EQ.2)GKY=KY(NFC)
      IF(NFC.LT.LALT1.AND.APM.EQ.1)GO TO 700
      IF(NFC.GT.NALT1.AND.APM.EQ.1)GO TO 700
      IF(NFC.LT.LALT2.AND.APM.EQ.2)GO TO 700
      IF(NFC.GT.NALT2.AND.APM.EQ.2)GO TO 700
      IF(NFC.LT.LALT3.AND.APM.EQ.3)GO TO 700
      IF(NFC.GT.NALT3.AND.APM.EQ.3)GO TO 700
      IF(NFC.LT.LALT4.AND.APM.EQ.4)GO TO 700
      IF(NFC.GT.NALT4.AND.APM.EQ.4)GO TO 700
800   CONTINUE
      NDIV=10
```

```
      CALL INTEG
      CALL PRINT
  700 CONTINUE
  650 CONTINUE
  600 CONTINUE
      STOP
    1 FORMAT(11I3)
    5 FORMAT(11F6.0)
   10 FORMAT(1X,'*****************************',/,1X,'AIRPLANE GEOMETRIC
     1 CONSTANTS',/,1X,'*****************************',/)
   15 FORMAT(1X,'WING GEOMETRIC CHORD,C',6X,F5.2,' FT.')
   20 FORMAT(1X,'TAIL GEOMETRIC CHORD,CT',5X,F5.2,' FT.')
   25 FORMAT(1X,'PITCH RAD. OF GYRATION,KAPPA ',F4.1,' FT.')
   30 FORMAT(1X,'TAIL MOMENT ARM,ET',10X,F5.1,' FT.')
   35 FORMAT(1X,'WING AREA,S',17X,F5.0,' SQ.FT.')
   40 FORMAT(1X,'TAIL AREA,ST',16X,F5.0,' SQ.FT.')
   45 FORMAT(1X,'WING ASPECT RATIO,AW',9X,F4.2)
   50 FORMAT(1X,'TAIL ASPECT RATIO,AT',9X,F4.2)
   55 FORMAT(1X,'TURBULENCE SCALE,L',10X,F5.0,' FT.')
   60 FORMAT(1X,'CUT-OFF FREQUENCY,FC',9X,F4.2,' HZ.')
   65 FORMAT(1X,'ELEVATQR RATE EFFECTIVENESS  ',F3.1,///)
  250 FORMAT(1X,'NFC',3X,'M',4X,'H',5X,'RHO',5X,'VS',5X,'AO',3X,'ETA',2X
     1,'FDEL',2X,' E ',3X,'S.M.',4X,'GK1',5X,'GK2',5X,'GK4',5X,'GKY')
  300 FORMAT(8F8.0)
  310 FORMAT(4F10.0)
  340 FORMAT(1X,I2,2X,F4.2,2X,F3.0,1X,F8.6,2X,F5.0,2X,F4.2,1X,F5.3,1X,F5
     1.3,1X,F4.2,2X,F4.1,4(2X,F6.3),/)
  420 FORMAT(3F5.0)
  500 FORMAT(///,1X,'GROSS WEIGHT',/)
  550 FORMAT(4X,'A=',F5.0/,4X,'B=',F5.0/,4X,'C=',F5.0//)
      END
      SUBROUTINE AUTO
      IMPLICIT REAL*8(A-H,K,O-Z)
```

```
      REAL*8 MU,M,NRSQ,NISQ,L
      INTEGER APM
      COMMON/GEN/TPT(4,10),TPB(4,10),TYT(4,10),TYB(4,10),COND(4),CONY(4)
     1,CONP(4),QUADA(4),QUADB(4),TDB(4),QUAPA(4),QUAPB(4),QUAYA(4),QUAYB
     2(4),QUAPTA(4),QUAPTB(4),QUAYTA(4),QUAYTB(4),NS(4),MS(4)
      COMMON/GEN2/K3(4),KPHI(4),NPT,NPB,NYT,NYB
      COMMON/INP/H,RHO,VS,AO,ETA,FDEL,FDLDT,W,C,CT,ET,S,ST,AW,AT,FC
     1,KAX(60),KAPPA,KAY,M,L
      COMMON/FLT/APM,NFC,NWT
      IF(APM.EQ.0)WRITE(6,460)
      IF(APM.EQ.0)RETURN
      IF(APM.EQ.1)WRITE(6,461)
      IF(APM.EQ.2)WRITE(6,462)
      IF(APM.EQ.3)WRITE(6,463)
      IF(APM.EQ.4)WRITE(6,464)
      I=APM
      DO 105 J=1,10
      TPT(I,J)=0.0
      TPB(I,J)=0.0
      TYT(I,J)=0.0
      TYB(I,J)=0.0
  105 CONTINUE
      READ(5,100)NPT,NPB,NYT,NYB
      READ(5,110)(TPT(I,J),J=1,NPT)
      READ(5,110)(TPB(I,J),J=1,NPB)
      READ(5,110)(TYT(I,J),J=1,NYT)
      READ(5,110)(TYB(I,J),J=1,NYB)
      READ(5,120)COND(I),CONP(I),CONY(I),QUADA(I),QUADB(I),TDB(I)
      READ(5,123)QUAPTA(I),QUAPTB(I),QUAYTA(I),QUAYTB(I)
      READ(5,125)QUAPA(I),QUAPB(I),QUAYA(I),QUAYB(I)
      READ(5,130)K3(I),KPHI(I)
      READ(5,135)NS(I),MS(I)
      WRITE(6,140)(TPT(I,J),J=1,NPT)
```

```
      WRITE(6,145)(TPB(I,J),J=1,NPB)
      WRITE(6,150)(TYT(I,J),J=1,NYT)
      WRITE(6,155)(TYB(I,J),J=1,NYB)
      WRITE(6,160)TDB(I)
      WRITE(6,161)QUADA(I),QUADB(I)
      WRITE(6,162)QUAPA(I),QUAPB(I)
      WRITE(6,172)QUAPTA(I),QUAPTB(I)
      WRITE(6,163)QUAYA(I),QUAYB(I)
      WRITE(6,173)QUAYTA(I),QUAYTB(I)
      WRITE(6,165)COND(I),CONP(I),CONY(I)
      WRITE(6,175)K3(I),KPHI(I)
      WRITE(6,170)NS(I),MS(I)
      RETURN
  100 FORMAT(4I3)
  110 FORMAT(10F7.0)
  120 FORMAT(6F10.0)
  123 FORMAT(4F10.0)
  125 FORMAT(4F10.0)
  130 FORMAT(2F10.0)
  135 FORMAT(2I3)
  140 FORMAT(1X,/,9X,'TAUS FOR NUMERATOR OF VPHI',4X,10F8.4)
  145 FORMAT(1X,/,9X,'TAUS FOR DENOMINATOR OF VPHI',2X,10F8.4)
  150 FORMAT(1X,/,9X,'TAUS FOR NUMERATOR OF V Y ',4X,10F8.4)
  155 FORMAT(1X,/,9X,'TAUS FOR DENOMINATOR OF V Y ',2X,10F8.4)
  160 FORMAT(1X,/,9X,'TAU FOR DENOMINATOR OF COMMON TERM',F10.6)
  161 FORMAT(1X,/,9X,'COMMON QUADRATIC COEFFICIENTS: A=',F10.6,2X,'B=',F
     110.6,/)
  162 FORMAT(9X,'DENOMINATOR PHI QUADRATIC COEFFICIENTS: A=',F10.6,2X,'B
     1=',F10.6,/)
  163 FORMAT(9X,'DENOMINATOR Y  QUADRATIC COEFFICIENTS: A=',F10.6,2X,'B=
     1',F10.6,/)
  165 FORMAT(9X,'FIXED GAIN OF COMMON TERM=',F10.6,//,9X,'FIXED GAIN OF
     1PHI TERM=',5X,F10.6,//,9X,'FIXED GAIN OF Y TERM=',5X,F10.6,/)
```

```
172 FORMAT(9X,'NUMERATOR PHI QUADRATIC COEFFICIENTS: A=',F10.6,2X,'B='
   1,F10.6,/)
173 FORMAT(9X,'NUMERATOR Y  QUADRATIC COEFFICIENTS: A=',F10.6,2X,'B=',
   1F10.6,/)
175 FORMAT(9X,'VARIABLE GAIN GK3=',F10.6,//,9X,'VARIABLE GAIN GKPHI=',
   1F10.6,/)
170 FORMAT(9X,'EXPONENTS: N=',I2,' M=',I2,/)
460 FORMAT(/////,2X,'APM ','0',2X,'A/P OFF',/)
461 FORMAT(2X,'APM ','1',2X,'PITCH HOLD',/)
462 FORMAT(2X,'APM ','2',2X,'PITCH+ALTITUDE HOLD',/)
463 FORMAT(2X,'APM ','3',2X,'TURBULENT MODE',/)
464 FORMAT(2X,'APM ','4',2X,'PITCH+RATE HOLD',/)
    END
    SUBROUTINE INTEG
    IMPLICIT REAL*8(A-H,K,O-Z)
    REAL*8 NO,M
    INTEGER APM
    COMMON/INP/H,RHO,VS,AO,ETA,FDEL,FDLDT,W,C,CT,ET,S,ST,AW,AT,FC
   1,KAX(60),KAPPA,KAY,M,L
    COMMON/FLT/APM,NFC,NWT
    COMMON/CALCU/V,VC,PI,APRI,BPRI,SMLA,SMLAT,R0,R1,E,C01,C02,C03,R2,S
   11,MU
    COMMON/INT/BIGK,ASIG,F1,KPRIME,KC,KO,NO
    COMMON/PRT/YDOTSQ,F2,F3,IP,JP
    COMMON/DIV/NDIV
    EXTERNAL FUN,FUN1
    KC=FC*PI/VC
    DELTA=KC/NDIV
    ANS=0.0D0
    ANS1=0.0D0
    BOT=0.0D0
    TOP=DELTA
    DO 10 I=1,NDIV
```

```
      ANS=ANS+GLEG15(BOT,TOP,FUN)
      ANS1=ANS1+GLEG15(BOT,TOP,FUN1)
      TOP=TOP+DELTA
      BOT=BOT+DELTA
   10 CONTINUE
      BIGK=DSQRT(ANS)
      KPRIME=DSQRT(ANS1)
      KO=KPRIME/BIGK
      NO=VC*KO/PI
      RETURN
      END
      FUNCTION GLEG15(A,B,FUNCT)
      IMPLICIT REAL*8(A-H,K,O-Z)
C
C FUNCTION GLEG15 EVALUATES INTEGRALS OF THE FORM
C
C          B
C     INTEGRAL  G(X)  DX
C          A
C
C WHERE A AND B ARE FINITE USING 15 POINT GAUSS-LEGENDRE QUADRATURE.
C
C USE
C
C     VALUE=GLEG15(A,B,FUNCT)
C
C           A......THE LOWER LIMIT OF INTEGRATION. MUST BE FINITE.
C
C           B......THE UPPER LIMIT OF INTEGRATION. MUST BE FINITE.
C
C           FUNCT..THE NAME OF AN EXTERNAL SUBROUTINE TO CALCULATE THE
C                  VALUE OF G(X) AT SPECIFIED POINTS.
C                  SUBROUTINE FUNCT(F,N)
```

```
C                              F..ON INPUT THE N VALUES OF X
C                                 ON OUTPUT THE N VALUES G(X)
C                              F(I)! I=1,...,N
C                              N..THE NUMBER OF FUNCTION EVALUATIONS.
C                    THE NAME GIVEN FUNCT MUST APPEAR IN AN EXTERNAL
C                    STATEMENT IN THE CALLING PROGRAM
C
C GLEG15 IS AVAILABLE IN FORTRAN
C
C RELEASED 25 AUGUST 1975
C
C PROGRAMMED BY S. BAUDENDISTEL  COMPUTER SCIENCES CORPORATION
C
      COMMON/FUNY/F(15),KAG(15),CALF1(15)
      DIMENSION W(8),R(8)
      W(1)=.202578241925561
      W(2)=.198431485327111
      W(3)=.186161000015562
      W(4)=.166269205816993
      W(5)=.139570677926154
      W(6)=.107159220467171
      W(7)=.070366047488108
      W(8)=.030753241996117
      R(1)=0.0D0
      R(2)=.201194093997434
      R(3)=.394151347077563
      R(4)=.570972172608538
      R(5)=.72441773136017
      R(6)=.848206583410427
      R(7)=.937273392400705
      R(8)=.987992518020485
      C=(B-A)*.5
      D=(B+A)*.5
```

```
      KAG(1)=D
      DO 10 I=2,8
      S=R(I)*C
      KAG(I)=D+S
      J=I+7
      KAG(J)=D-S
10    CONTINUE
      CALL FUNCT
      D=W(1)*F(1)
      DO 20 I=2,8
      J=I+7
20    D=D+W(I)*(F(I)+F(J))
      GLEG15=C*D
      RETURN
      END
      SUBROUTINE FUN
      IMPLICIT REAL*8(A-H,K,O-Z)
      REAL*8 M
      REAL*8 L
      INTEGER APM
      COMMON/INP/H,RHO,VS,AO,ETA,FDEL,FDLDT,W,C,CT,ET,S,ST,AW,AT,FC
     1,KAX(60),KAPPA,KAY,M,L
      COMMON/FLT/APM,NFC,NWT
      COMMON/CALCU/V,VC,PI,APRI,BPRI,SMLA,SMLAT,R0,R1,E,C01,C02,C03,R2,S
     11,MU
      COMMON/INT/BIGK,ASIG,F1,KPRIME,KC,KO,NO
      COMMON/PRT/YDOTSQ,F2,F3,IP,JP
      COMMON/FUNY/F(15),KAG(15),CALF1(15)
      DO 10 J=1,15
      KAY=KAG(J)
      CALL CALC
      CALF1(J)=F1
      TLC=2.*L/C
```

```
      TLCK=(1.339*TLC*KAY)**2
      PHISIG=(TLC**(5./3.))*(1.+(8./3.)*TLCK)/((1.+TLCK)**(11./6.))
      F(J)=F1*PHISIG
   10 CONTINUE
      RETURN
      END
      SUBROUTINE FUN1
      IMPLICIT REAL*8(A-H,K,O-Z)
      REAL*8 M
      REAL*8 L
      INTEGER APM
      COMMON/INP/H,RHO,VS,AO,ETA,FDEL,FDLDT,W,C,CT,ET,S,ST,AW,AT,FC
     1,KAX(60),KAPPA,KAY,M,L
      COMMON/FLT/APM,NFC,NWT
      COMMON/CALCU/V,VC,PI,APRI,BPRI,SMLA,SMLAT,R0,R1,E,CO1,CO2,CO3,R2,S
     11,MU
      COMMON/INT/BIGK,ASIG,F1,KPRIME,KC,KO,NO
      COMMON/PRT/YDOTSQ,F2,F3,IP,JP
      COMMON/FUNY/F(15),KAG(15),CALF1(15)
      DO 10 J=1,15
      KAY=KAG(J)
      F1=CALF1(J)
      TLC=2.*L/C
      TLCK=(1.339*TLC*KAY)**2
      PHISIG=(TLC**(5./3.))*(1.+(8./3.)*TLCK)/((1.+TLCK)**(11./6.))
      F(J)=(KAY**2)*F1*PHISIG
   10 CONTINUE
      RETURN
      END
      SUBROUTINE CALC
      IMPLICIT REAL*8(A-H,K,O-Z)
      REAL*8 MU,M,NRSQ,NISQ,L
      INTEGER APM
```

```
      COMPLEX*16 DCMPLX,DCONJG,YDOT,YDTC,Y,YTOP,YBOT
      COMPLEX*16 A1COM,A2COM,B1COM,B2COM,C1COM,C2COM
      COMPLEX*16 SOP,ABPHI,ABY,PN,PD,YN,YD,DN,DD,PA1,PB1,PA2,PB2
      COMMON/INP/H,RHO,VS,AO,ETA,FDEL,FDLDT,W,C,CT,ET,S,ST,AW,AT,FC
     1,KAX(60),KAPPA,KAY,M,L
      COMMON/FLT/APM,NFC,NWT
      COMMON/CALCU/V,VC,PI,APRI,BPRI,SMLA,SMLAT,R0,R1,E,CO1,CO2,CO3,R2,S
     11,MU
      COMMON/INT/BIGK,ASIG,F1,KPRIME,KC,KO,NO
      COMMON/PRT/YDOTSQ,F2,F3,IP,JP
      COMMON/FAST/TVC,GK1,GK2,GK3,GK4,GKPHI,GKY
      COMMON/GEN/TPT(4,10),TPB(4,10),TYT(4,10),TYB(4,10),COND(4),CONY(4)
     1,CONP(4),QUADA(4),QUADB(4),TDB(4),QUAPA(4),QUAPB(4),QUAYA(4),QUAYB
     2(4),QUAPTA(4),QUAPTB(4),QUAYTA(4),QUAYTB(4),NS(4),MS(4)
      COMMON/GEN2/K3(4),KPHI(4),NPT,NPB,NYT,NYB
      IF(KAY.EQ.0.)F1=0.0D0
      IF(KAY.EQ.0.)GO TO 800
      OMEGA=TVC*KAY
      SOP=DCMPLX(0.0D0,OMEGA)
      DN=DCMPLX(1.0D0,0.0D0)
      DD=DCMPLX(0.0D0,0.0D0)
      PN=DCMPLX(1.0D0,0.0D0)
      IF(APM.EQ.0)PN=DCMPLX(0.0D0,0.0D0)
      PD=DCMPLX(1.0D0,0.0D0)
      YN=DCMPLX(1.0D0,0.0D0)
      IF(APM.EQ.0)YN=DCMPLX(0.0D0,0.0D0)
      YD=DCMPLX(1.0D0,0.0D0)
      IF(APM.EQ.0)GO TO 50
      DO 10 J=1,NPT
   10 PN=PN*(TPT(APM,J)*SOP+1.)
      DO 20 J=1,NPB
   20 PD=PD*(TPB(APM,J)*SOP+1.)
      DO 30 J=1,NYT
```

```
30  YN=YN*(TYT(APM,J)*SOP+1.)
    DO 40 J=1,NYB
40  YD=YD*(TYB(APM,J)*SOP+1.)
    DD=COND(APM)*GK1*GK2*GK3*(QUADA(APM)*SOP**2+QUADB(APM)*SOP+1.)
    DN=TDB(APM)*SOP/GK4+1.
    PN=CONP(APM)*GKPHI*(QUAPTA(APM)*SOP**2+QUAPTB(APM)*SOP+1.)*PN
    PD=(QUAPA(APM)*SOP**2+QUAPB(APM)*SOP+1.)*(SOP**NS(APM))*PD
    YN=CONY(APM)*GKY*(V/57.3)*(QUAYTA(APM)*SOP**2+QUAYTB(APM)*SOP+1.)*
   1YN
    YD=(QUAYA(APM)*SOP**2+QUAYB(APM)*SOP+1.)*(SOP**MS(APM))*YD
50  STAB=FDLDT*CO2*KAY
    TAIL=-DCMPLX(FDEL,STAB)
    ABPHI=TAIL*(DD/DN)*(PN/PD)
    ABY=TAIL*(DD/DN)*(YN/YD)
    PAR1=-2.*MU*TVC*(KAY**2.)
    PAI1=TVC*(R0+R1*(1.-ETA))*KAY
    PBR1=-(R0+R1*(1.-ETA))
    PBI1=(R0*(2.*CO3-1.)-R1*R2)*KAY
    C1=R0+R1*(DCOS(KAY*S1)-ETA)
    C1BAR=-R1*DSIN(KAY*S1)
    PAR2=0.0D0
    PAI2=TVC*(CO3*R0-CO1*R1*(1.-ETA))*KAY
    PBR2=-(CO3*R0-CO1*R1*(1.-ETA)+4.*MU*(KAPPA**2)*(KAY**2)/(C**2))
    PBI2=(CO3*R0*(2.*CO3-1.)+CO1*R1*R2)*KAY
    C2=CO3*R0-CO1*R1*(DCOS(KAY*S1)-ETA)
    C2BAR=CO1*R1*DSIN(KAY*S1)
    PA1=DCMPLX(PAR1,PAI1)
    PB1=DCMPLX(PBR1,PBI1)
    PA2=DCMPLX(PAR2,PAI2)
    PB2=DCMPLX(PBR2,PBI2)
    A1COM=R1*ABY+PA1
    A2COM=-CO1*R1*ABY+PA2
    B1COM=R1*ABPHI+PB1
```

```
      B2COM=-CO1*R1*ABPHI+PB2
      C1COM=DCMPLX(C1,C1BAR)
      C2COM=DCMPLX(C2,C2BAR)
      YTOP=C1COM*B2COM-C2COM*B1COM
      YBOT=A1COM*B2COM-A2COM*B1COM
      Y=YTOP/YBOT
  700 YDOT=TVC*KAY*Y
      YDTC=DCONJG(YDOT)
      YDOTSQ=YDOT*YDTC
      BETASQ=1.-(M**2)
      F2=1./(1.+(1.5*PI*KAY/BETASQ)+((PI**2)*M*(KAY**2)/BETASQ))
      F3=1./(1.+(.55*AW*KAY))
      F1=4.*(MU**2)*(KAY**2)*YDOTSQ*F2*F3
  800 RETURN
      END
      SUBROUTINE PRINT
      IMPLICIT REAL*8(A-H,K,O-Z)
      REAL*8 MU,M,L,NO
      INTEGER APM
      COMMON/INP/H,RHO,VS,AO,ETA,FDEL,FDLDT,W,C,CT,ET,S,ST,AW,AT,FC
     1,KAX(60),KAPPA,KAY,M,L
      COMMON/FLT/APM,NFC,NWT
      COMMON/CALCU/V,VC,PI,APRI,BPRI,SMLA,SMLAT,R0,R1,E,CO1,CO2,CO3,R2,S
     11,MU
      COMMON/INT/BIGK,ASIG,F1,KPRIME,KC,KO,NO
      COMMON/PRT/YDOTSQ,F2,F3,IP,JP
      COMMON/FAST/TVC,GK1,GK2,GK3,GK4,GKPHI,GKY
      DIMENSION F1X(60),YDTSQ(60),F2X(60),F3X(60),FISIG(60)
      IPRT=0
      IF(NWT.NE.2)GO TO 20
      IPRT=1
      DO 10 J=1,41
      KAY=KAX(J)
```

```
      CALL CALC
      F1X(J)=F1
      TLC=2.*L/C
      TLCK=(1.339*TLC*KAY)**2
      YDTSQ(J)=YDOTSQ
      F2X(J)=F2
      F3X(J)=F3
      FISIG(J)=(TLC**(5./3.))*(1.+(8./3.)*TLCK)/((1.+TLCK)**(11./6.))
10    CONTINUE
20    CONTINUE
      JP=JP+1
      KP=(JP-1)/3
      KP=3*KP+1
      IF(JP.EQ.KP)IP=IP+1
      IF(JP.EQ.KP)WRITE(6,30)IP
      CALL CODE(NFC,NWT,APM)
      ASIG=VC*BIGK/(32.2*MU)
      ASIGVC=ASIG/VC
      WRITE(6,40)M,H,V,VC,MU,KC
      WRITE(6,50)AO,SMLA,SMLAT
      WRITE(6,60)R0,R1,R2,S1
      WRITE(6,70)BIGK,KPRIME,ASIG,ASIGVC,KO,NO
      IF(IPRT.EQ.0)GO TO 100
      IP=IP+1
      JP=0
      WRITE(6,30)IP
      CALL CODE(NFC,NWT,APM)
      WRITE(6,80)
      DO 90 J=1,41
      KAY=KAX(J)
      F2F3=F2X(J)*F3X(J)
      FUNF1=F1X(J)*FISIG(J)
      FUN1F1=(KAY**2)*FUNF1
```

```
      GFPSD=KAY*F1X(J)*FISIG(J)
      GNFPSD=((VC/(32.2*MU))**2)*GFPSD/(PI*(TLC**(2./3.)))
      ANFPSD=GFPSD/(BIGK**2)
      WRITE(6,85)KAY,YDTSQ(J),F2F3,F1X(J),FISIG(J),FUNF1,FUN1F1,GFPSD,GN
     1FPSD,ANFPSD
   90 CONTINUE
  100 RETURN
   30 FORMAT('1',10X,'GUST RESPONSE INTEGRATIONS',10X,'PAGE',I3///)
   40 FORMAT(6X,'M',10X,'H',10X,'V',9X,'V/C',8X,'MU',9X,'KC',/,1X,1P6E11
     1.3/)
   50 FORMAT(5X,'AO',10X,'A',9X,'AT',/,1X,1P3E11.3/)
   60 FORMAT(5X,'R0',9X,'R1',9X,'R2',9X,'S1',/,1X,1P4E11.3/)
   70 FORMAT(6X,'K',8X,'KPRIME',7X,'ASIG',5X,'ASIG/V/C',6X,'KO',9X,'NO',
     1/,1X,1P6E11.3//////)
   80 FORMAT(5X,'KAY',8X,'YDOTSQ',5X,'F2*F3',7X,'F1',7X,'PHI/SIG',2X,'F1
     1*PHI/SIG',2X,'KSQ*F1*PHI/SIG',3X,'GFPSD',5X,'GNFPSD',5X,'ANFPSD',/
     1)
   85 FORMAT(1X,1P6E11.3,3X,1PE11.3,2X,1P3E11.3/)
      END
      SUBROUTINE CODE(NFC,NWT,APM)
      INTEGER APM
      WRITE(6,800)
      IF(NWT.NE.1)GOTO 620
      WRITE(6,600)NFC,APM
      GO TO 700
  620 IF(NWT.NE.2)GOTO 660
      WRITE(6,640)NFC,APM
      GOTO 700
  660 WRITE(6,680)NFC,APM
  700 WRITE(6,800)
      RETURN
  600 FORMAT(1X,'CASE NUMBER',2X,I2,'-A-',I1)
  640 FORMAT(1X,'CASE NUMBER',2X,I2,'-B-',I1)
```

```
680 FORMAT(1X,'CASE NUMBER',2X,I2,'-C-',I1)
800 FORMAT(1X,'--------------------')
    END
```

REFERENCES

1. Houbolt, J. C.;and Williamson, G. G.: Spectral Gust Response For An Airplane with Vertical Motion and Pitch. AFFDL-TR-75-121 Air Force Flight Dynamics Lab., October, 1975.
2. Houbolt, J. C.: On Turbulence Environment and Design Criteria. AGARD Conference Proceedings No. 140 on Flight in Turbulence, 1974, pp. 14.1-14.15.
3. Houbolt, J. C.: Dynamic Response of Airplanes to Atmospheric Turbulence Including Flight Data on Input and Response. NASA TR R-199, June, 1964.
4. Iliff, K. W.: Identification and Stochastic Control of an Aircraft Flying in Turbulence. Journal of Guidance and Control, Vol. 1, March-April 1978, pp. 101-108.
5. Chapman, J. W.: Correlation of Measured and Analytical Continuous Turbulence Loads and Accelerations. Proceedings of AIAA/ASME 18th Structures, Structural Dynamics and Materials Conference, Vol. B, 1977, pp. 10-18.
6. Ingram, C. T.; and Eichenbaum, F. D.: A Comparison of C-141A Flight Test Measured and Theoretical Vertical Gust Response. Journal of Aircraft, Vol. 6, Nov-Dec 1969, pp. 532-536.
7. Dempster, J. B.; and Roger, K. L.: Evaluation of B-52 Structural Response to Random Turbulence with Stability Augmentation Systems. Journal of Aircraft, Vol. 4, Nov-Dec 1967, pp. 507-512.
8. Hunter, P. A.: Initial VGH Data on Operations of Small Turbojets in Commercial Transport Service. Journal of Aircraft, Vol. 4, Nov-Dec 1967, pp. 513-517.

9. Firebaugh, J. M.: Evaluations of a Spectral Gust Model Using VGH and V-G Flight Data. Journal of Aircraft, Vol. 4, Nov-Dec 1967, pp. 518-525.

10. Goldberg, J. H.: Analysis of AFFDL-TR-75-121 Extended to Include a Longitudinal Motion Control Autopilot. NASA-ASEE 1979 Summer Faculty Fellowship Program, September, 1979.

AIRPLANE	A			B			C			D		
S_t/S	0.371			0.267			0.367			0.241		
c_t/c	0.803			0.716			0.815			0.758		
e_t/c	2.61			3.69			2.43			4.24		
k/c	1.55			1.48			1.56			1.97		
FLIGHT CONDITION	C/D	LO CR	HI CR	C/D	LO CR	HI CR	C/D	LO CR	HI CR	C/D	LO CR	HI CR
M	0.50	0.80	.89	0.56	0.81	0.85	0.50	0.80	.89	0.58	0.81	0.84
hp(1000 ft)	20	30	40	15	30	38	20	30	40	10	28	32
a/a_0	0.950	0.950	0.950	0.896	0.906	0.912	0.867	0.889	0.910	0.880	0.894	0.903
a_t/a_0	0.798	0.778	0.749	0.741	0.741	0.733	0.719	0.721	0.706	0.682	0.661	0.656
$r_1(1-\eta)$	0.148	0.118	0.110	0.104	0.094	0.088	0.133	0.111	0.090	0.120	0.106	0.097
e/c	0.030	0.030	0.030	0.157	0.123	0.096	0.156	0.101	0	0.274	0.279	0.239
k_c	0.162	0.106	0.098	0.112	0.082	0.080	0.179	0.117	0.108	0.113	0.088	0.086

Table 1 Airplane Characteristics

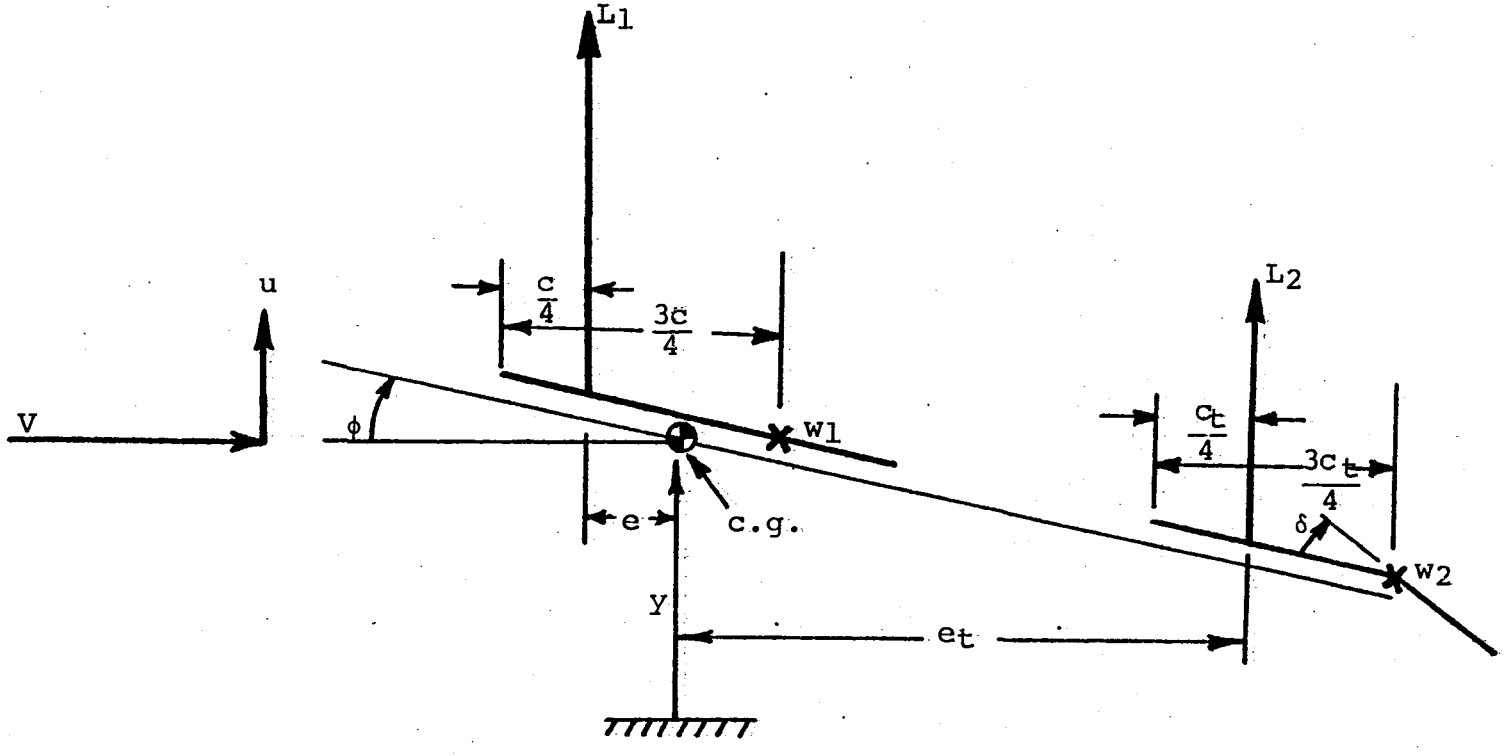

Figure 1.- Wing and tail lift, geometry, and notation, all dimensions and angles are positive as shown.

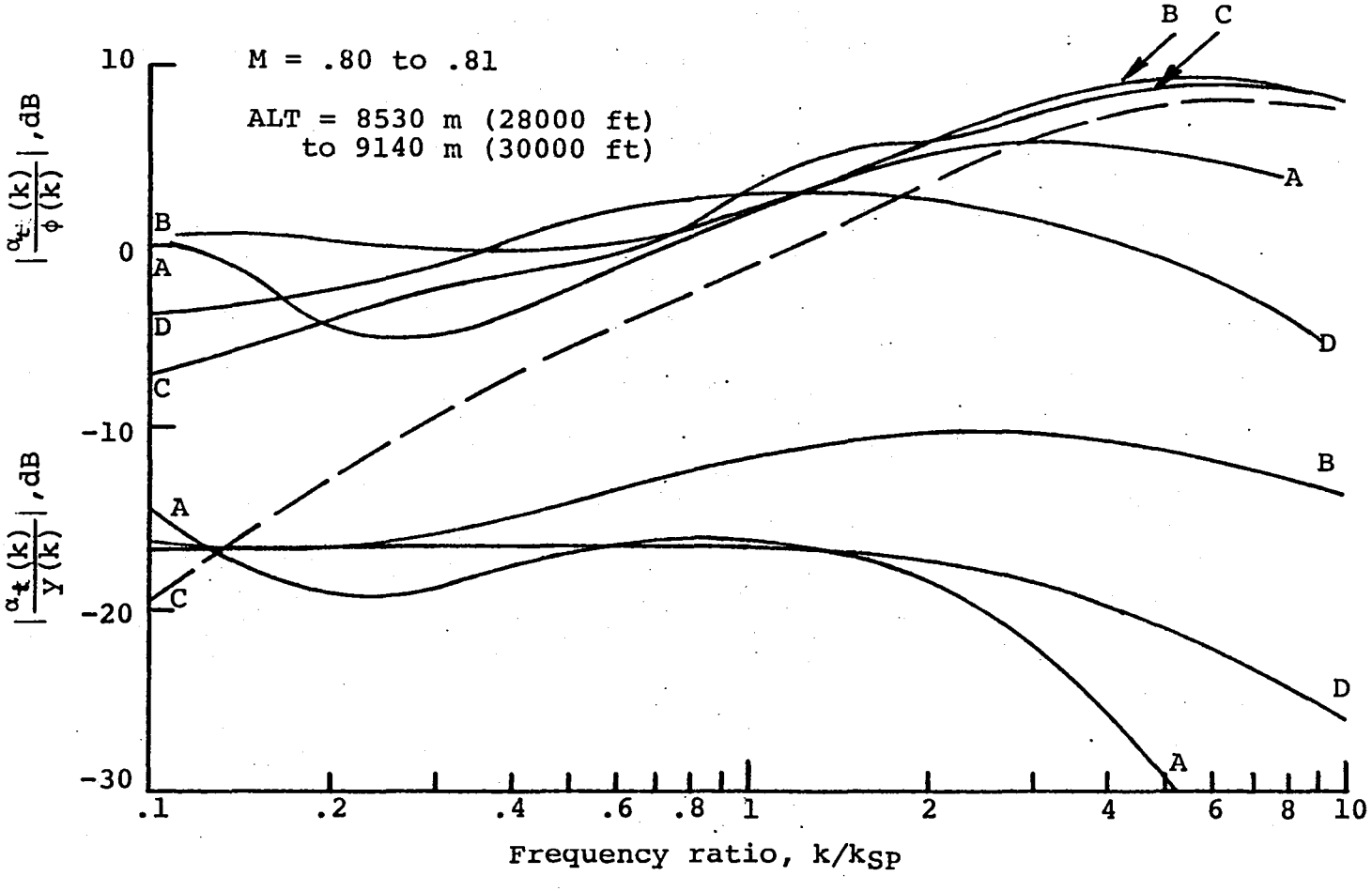

Figure 2.- Autopilot frequency response, Low Cruise, A/P mode Cruise.

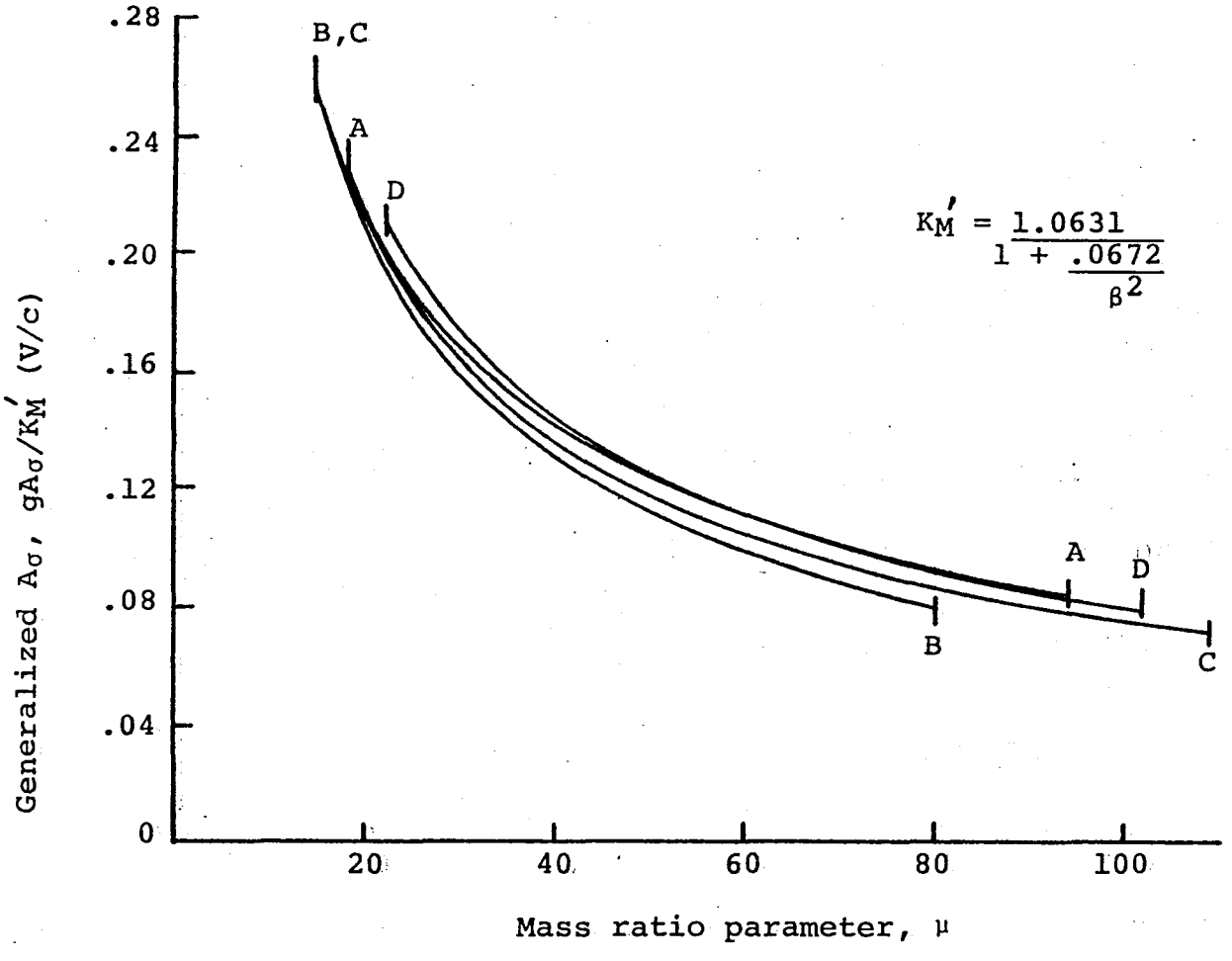

Figure 3.- Generalized A_σ versus mass ratio, A/P mode Off.

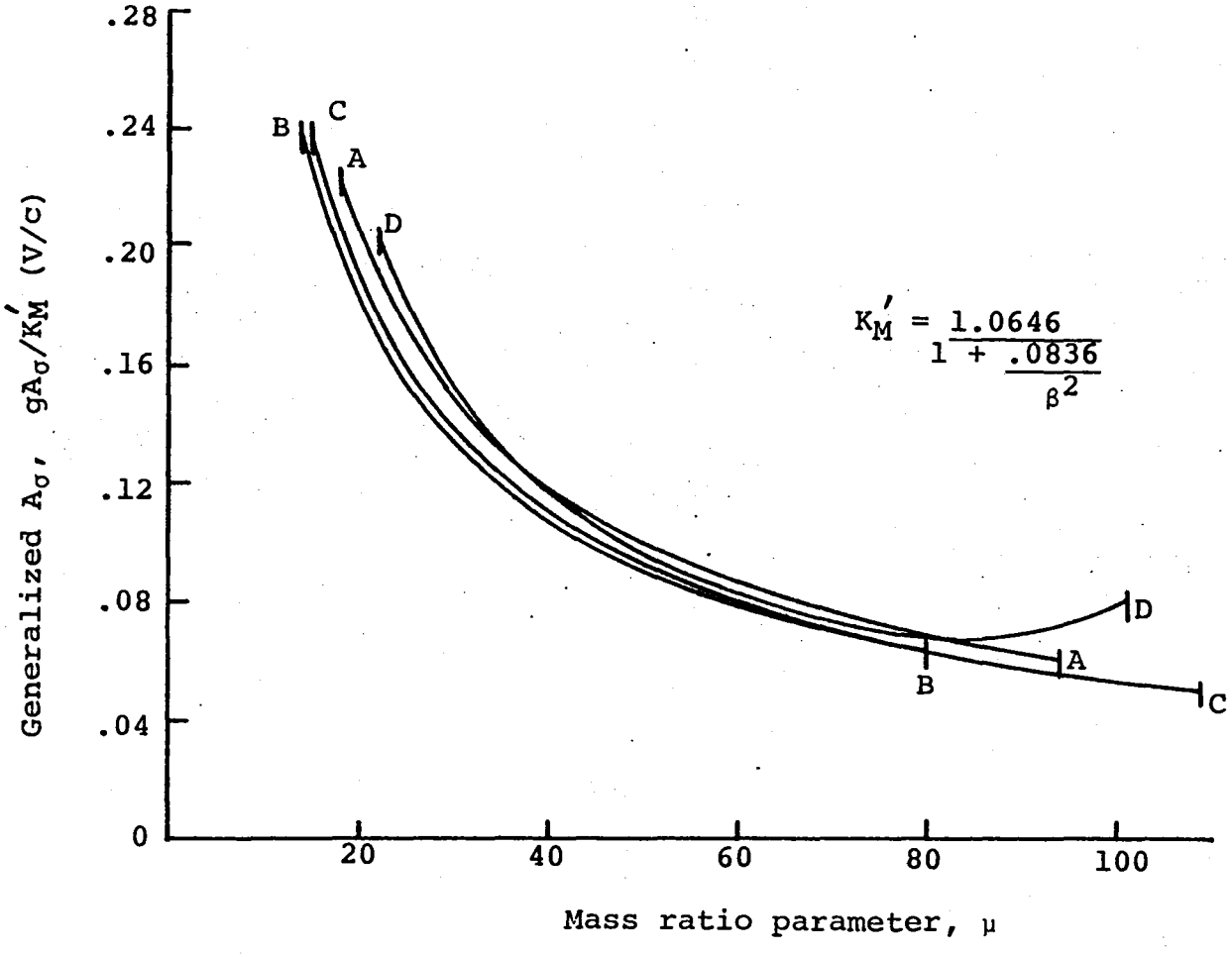

Figure 4.- Generalized A_σ versus mass ratio, A/P mode Climb/Descent.

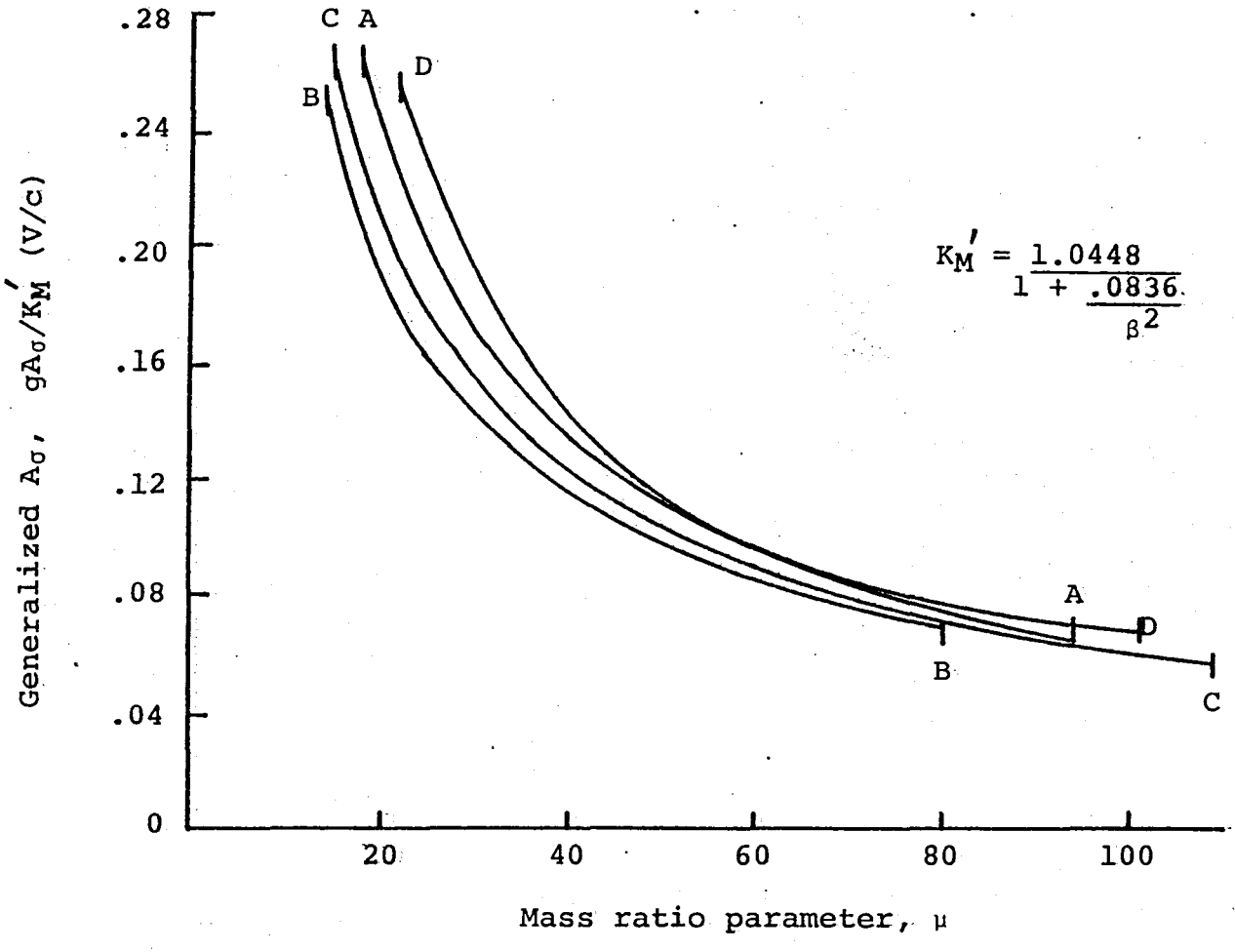

Figure 5.- Generalized A_σ versus mass ratio, A/P mode Cruise.

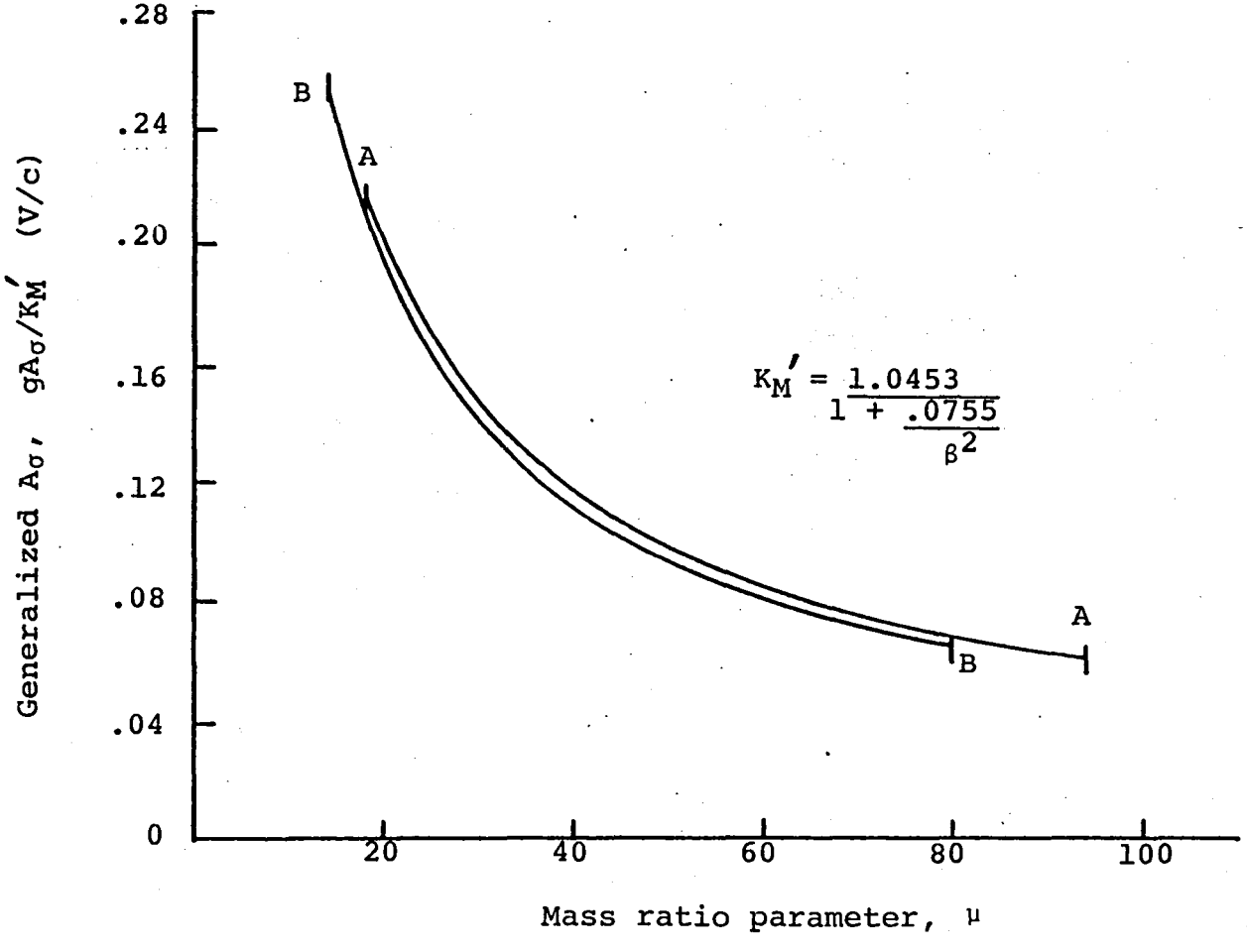

Figure 6.- Generalized A_σ versus mass ratio, A/P mode Turbulent.

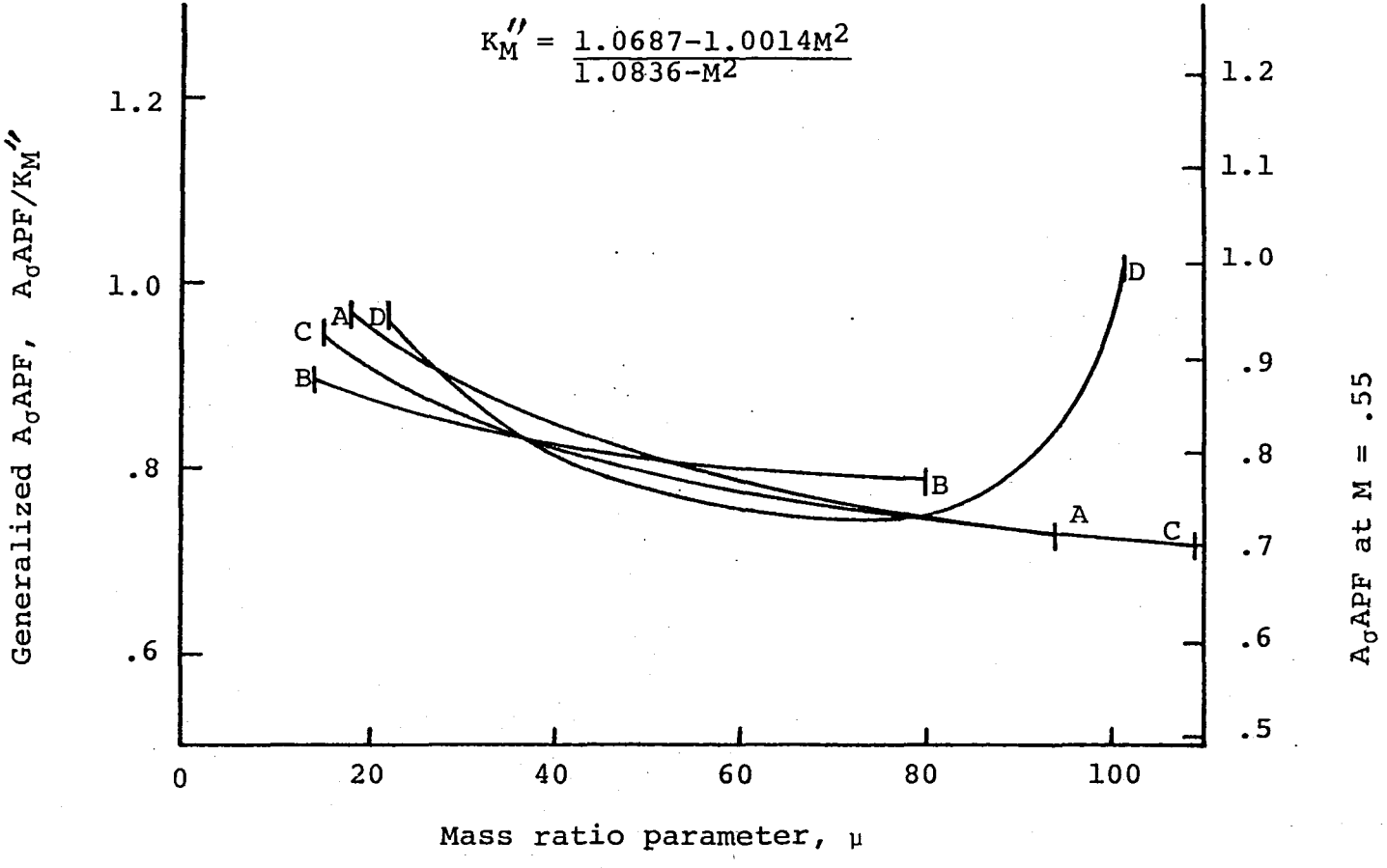

Figure 7.- Generalized $A_\sigma APF$ versus mass ratio parameter, A/P mode Climb/Descent.

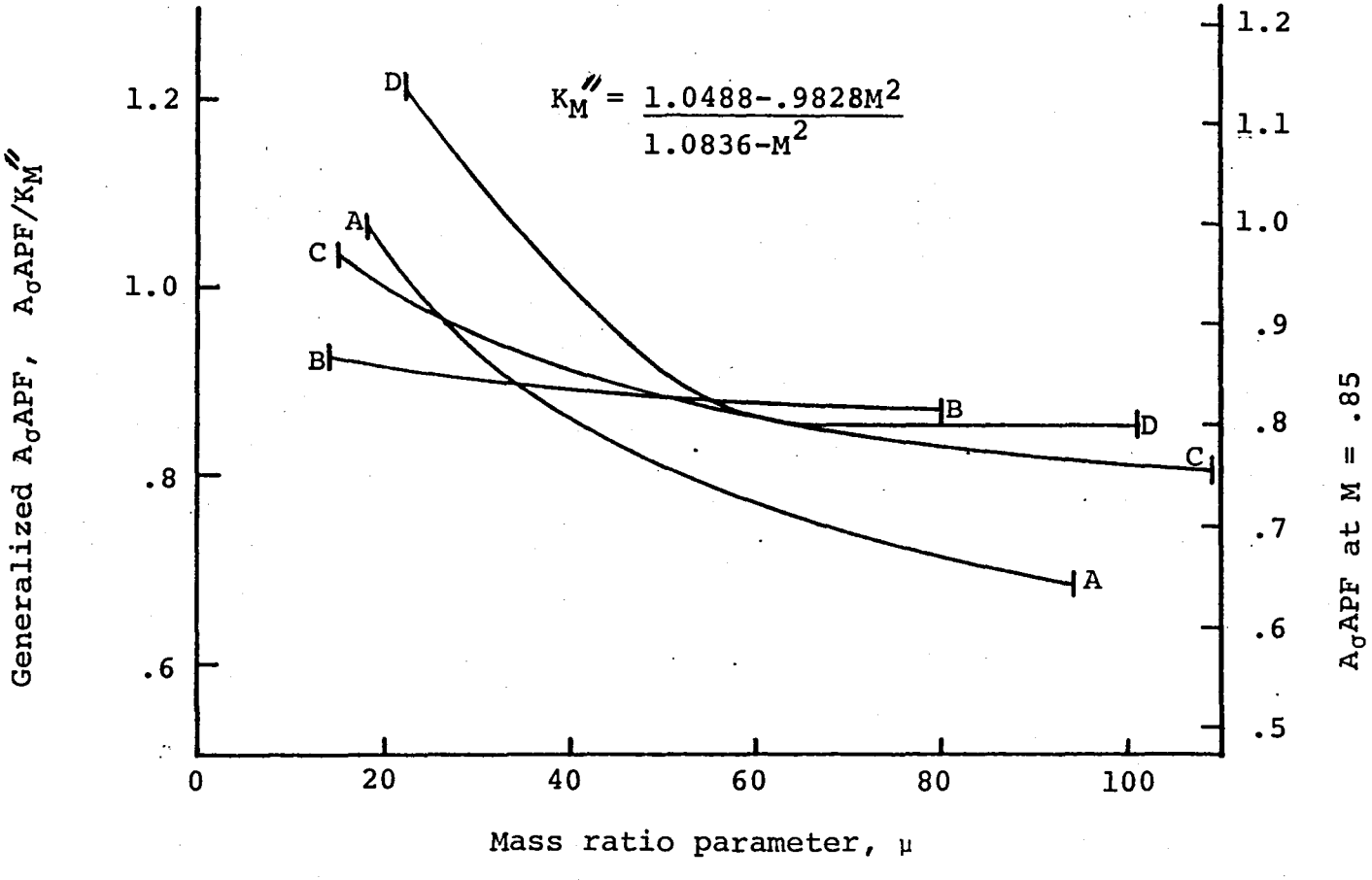

Figure 8.- Generalized $A_\sigma APF$ versus mass ratio parameter, A/P mode Cruise.

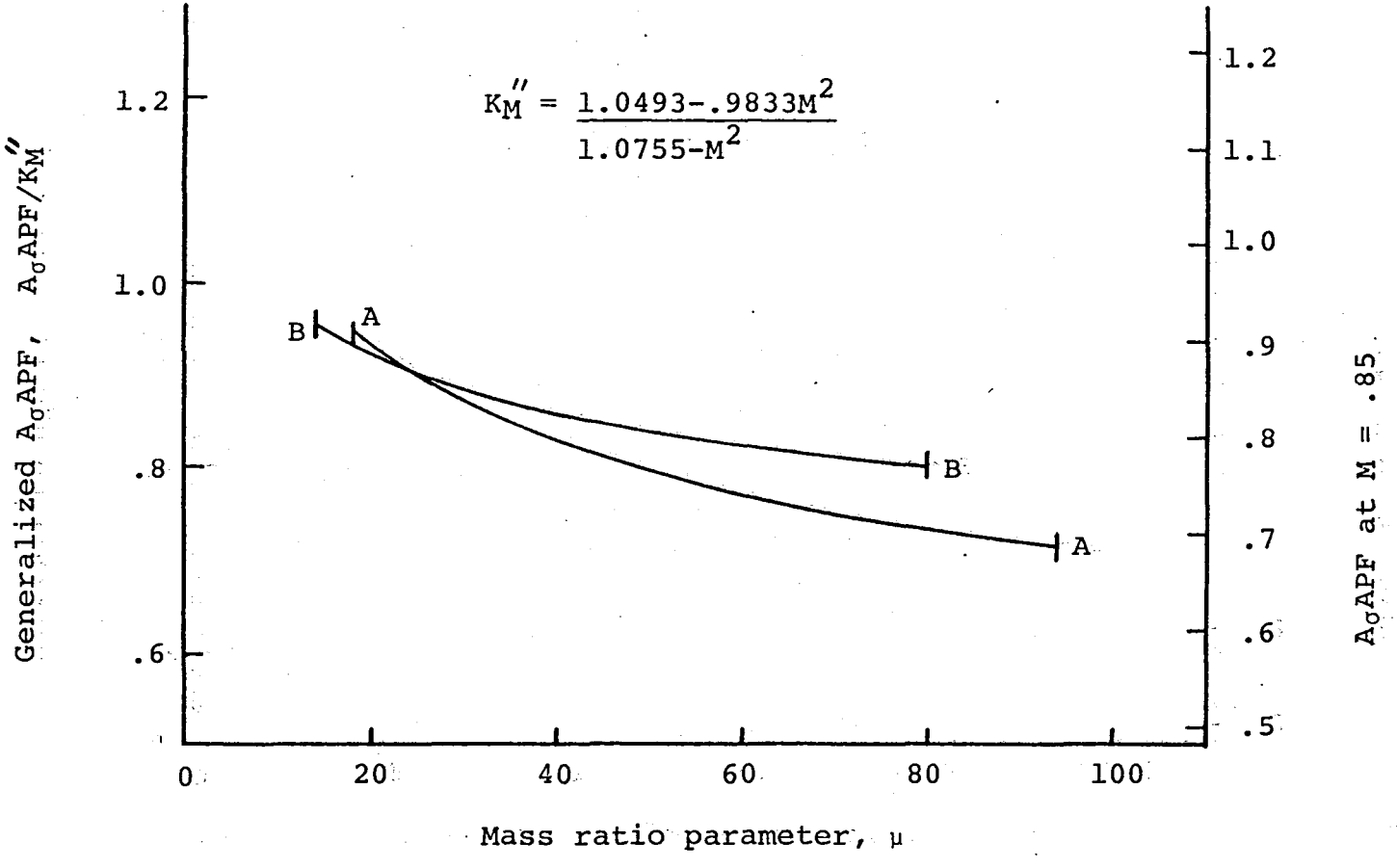

Figure 9.- Generalized $A_\sigma APF$ versus mass ratio parameter, A/P mode Turbulent.

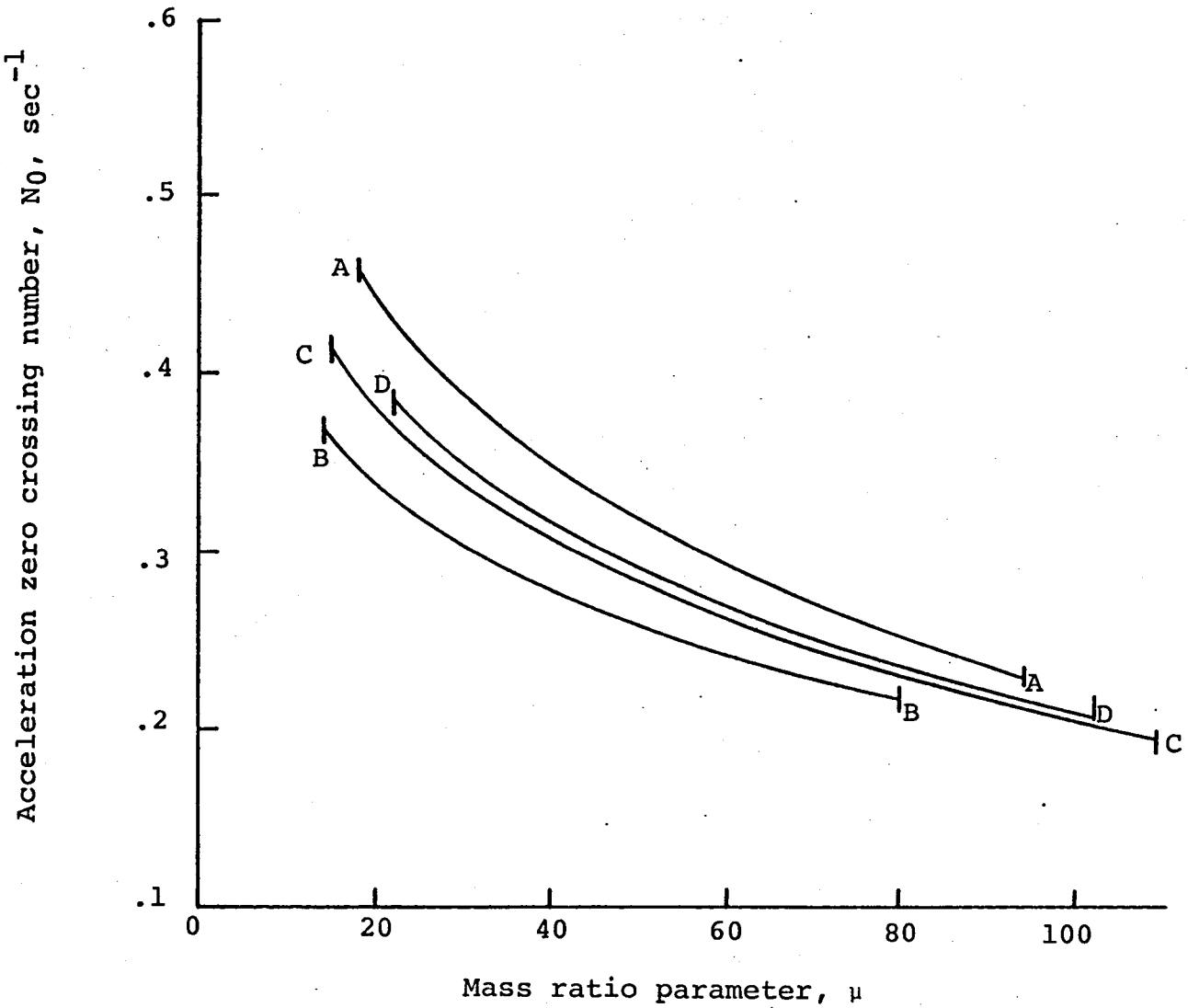

Figure 10.- Acceleration increment zero crossing number versus mass ratio parameter, A/P mode Off, V/c = 20 sec^{-1}.

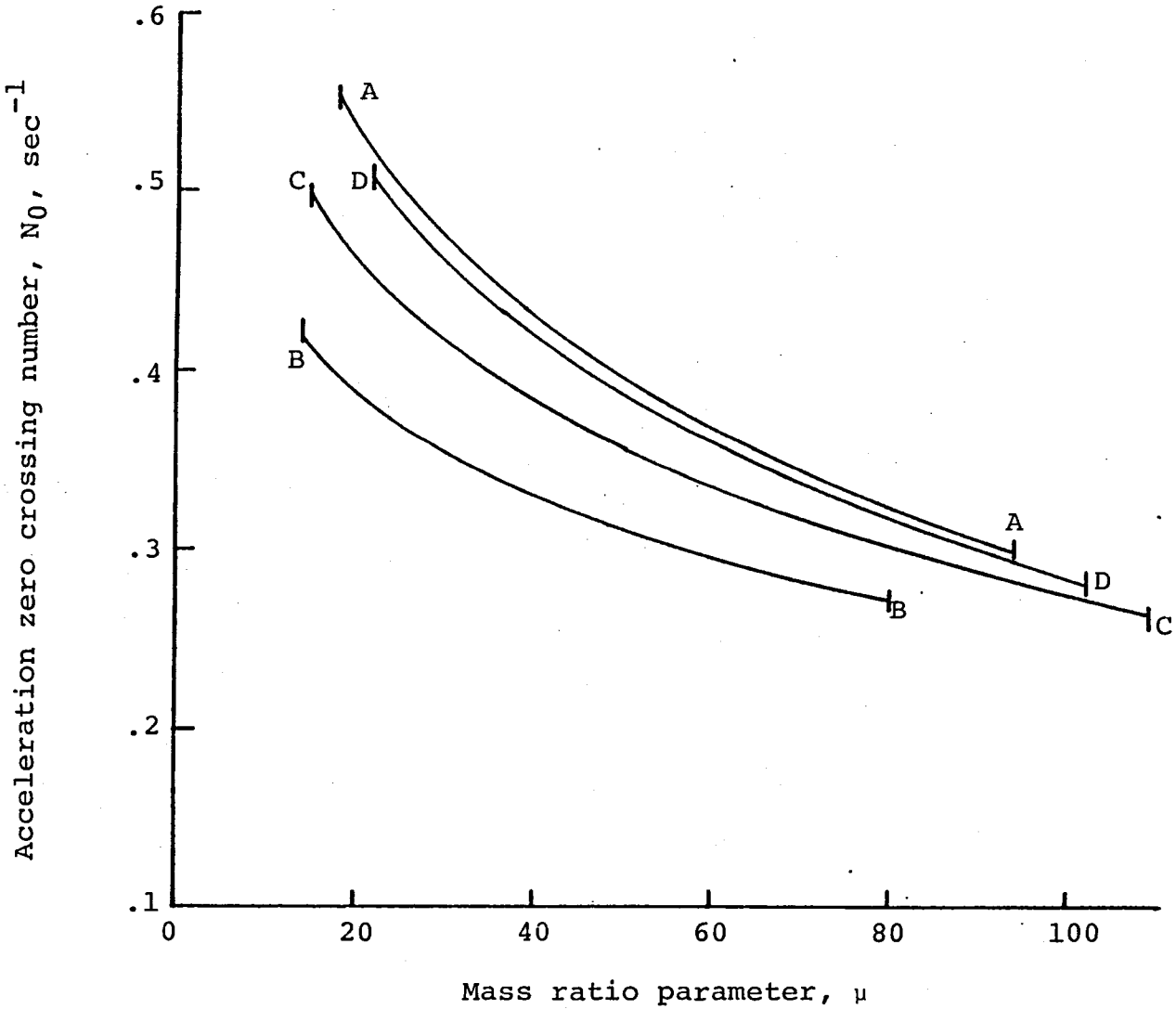

Figure 11.- Acceleration increment zero crossing number versus mass ratio parameter, A/P mode Off, V/c = 30 sec^{-1}.

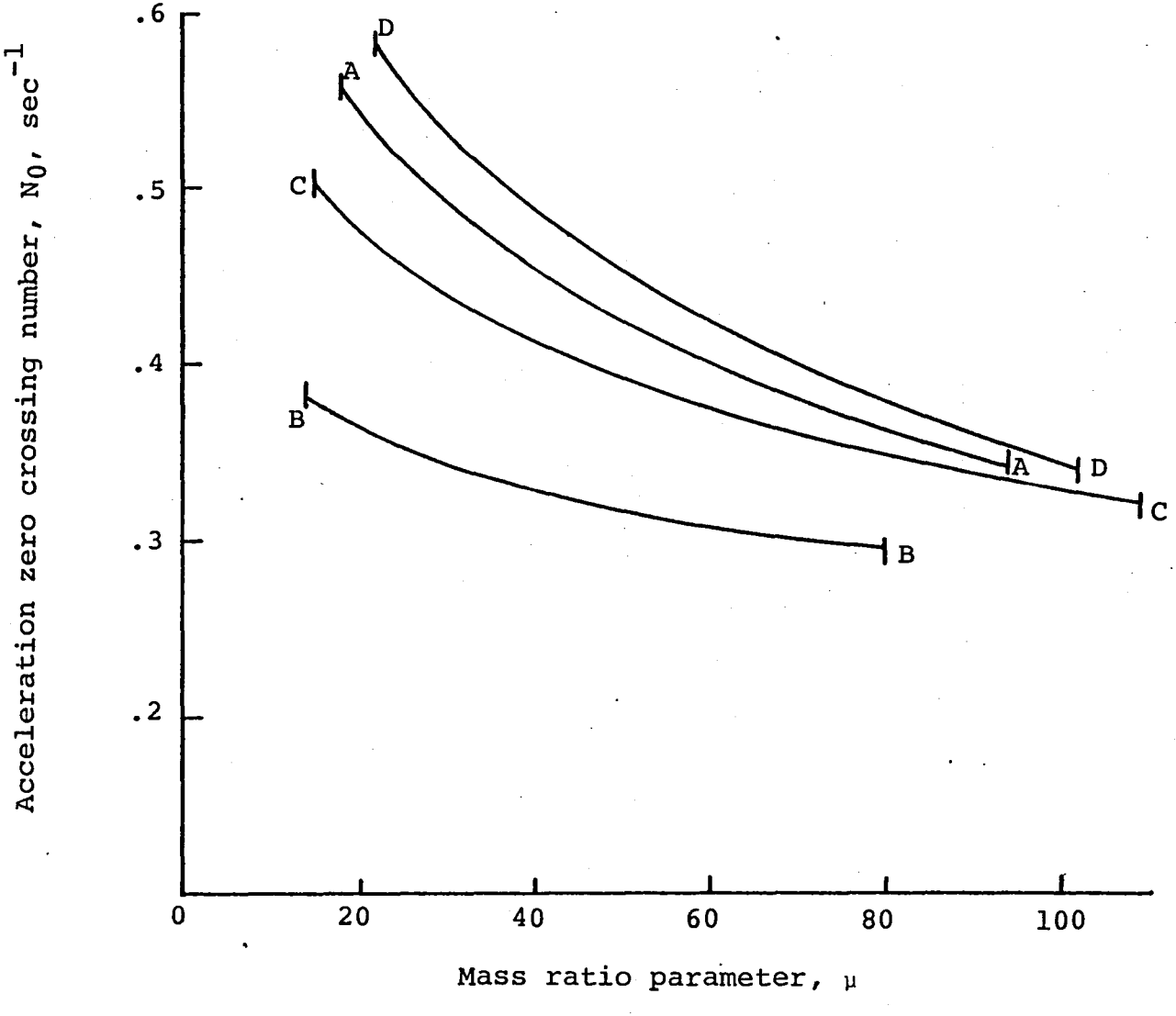

Figure 12.- Acceleration increment zero crossing number versus mass ratio parameter, A/P mode Off, V/c = 40 sec^{-1}.

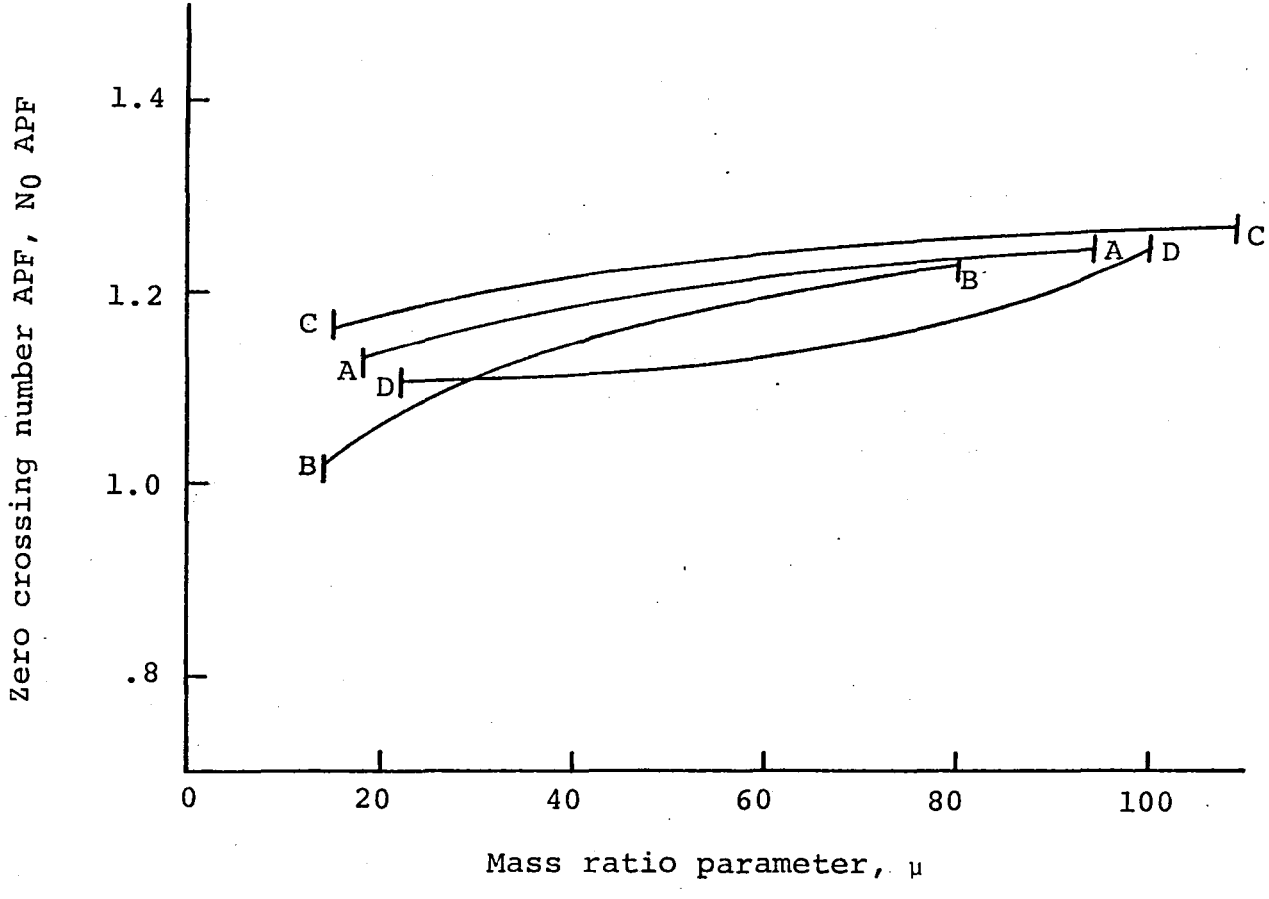

Figure 13.- Zero crossing number APF versus mass ratio parameter, A/P mode Climb/Descent, V/c = 20 sec^{-1}.

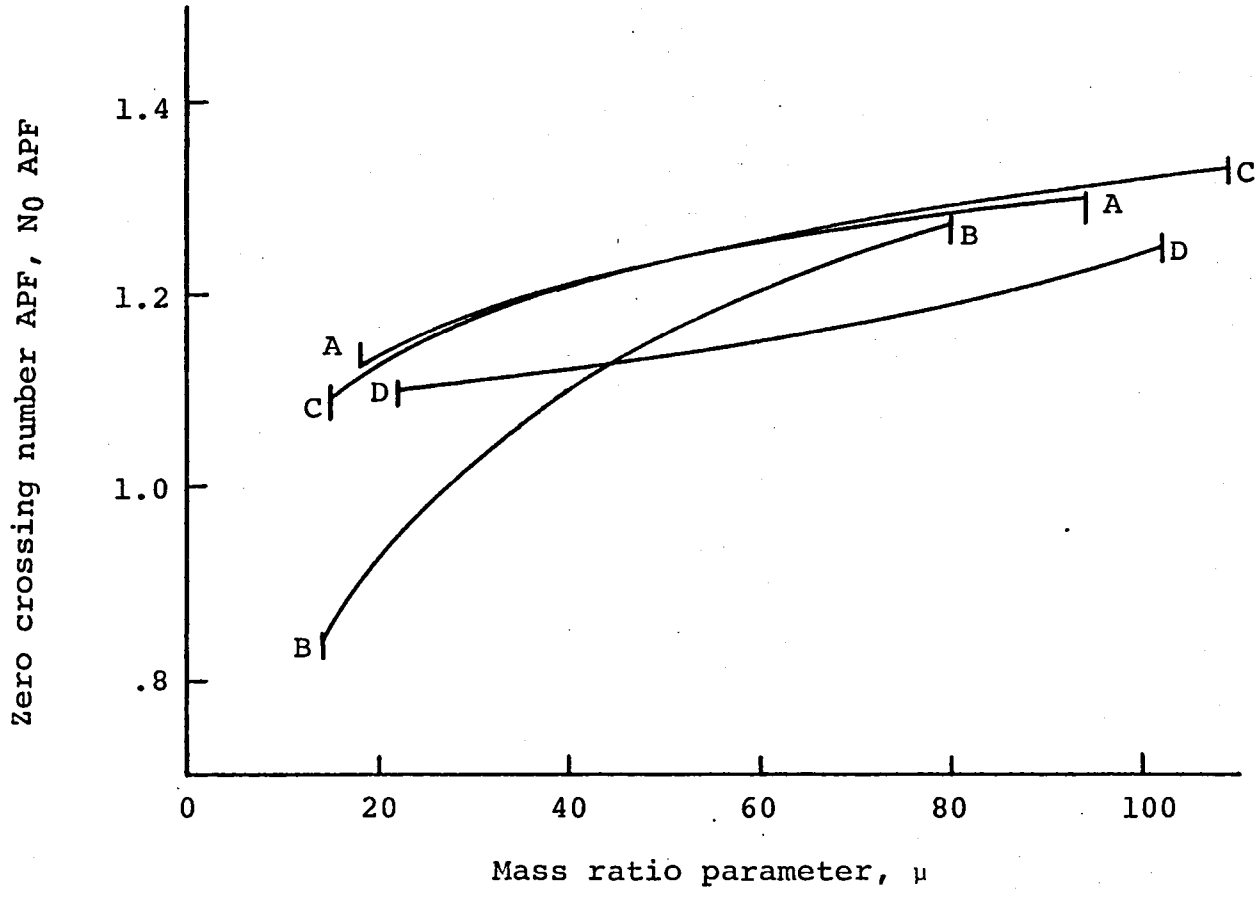

Figure 14.- Zero crossing number APF versus mass ratio parameter, A/P mode Climb/Descent, V/c = 30 sec^{-1}.

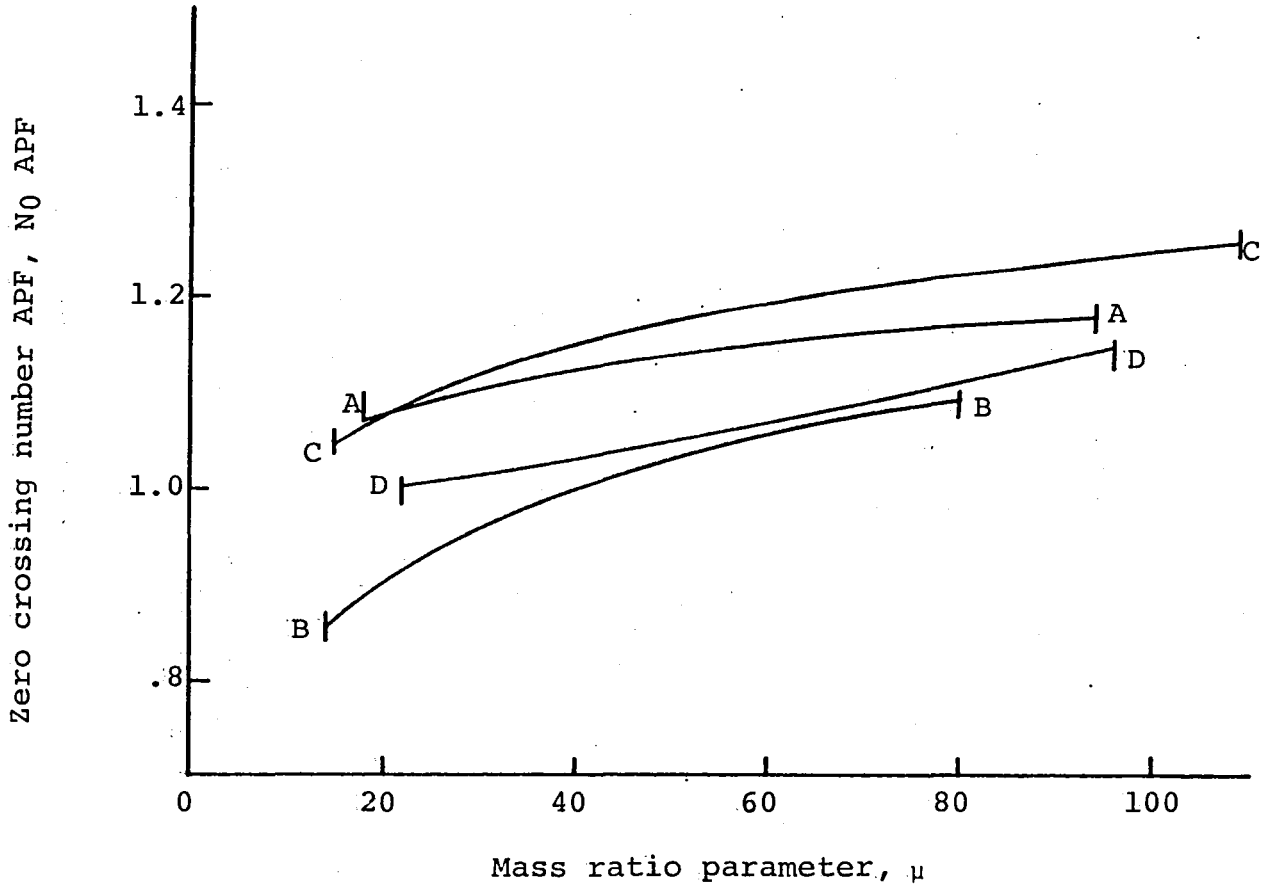

Figure 15.- Zero crossing number APF versus mass ratio parameter, A/P mode Cruise, V/c = 30 sec^{-1}.

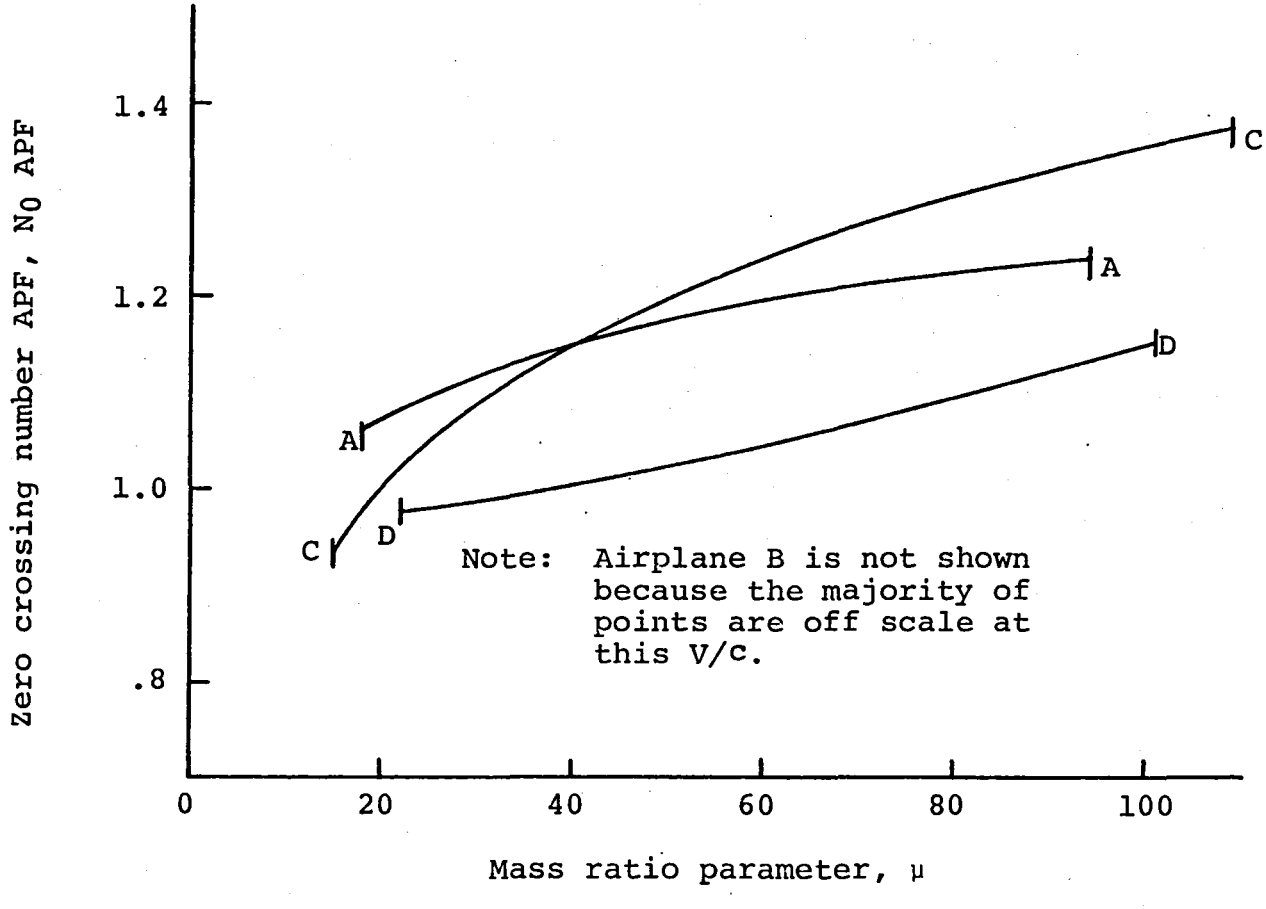

Figure 16.- Zero crossing number APF versus mass ratio parameter, A/P mode Cruise, V/c = 40 sec^{-1}.

Figure 17.- Zero crossing number APF versus mass ratio parameter, A/P mode Turbulent, V/c = 30 sec^{-1}.

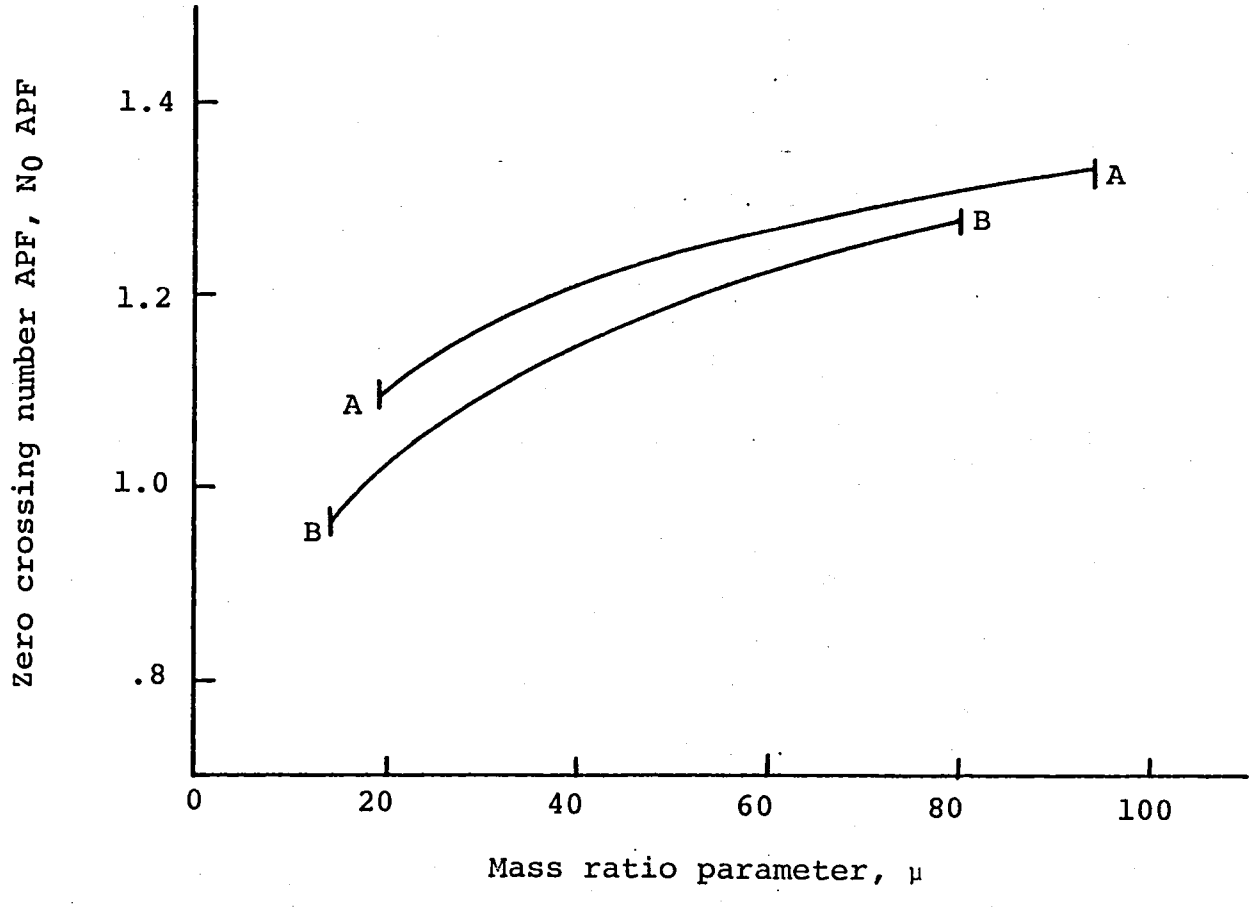

Figure 18.- Zero crossing number APF versus mass ratio parameter, A/P mode Turbulent, V/c = 40 sec^{-1}.

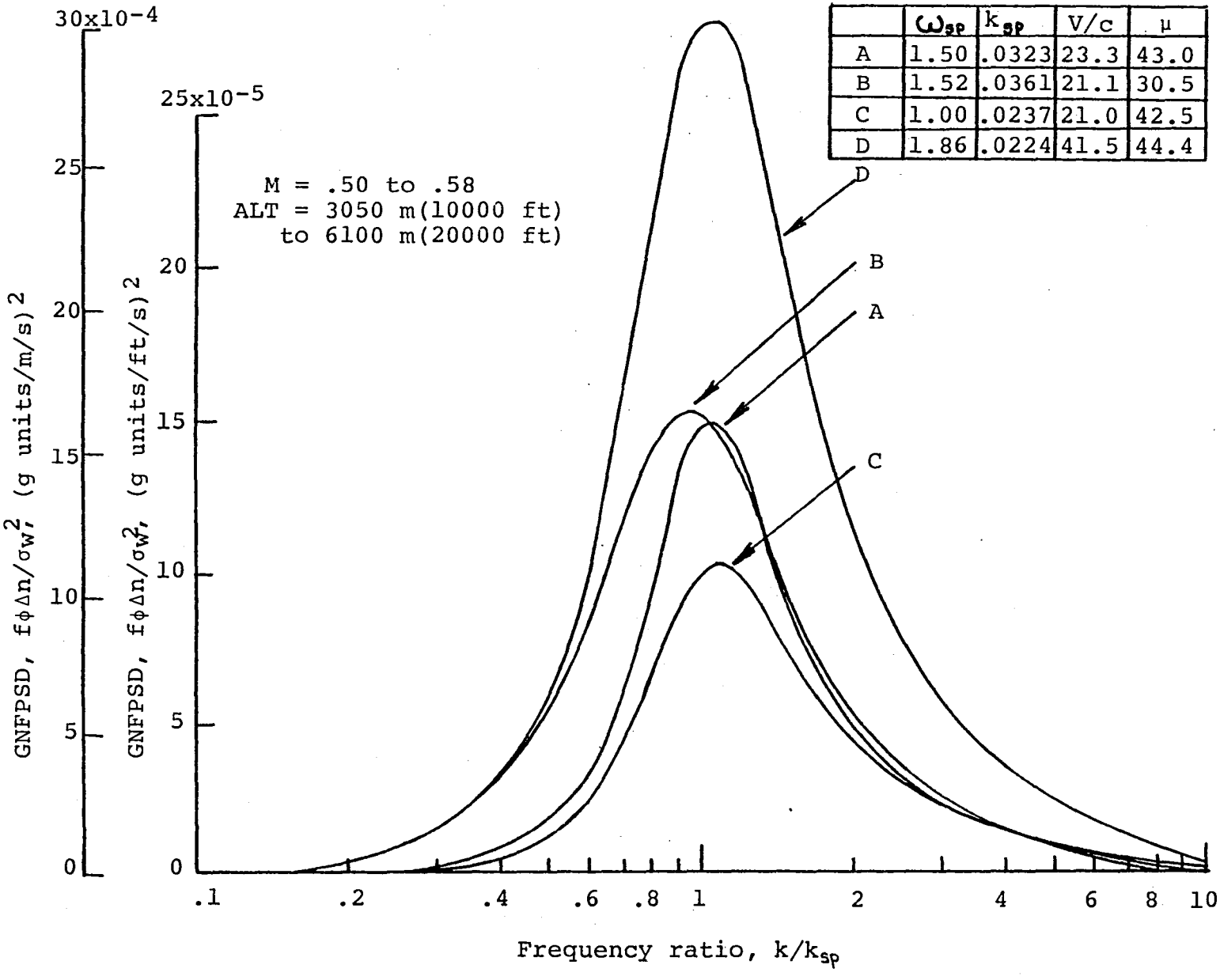

	ω_{sp}	k_{sp}	V/c	μ
A	1.50	.0323	23.3	43.0
B	1.52	.0361	21.1	30.5
C	1.00	.0237	21.0	42.5
D	1.86	.0224	41.5	44.4

Figure 19.- GNFPSD versus frequency ratio, Climb and descent, A/P mode Off.

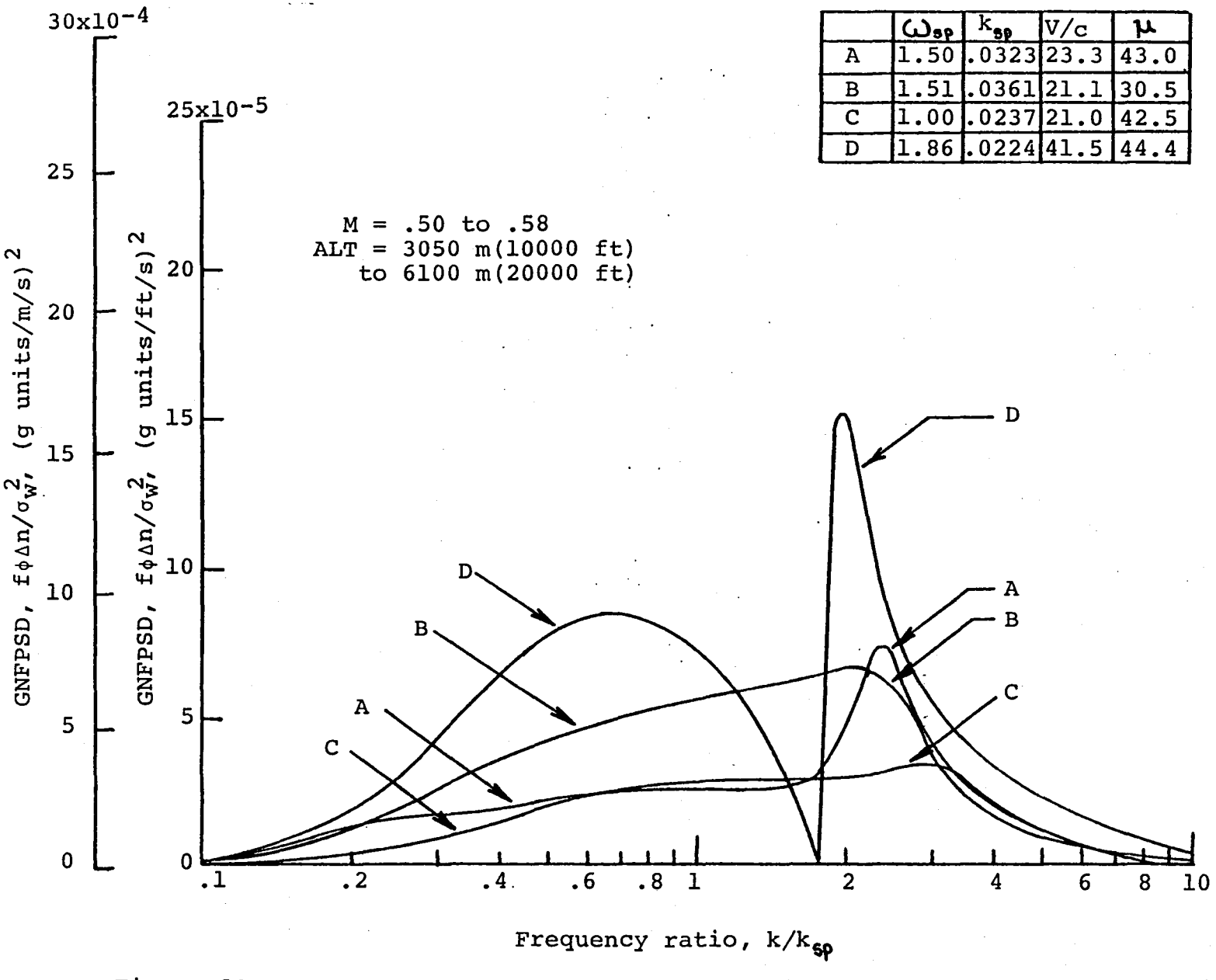

	ω_{sp}	k_{sp}	V/c	μ
A	1.50	.0323	23.3	43.0
B	1.51	.0361	21.1	30.5
C	1.00	.0237	21.0	42.5
D	1.86	.0224	41.5	44.4

Figure 20.- GNFPSD versus frequency ratio, Climb and descent, A/P mode Climb/Descent.

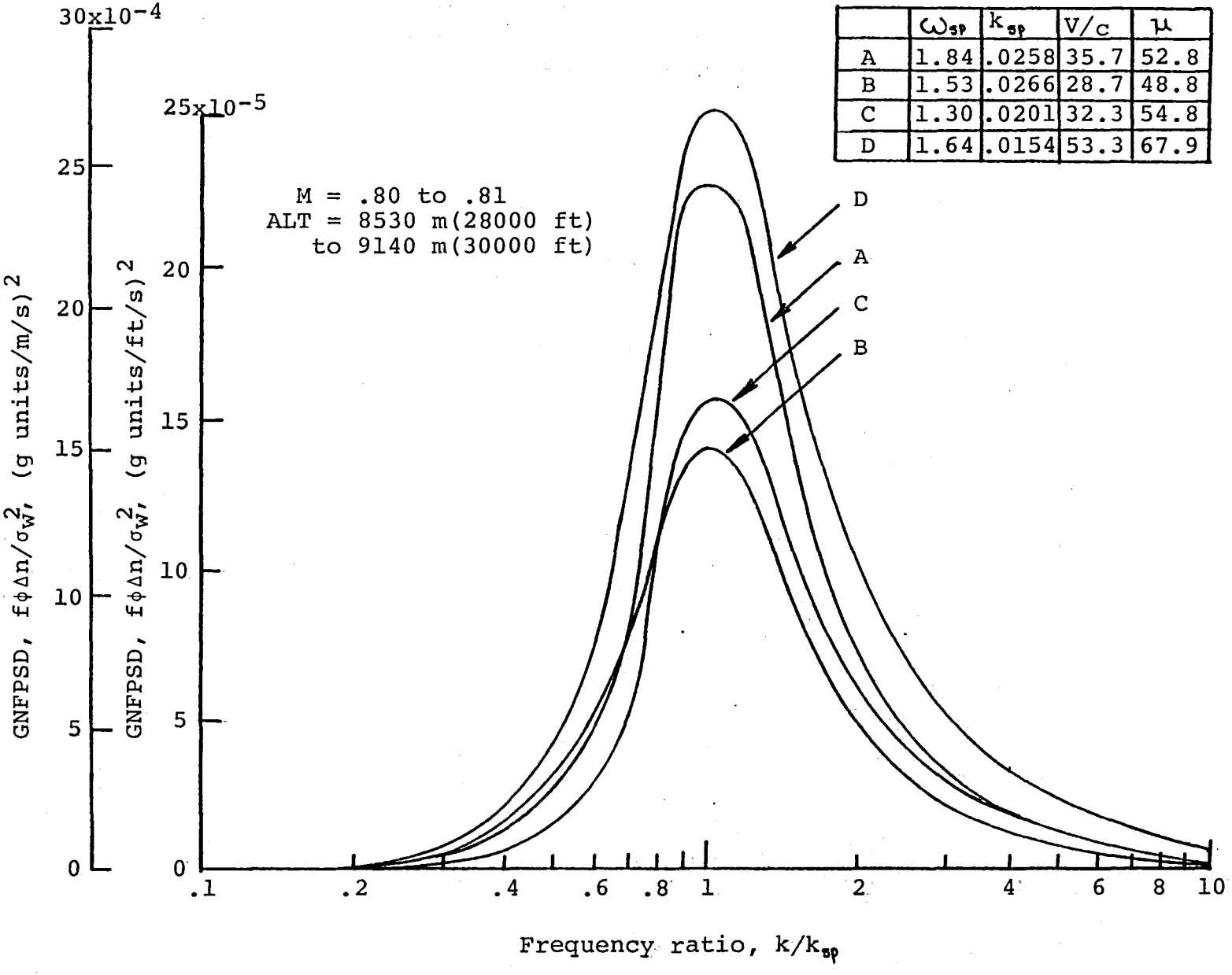

	ω_{sp}	k_{sp}	V/c	μ
A	1.84	.0258	35.7	52.8
B	1.53	.0266	28.7	48.8
C	1.30	.0201	32.3	54.8
D	1.64	.0154	53.3	67.9

Figure 21.- GNFPSD versus frequency ratio, Low cruise, A/P mode Off.

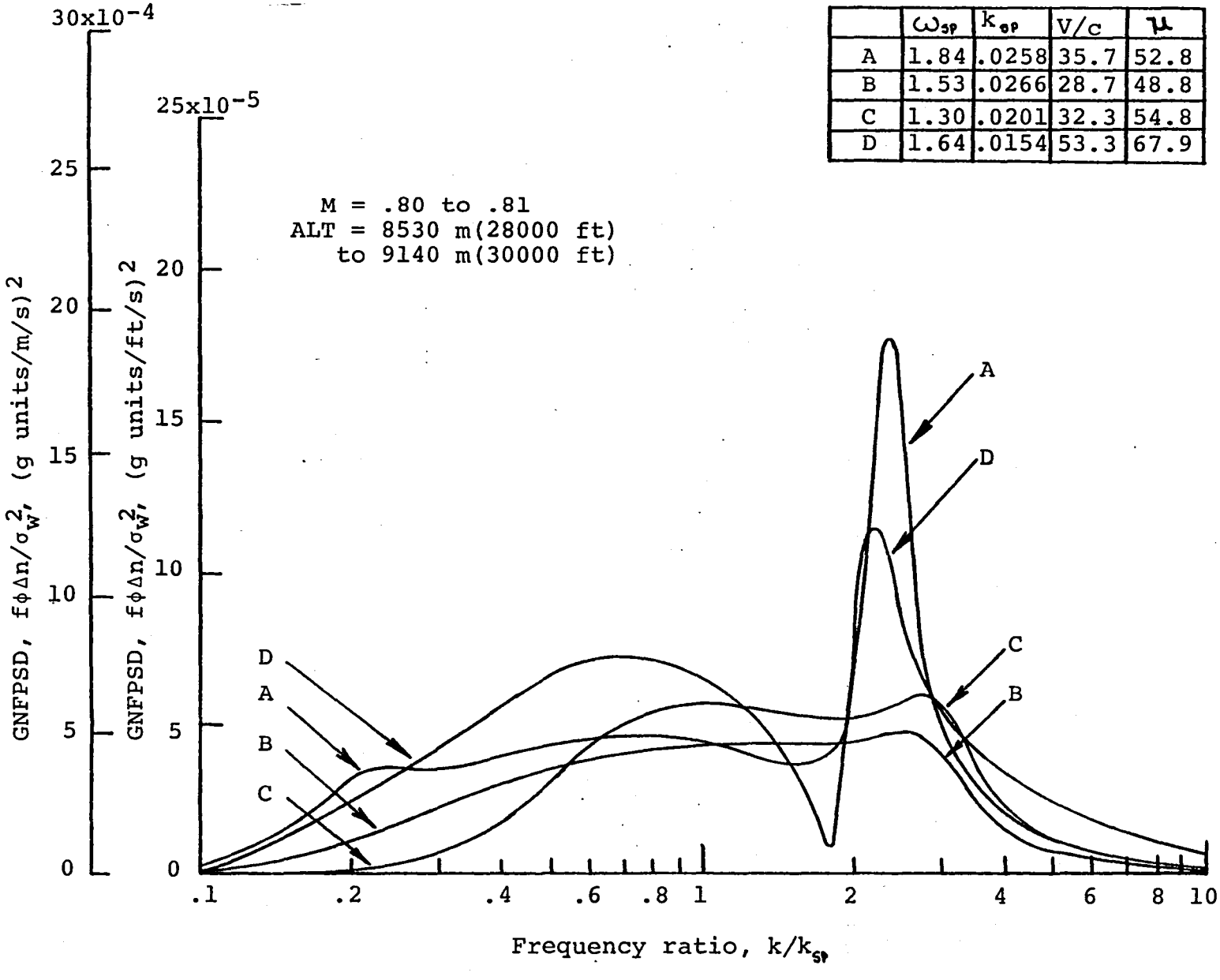

	ω_{sp}	k_{sp}	V/c	μ
A	1.84	.0258	35.7	52.8
B	1.53	.0266	28.7	48.8
C	1.30	.0201	32.3	54.8
D	1.64	.0154	53.3	67.9

Figure 22.- GNFPSD versus frequency ratio, Low cruise, A/P mode Cruise.

	ω_{sp}	k_{sp}	V/c	μ
A	1.84	.0258	35.7	52.8
B	1.53	.0266	28.7	48.8

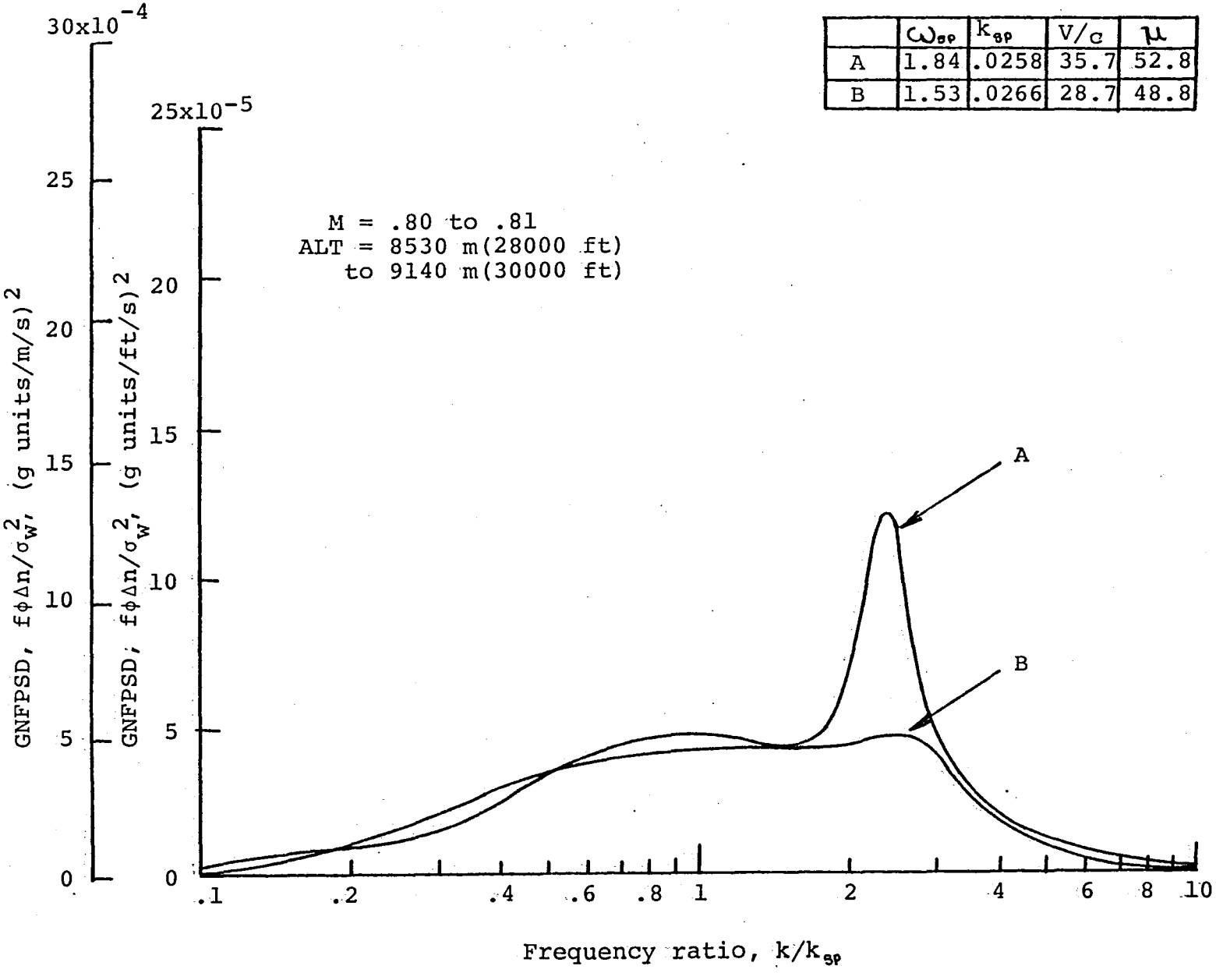

Figure 23.- GNFPSD versus frequency ratio, Low cruise, A/P mode Turbulent.

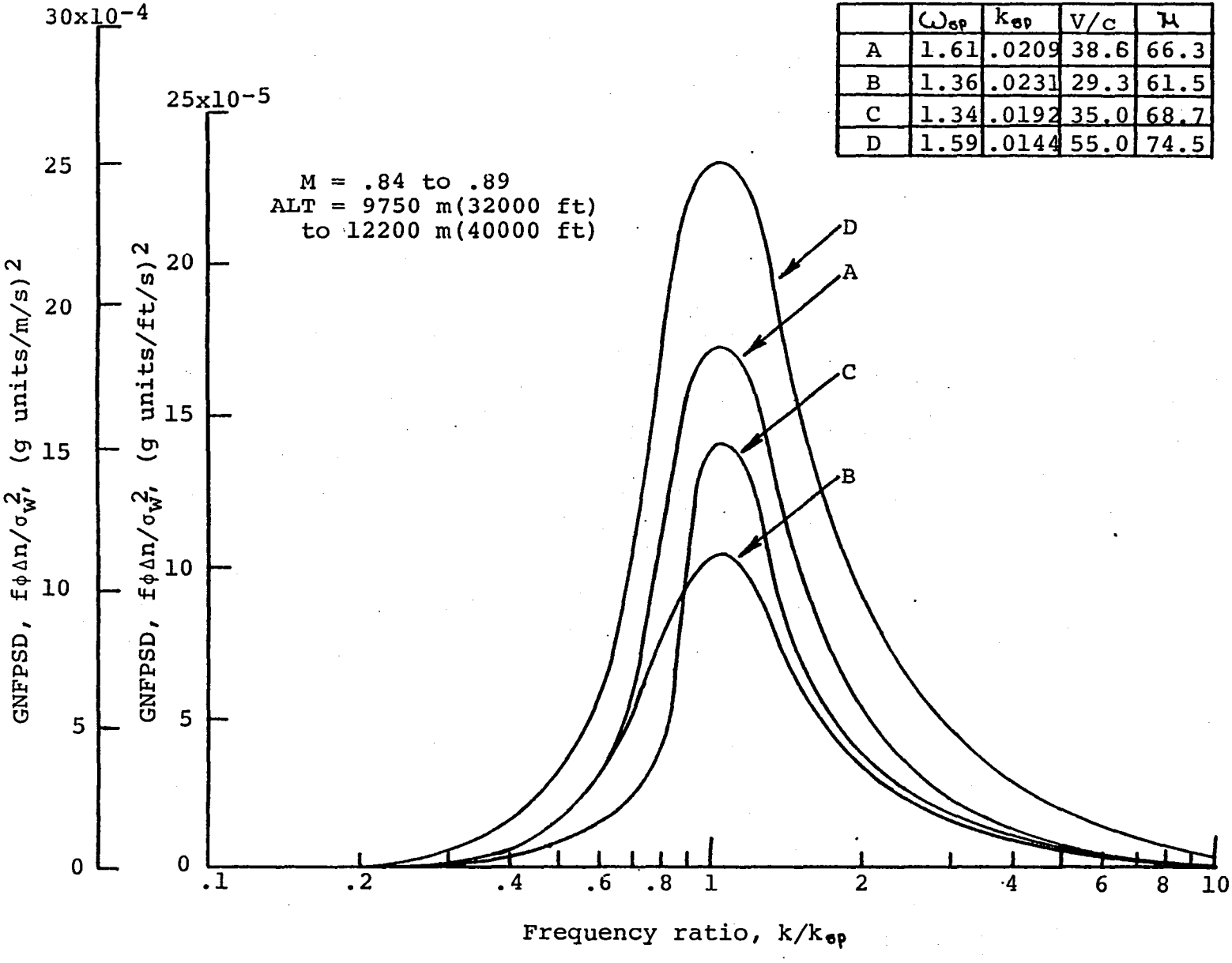

	ω_{op}	k_{op}	V/c	μ
A	1.61	.0209	38.6	66.3
B	1.36	.0231	29.3	61.5
C	1.34	.0192	35.0	68.7
D	1.59	.0144	55.0	74.5

Figure 24.- GNFPSD versus frequency ratio, High cruise, A/P mode Off.

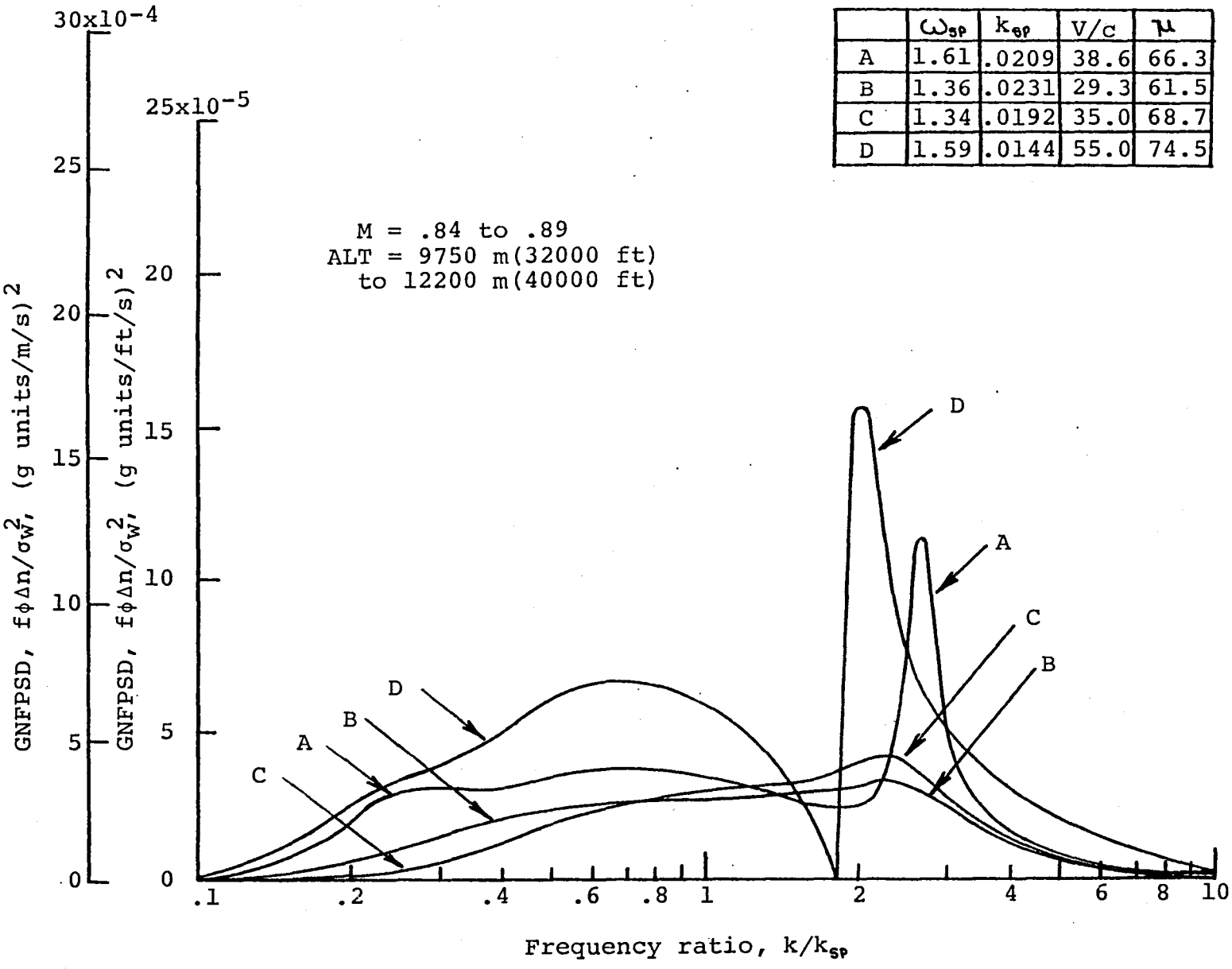

	ω_{sp}	k_{sp}	V/c	μ
A	1.61	.0209	38.6	66.3
B	1.36	.0231	29.3	61.5
C	1.34	.0192	35.0	68.7
D	1.59	.0144	55.0	74.5

Figure 25.- GNFPSD versus frequency ratio, High cruise, A/P mode Cruise.

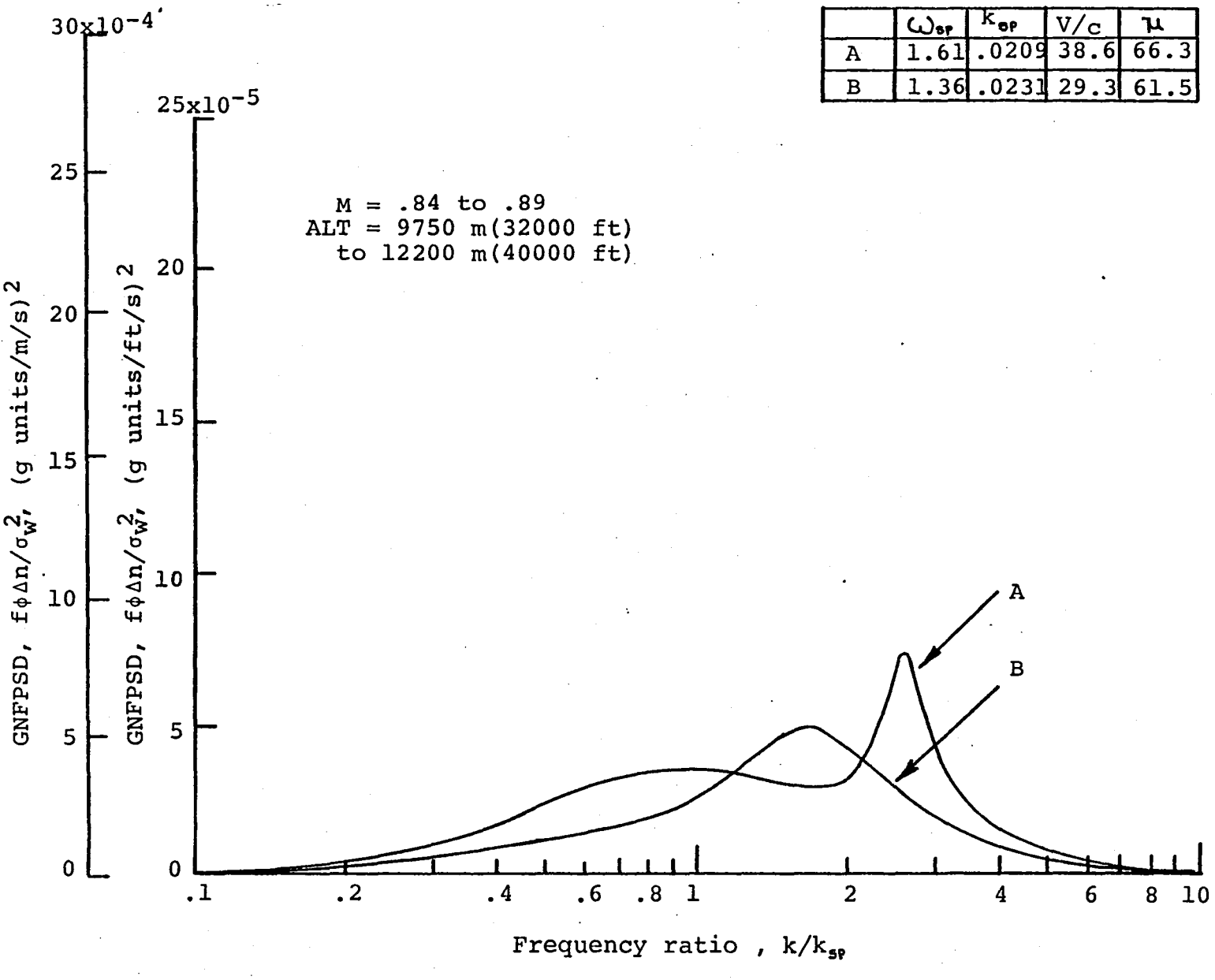

	ω_{sp}	k_{sp}	V/c	μ
A	1.61	.0209	38.6	66.3
B	1.36	.0231	29.3	61.5

Figure 26.- GNFPSD versus frequency ratio, High cruise, A/P mode Turbulent.

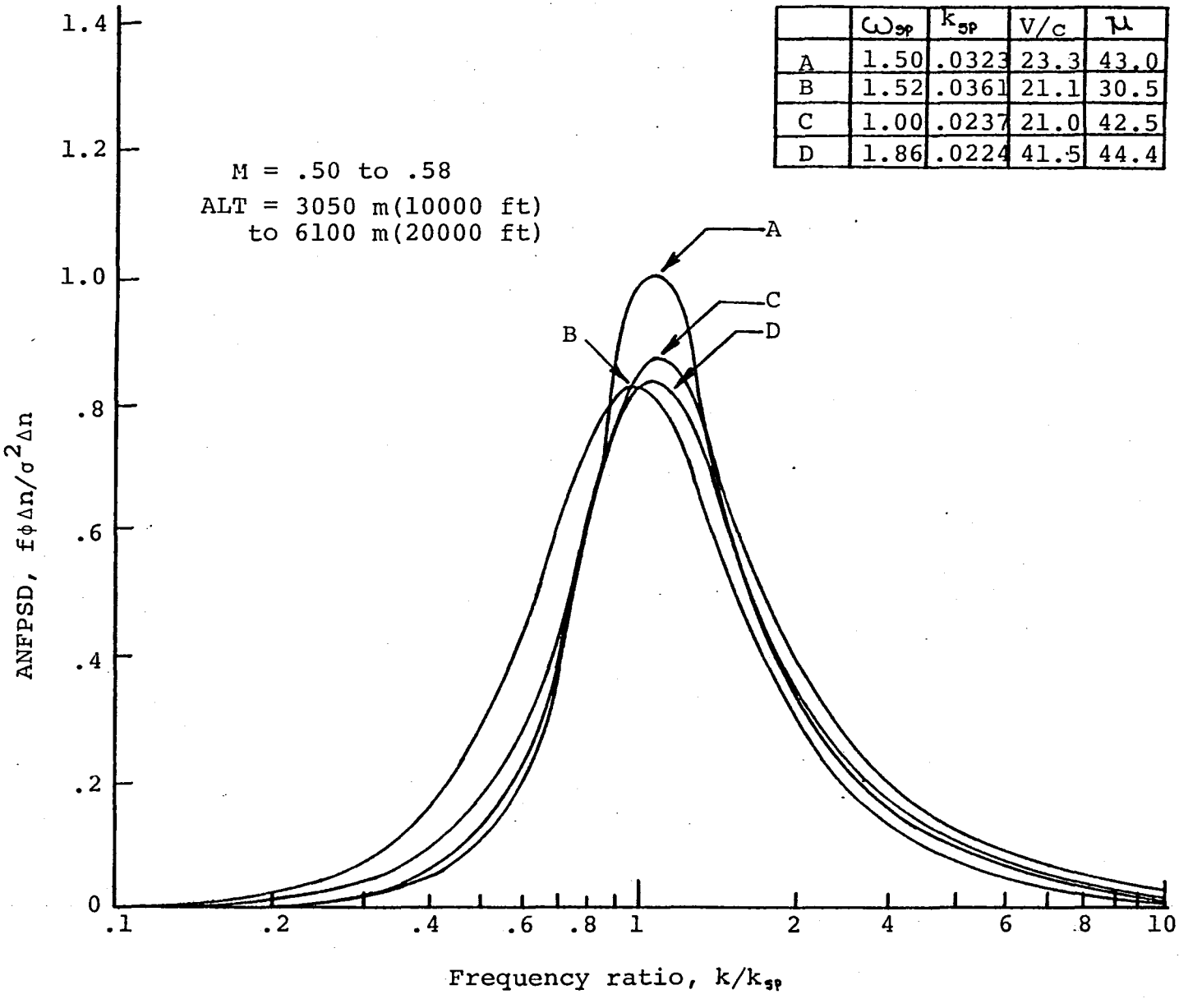

	ω_{sp}	k_{sp}	V/c	μ
A	1.50	.0323	23.3	43.0
B	1.52	.0361	21.1	30.5
C	1.00	.0237	21.0	42.5
D	1.86	.0224	41.5	44.4

Figure 27.- ANFPSD versus frequency ratio, Climb and descent, A/P mode Off.

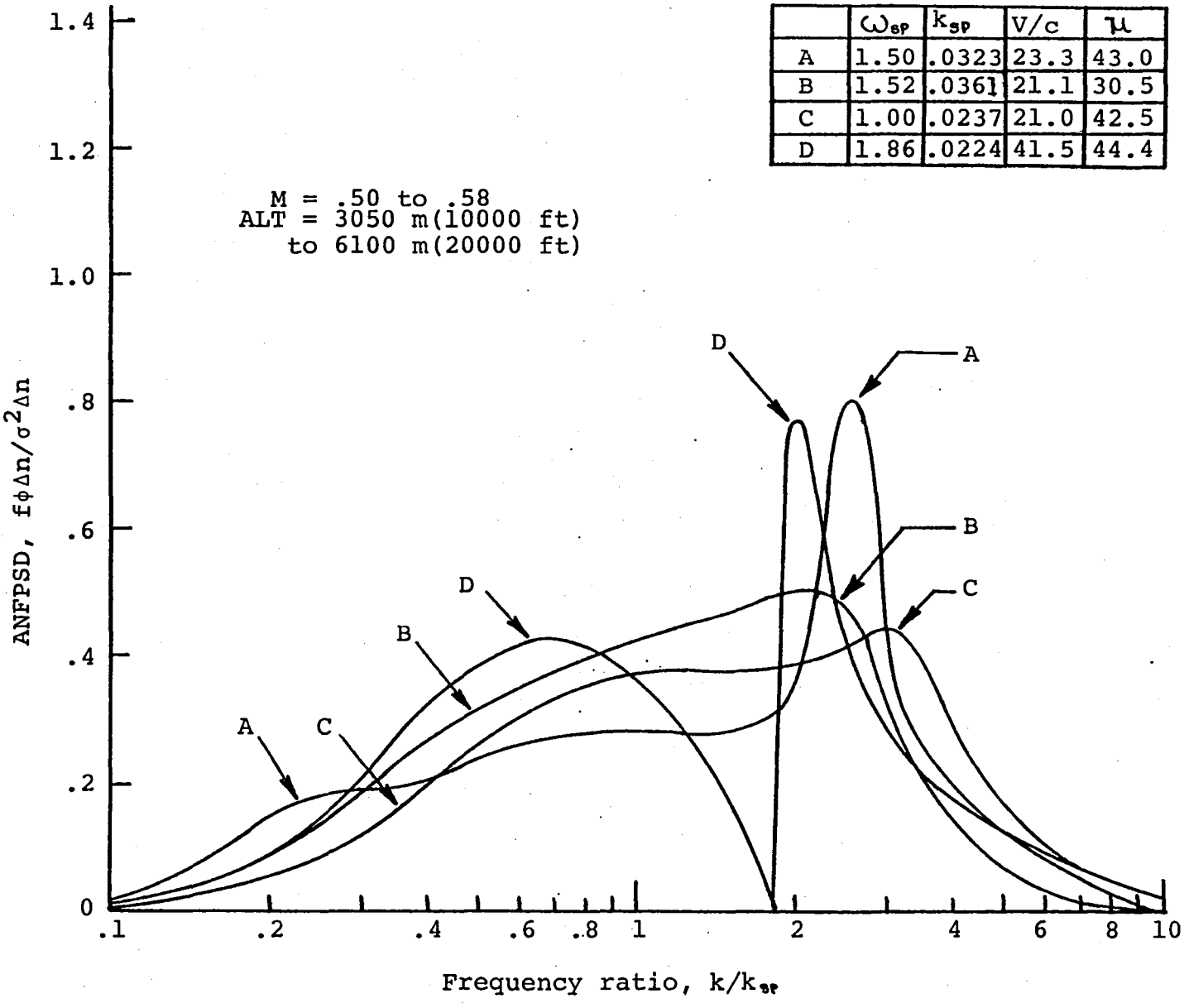

	ω_{sp}	k_{sp}	V/c	μ
A	1.50	.0323	23.3	43.0
B	1.52	.0361	21.1	30.5
C	1.00	.0237	21.0	42.5
D	1.86	.0224	41.5	44.4

Figure 28.- ANFPSD versus frequency ratio, Climb and descent, A/P mode Climb/Descent.

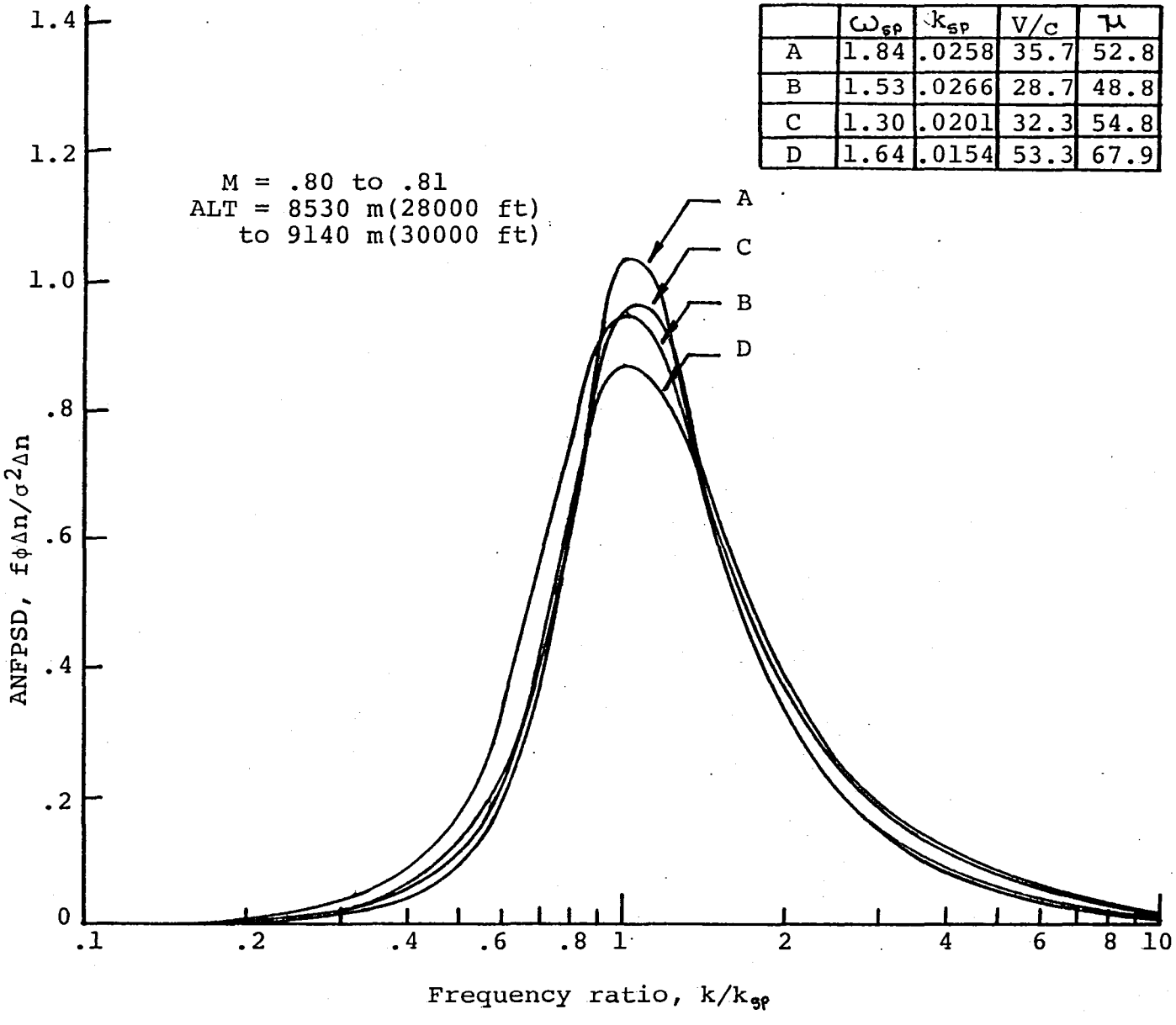

	ω_{sp}	k_{sp}	V/c	μ
A	1.84	.0258	35.7	52.8
B	1.53	.0266	28.7	48.8
C	1.30	.0201	32.3	54.8
D	1.64	.0154	53.3	67.9

Figure 29.- ANFPSD versus frequency ratio, Low cruise, A/P mode Off.

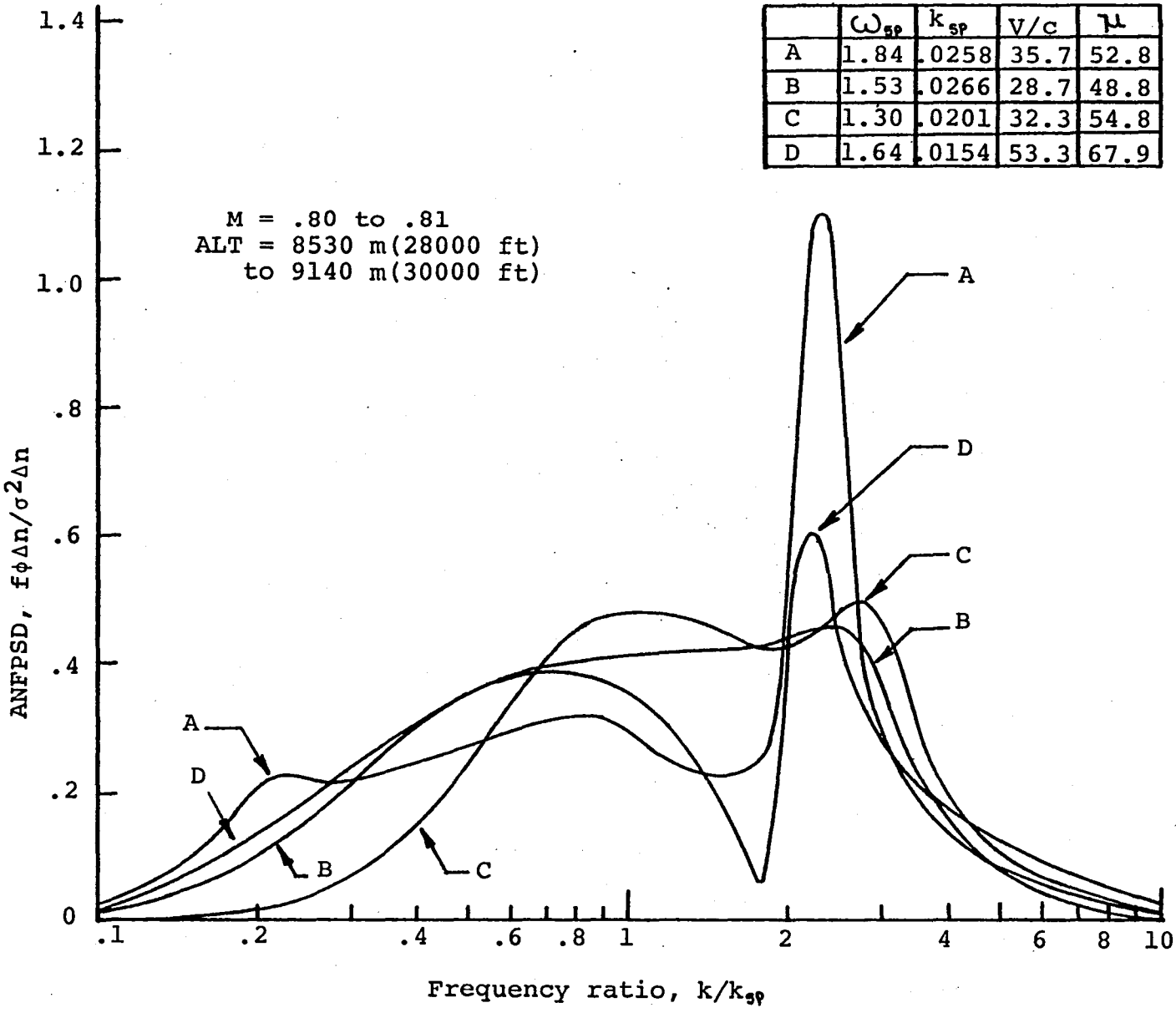

	ω_{sp}	k_{sp}	V/c	μ
A	1.84	.0258	35.7	52.8
B	1.53	.0266	28.7	48.8
C	1.30	.0201	32.3	54.8
D	1.64	.0154	53.3	67.9

Figure 30.- ANFPSD versus frequency ratio, Low cruise, A/P mode Cruise.

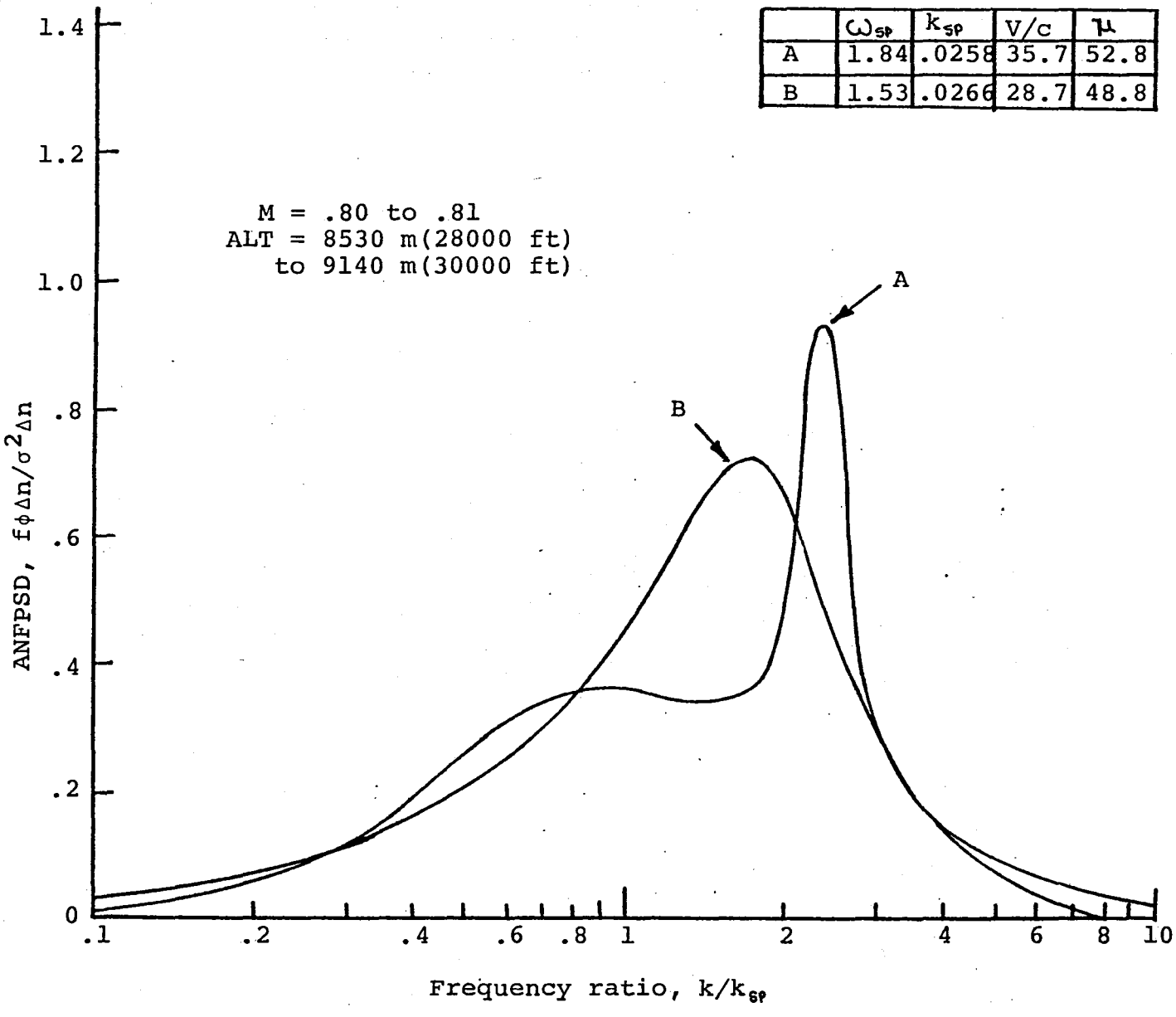

	ω_{sp}	k_{sp}	V/c	μ
A	1.84	.0258	35.7	52.8
B	1.53	.0266	28.7	48.8

Figure 31.- ANFPSD versus frequency ratio, Low cruise, A/P mode Turbulent.

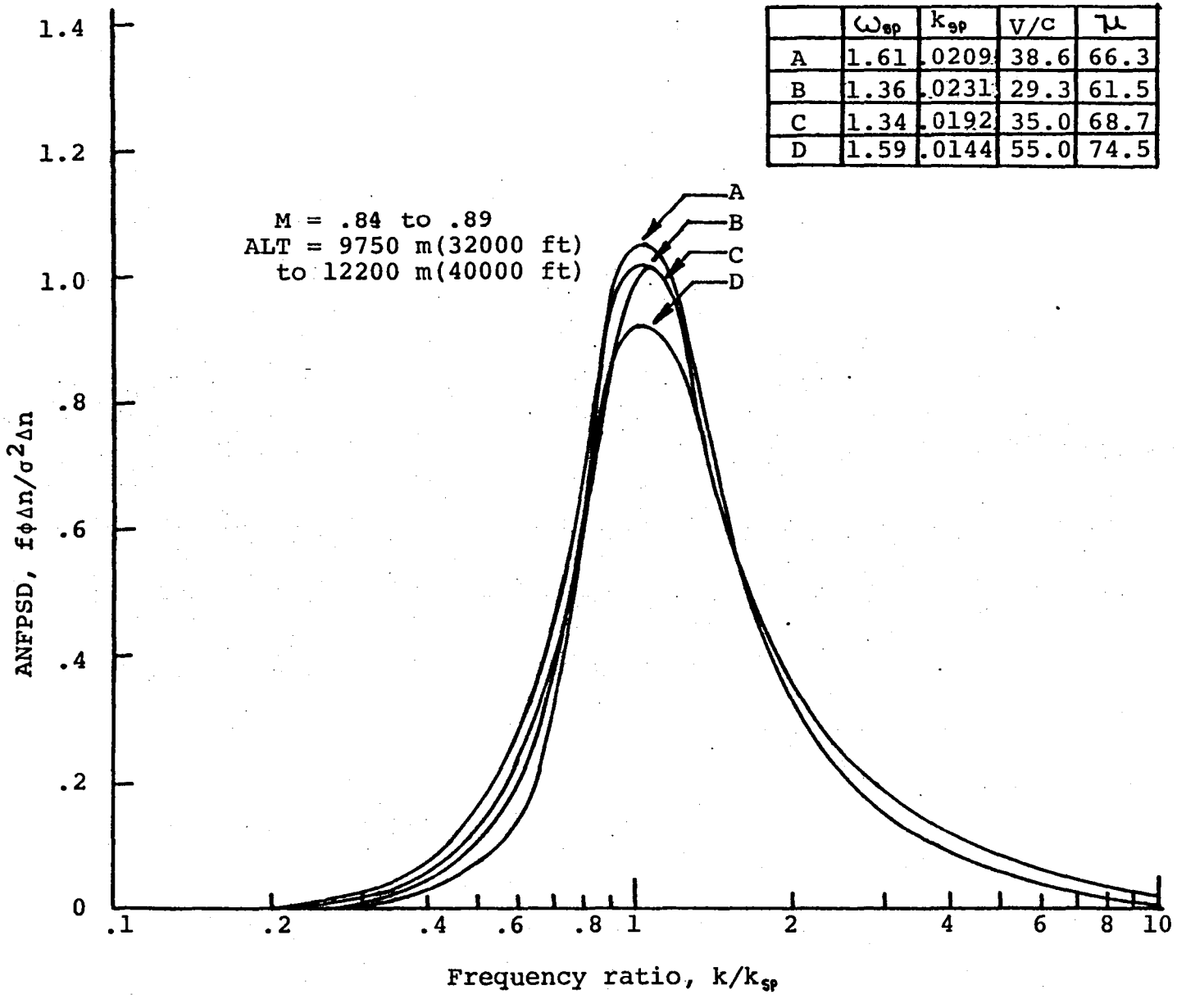

Figure 32.- ANFPSD versus frequency ratio, High cruise, A/P mode Off.

	ω_{sp}	k_{sp}	V/c	μ
A	1.61	.0209	38.6	66.3
B	1.36	.0231	29.3	61.5
C	1.34	.0192	35.0	68.7
D	1.59	.0144	55.0	74.5

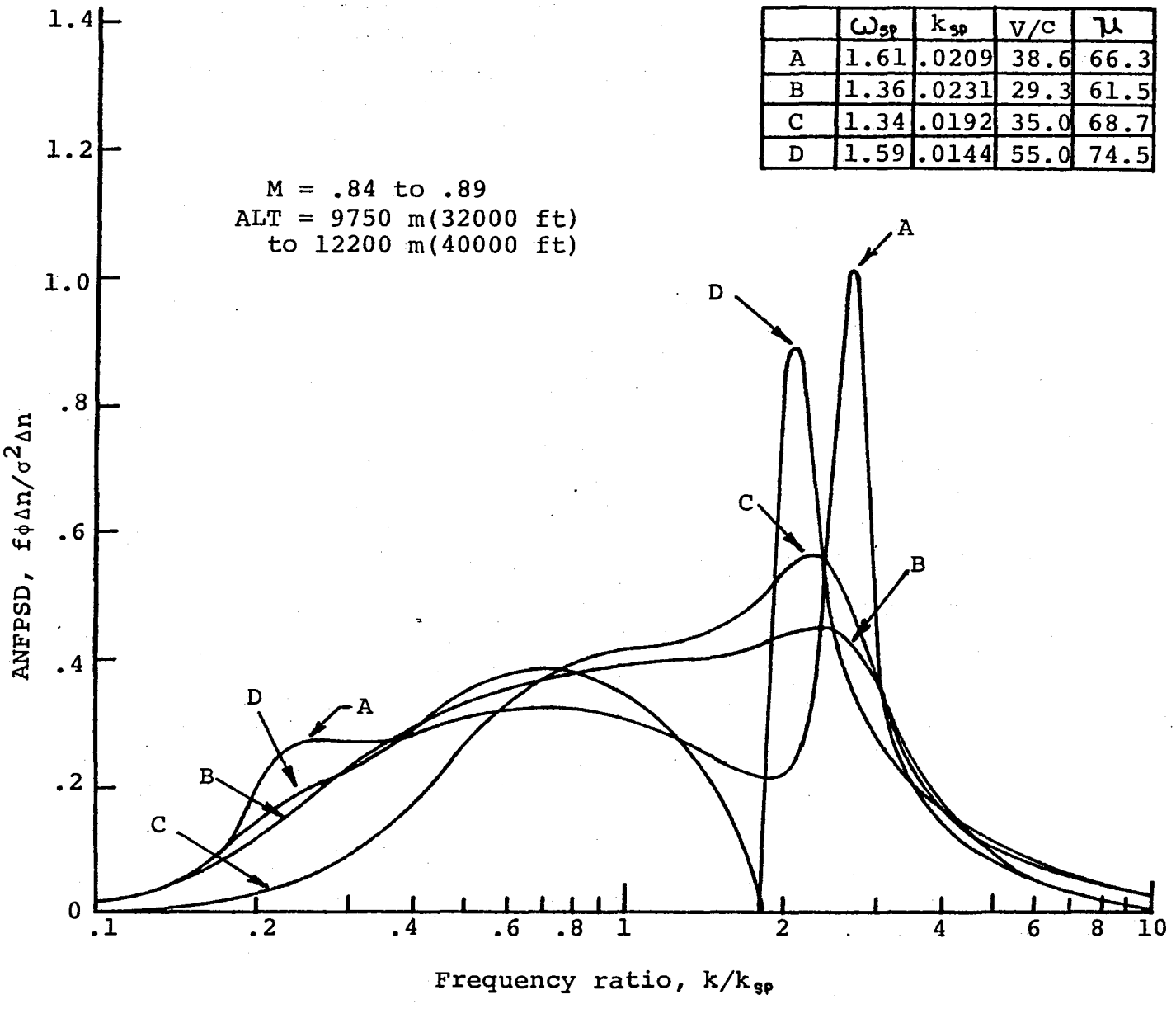

Figure 33.- ANFPSD versus frequency ratio, High cruise, A/P mode Cruise.

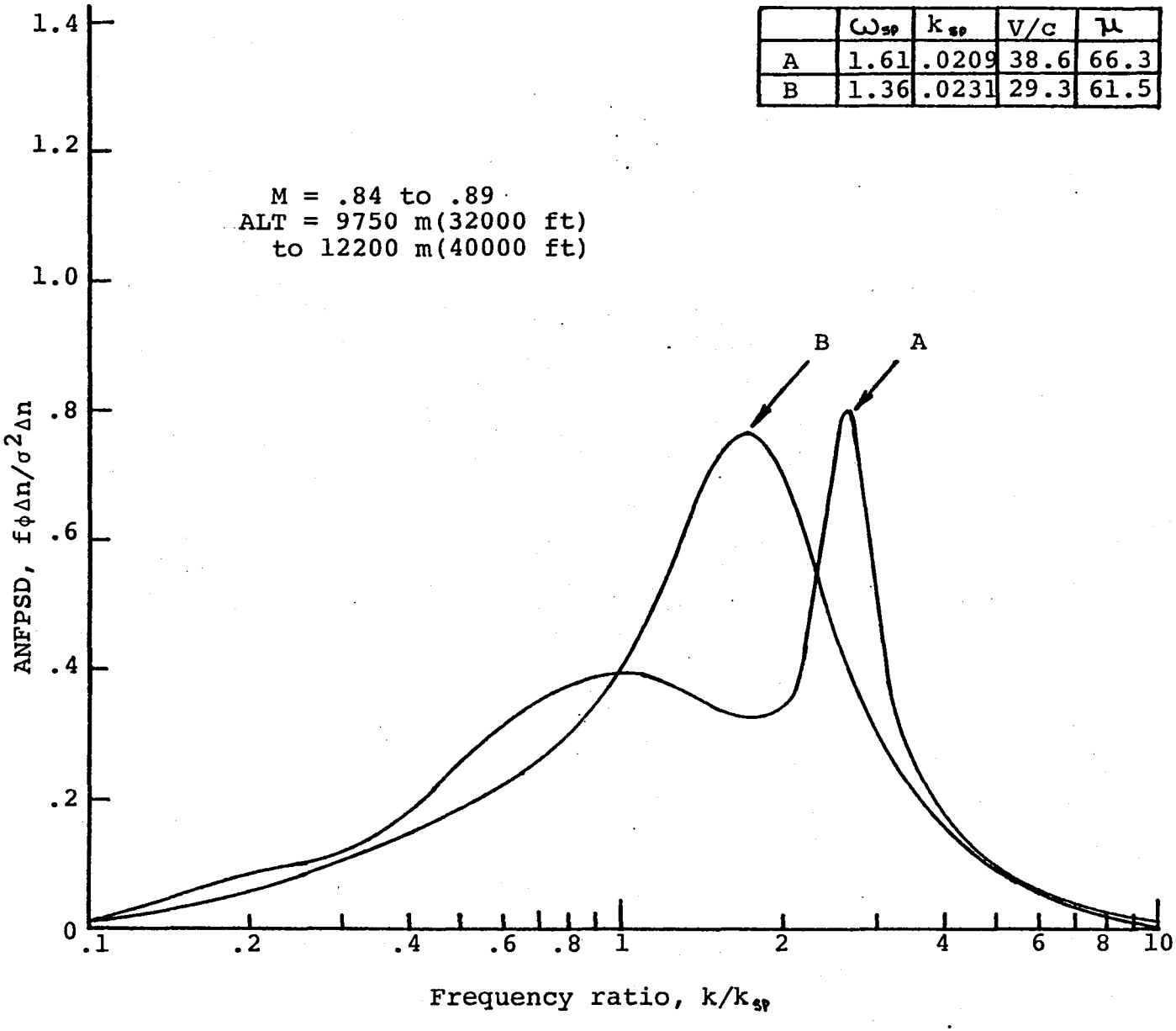

	ω_{sp}	k_{sp}	V/c	μ
A	1.61	.0209	38.6	66.3
B	1.36	.0231	29.3	61.5

Figure 34.- ANFPSD versus frequency ratio, High cruise, A/P mode Turbulent.

1. Report No.	2. Government Accession No.	3. Recipient's Catalog No.
NASA CR-165919		

4. Title and Subtitle	5. Report Date
GUST RESPONSE OF COMMERCIAL JET AIRCRAFT INCLUDING EFFECTS OF AUTOPILOT OPERATION	June 1982
	6. Performing Organization Code
7. Author(s)	8. Performing Organization Report No.
Joseph H. Goldberg	
	10. Work Unit No.
9. Performing Organization Name and Address	
Villanova University Villanova, Pennsylvania 19085	11. Contract or Grant No. NAS1-16095
	13. Type of Report and Period Covered Contractor report
12. Sponsoring Agency Name and Address	
National Aeronautics and Space Administration Washington, DC 20546	14. Sponsoring Agency Code

15. Supplementary Notes

Final Report
Langley technical monitor: Norman L. Crabill

16. Abstract

Presented is a simplified theory of aircraft vertical acceleration gust response based on a model including pitch, vertical displacement and control motions due to autopilot operation. High-order autopilot transfer functions are utilized for improved accuracy in the determination of the overall response characteristics. Four representative commercial jet aircraft were studied over a wide range of operating conditions and comparisons of individual responses are given. It is shown that autopilot operation relative to the controls - fixed case causes response attenuation of from 10 percent to approximately 25 percent depending on flight condition and increases in crossing number up to 30 percent, with variations between aircraft of from 5 percent to 10 percent, in general, reflecting the differences in autopilot design. A detailed computer program description and listing of the calculation procedure suitable for the general application of the theory to any airplane - autopilot combination is also included.

17. Key Words (Suggested by Author(s))	18. Distribution Statement
Gust response, Commercial jets Autopilot effects	Unclassified-Unlimited Subject Category - 03

19. Security Classif. (of this report)	20. Security Classif. (of this page)	21. No. of Pages	22. Price
Unclassified	Unclassified	123	

For sale by the National Technical Information Service, Springfield, Virginia 22161

End of Document